
[All ETDs from UAB](#)

[UAB Theses & Dissertations](#)

2005

Design of wrap around steel gusset plates.

Ronald Scott Dowswell
University of Alabama at Birmingham

Follow this and additional works at: <https://digitalcommons.library.uab.edu/etd-collection>

Recommended Citation

Dowswell, Ronald Scott, "Design of wrap around steel gusset plates." (2005). *All ETDs from UAB*. 5444.
<https://digitalcommons.library.uab.edu/etd-collection/5444>

This content has been accepted for inclusion by an authorized administrator of the UAB Digital Commons, and is provided as a free open access item. All inquiries regarding this item or the UAB Digital Commons should be directed to the [UAB Libraries Office of Scholarly Communication](#).

NOTE TO USERS

This reproduction is the best copy available.

UMI[®]

DESIGN OF WRAP-AROUND STEEL GUSSET PLATES

by

RONALD SCOTT DOWSWELL

A DISSERTATION

Submitted to the graduate faculty of The University of Alabama at Birmingham,
in partial fulfillment of the requirements for the degree of
Doctor of Philosophy

BIRMINGHAM, ALABAMA

2005

UMI Number: 3201151

INFORMATION TO USERS

The quality of this reproduction is dependent upon the quality of the copy submitted. Broken or indistinct print, colored or poor quality illustrations and photographs, print bleed-through, substandard margins, and improper alignment can adversely affect reproduction.

In the unlikely event that the author did not send a complete manuscript and there are missing pages, these will be noted. Also, if unauthorized copyright material had to be removed, a note will indicate the deletion.

UMI[®]

UMI Microform 3201151

Copyright 2006 by ProQuest Information and Learning Company.

All rights reserved. This microform edition is protected against unauthorized copying under Title 17, United States Code.

ProQuest Information and Learning Company
300 North Zeeb Road
P.O. Box 1346
Ann Arbor, MI 48106-1346

ABSTRACT OF DISSERTATION
GRADUATE SCHOOL, UNIVERSITY OF ALABAMA AT BIRMINGHAM

Degree PhD Program Civil Engineering

Name of Candidate Ronald Scott Dowswell

Committee Chair Fouad H. Fouad

Title Design of Wrap-Around Steel Gusset Plates

Gusset plates are used in steel buildings to connect bracing members to other structural members in the lateral force resisting system. Horizontal bracing is commonly used to resist lateral loads in industrial structures and in commercial buildings where floor and roof diaphragms cannot carry the loads. Wrap-around gusset plates are L-shaped plates that are used where an opening is required at the corner of the plate. This typically occurs at horizontal bracing where the gusset plate is cut out around a column.

The purposes of this research were to gain a better understanding of the behavior of wrap-around gusset plates, identify potential failure modes, and formulate a design method for these connections. Ten experimental specimens were tested in compression and five were tested in tension. All of the specimens were modeled using the finite element method with material and geometric nonlinearities.

The experiments and finite element models indicated that wrap-around gusset plates are subject to limit states common to flexural members. The results were used to formulate a design method for wrap-around gusset plates, which is based on a cantilever beam model. The accuracy of the proposed design method was verified by comparing the calculated capacities to experimental and finite element results. The accuracy of the proposed method is similar to that of the current design procedure for standard gusset plates without cutouts.

ACKNOWLEDGEMENTS

I would like to thank Dr. Fouad H. Fouad for serving as my graduate committee chair, and Dr. James S. Davidson, Dr. Talat Abu-Amra, Dr. Bobby J. Stephens, and Dr. Houssam A. Toutanji for serving on my graduate committee. The assistance of lab supervisor Richard Hawkins was invaluable and is appreciated.

The test frame and specimens were fabricated and donated to the project by Gipson Steel, Inc. Structural Steel Services, Inc., also fabricated parts of the test frame. Bell Steel Company supplied the bolts. The technical assistance of Elton Hogan and Mark Gipson of Gipson Steel, George Reed and Kane Combs of Structural Steel Services, and Curtis Smith of Bell Steel is greatly appreciated.

TABLE OF CONTENTS

	<i>Page</i>
ABSTRACT	ii
ACKNOWLEDGMENTS	iii
LIST OF TABLES	v
LIST OF FIGURES	vii
INTRODUCTION	1
DESIGN CONSIDERATIONS FOR WRAP-AROUND GUSSET PLATES	3
WRAP-AROUND GUSSET PLATES IN TENSION	33
WRAP-AROUND GUSSET PLATES IN COMPRESSION	50
MODELING TECHNIQUES FOR WRAP-AROUND GUSSET PLATES	74
FINITE ELEMENT ANALYSIS OF WRAP-AROUND GUSSET PLATES	102
A PROPOSED DESIGN METHOD FOR WRAP-AROUND GUSSET PLATES	123
CONCLUSION	150
APPENDIX: NOTATION	152

LIST OF TABLES

<i>Table</i>	<i>Page</i>
DESIGN CONSIDERATIONS FOR WRAP-AROUND GUSSET PLATES	
1 Experimental Residual Stress Patterns in Flame-cut Plates	16
WRAP-AROUND GUSSET PLATES IN TENSION	
1 Measured Plate Thickness	36
2 Test Loads	40
WRAP-AROUND GUSSET PLATES IN COMPRESSION	
1 Measured Plate Thickness	56
2 Test Data	62
MODELING TECHNIQUES FOR WRAP-AROUND GUSSET PLATES	
1 Summary of Boundary Conditions	80
2 Summary of Linear Elastic Mesh Study	81
3 Experimental Residual Stress Patterns in Flame-cut Plates	84
4 Summary of Models Analyzed for Nonlinear Inelastic Analysis	87
FINITE ELEMENT ANALYSIS OF WRAP-AROUND GUSSET PLATES	
1 Measured Plate Thickness	105
2 Summary of Boundary Conditions	107
3 Loads from Finite Element Models and Experiments	112
A PROPOSED DESIGN METHOD FOR WRAP-AROUND GUSSET PLATES	
1 Calculated Capacities	132

LIST OF TABLES (Continued)

<i>Table</i>	<i>Page</i>
2 Experimental and Finite Element Loads	133

LIST OF FIGURES

<i>Figure</i>	<i>Page</i>
DESIGN CONSIDERATIONS FOR WRAP-AROUND GUSSET PLATES	
1 Standard vertical brace connection	24
2 Horizontal brace connection at beam-to-beam intersection	24
3 Wrap-around gusset plate connection	25
4 Wrap-around gusset plate connection at a large column	25
5 Effective width for various connection configurations	26
6 Geometry of effective column	26
7 Interface loads for a standard gusset plate	26
8 Various force distributions for horizontal brace connections	27
9 Force system for wrap-around gusset plates	27
10 Elastic bending stresses in gusset plate legs	28
11 Flexural stresses for rectangular beams	29
12 Force system with bilinear moment diagram at Leg 1	30
13 Residual stress pattern in a flame-cut plate	30
14 Biaxial stress at the interior corner	31
15 Plane stress element	31
16 Plastic bending stresses in each leg	32
WRAP-AROUND GUSSET PLATES IN TENSION	
1 Horizontal brace connection at beam-to-beam intersection	42

LIST OF FIGURES (Continued)

<i>Figure</i>	<i>Page</i>
2 Horizontal brace connection at beam-to-column intersection	42
3 Fabrication drawings	43
4 Strain gage locations	44
5 Test frame drawings	45
6 Picture of testing machine and test frame	46
7 Load vs. deflection plots	47
8 In-plane deformation of Specimen 2T after test	48
9 Out-of-plane deformation of Specimen 2T after test	48
10 Apparent stress vs. load plot for Specimens 9T and 10T	49

WRAP-AROUND GUSSET PLATES IN COMPRESSION

1 Horizontal brace connection at beam-to-beam intersection	65
2 Horizontal brace connection at beam-to-column intersection	65
3 Fabrication drawings	66
4 Strain gage locations	67
5 Test frame drawings	68
6 Photographs of test frame	69
7 Load vs. deflection plots	70
8 Specimens 4C, 6C, and 7C after test	71
9 Stress vs. load plot for Specimen 6C	72
10 Apparent stress vs. load plot for Specimen 7C	72
11 Apparent stress vs. load plot for Specimen 9C	73

LIST OF FIGURES (Continued)

<i>Figure</i>	<i>Page</i>
MODELING TECHNIQUES FOR WRAP-AROUND GUSSET PLATES	
1 Standard vertical brace connection	92
2 Horizontal brace connection at beam-to-column intersection	92
3 Dimensions of the plate modeled	93
4 Boundary conditions	93
5 Von Mises stress contour for Mesh 1	94
6 Mesh Schemes Studied	95
7 Buckled shape for elastic buckling analysis	96
8 Residual deformation of Specimen 2 from Dowswell and Fouad (2005)	97
9 Experimental stress-strain curve by Dowswell and Fouad (2005)	97
10 Residual stress pattern in a flame-cut plate	98
11 Simplified residual stress pattern	98
12 Model with residual stresses at edges	98
13 Load vs. in-plane deflection for models with residual stresses and experimental stress strain curve	99
14 Load vs. in-plane deflection for model with residual stresses and without residual stresses incorporated	100
15 Load vs. in-plane deflection for model with elastic-plastic curve and experimental curve	101
FINITE ELEMENT ANALYSIS OF WRAP-AROUND GUSSET PLATES	
1 Wrap-around gusset plate connection	114
2 Details of specimens from Dowswell and Fouad (2006b)	115
3 Mesh scheme	116

LIST OF FIGURES (Continued)

<i>Figure</i>	<i>Page</i>
4 Boundary conditions	116
5 Residual stress pattern in a flame-cut plate	117
6 Simplified residual stress pattern	117
7 Buckled shape for Model 2T	118
8 Buckled shape for Model 6C	118
9 Bending stresses in gusset plate legs	119
10 Elastic stress contours for Model 2T	119
11 Flexural stresses in 8-in. leg of plate 2T at a brace load of 65 k	120
12 Load versus deflection plots for finite element models	121
13 In-plane deformation of Model 2T	122
14 Load versus deflection data for Model 2C and Specimen 2C	122
A PROPOSED DESIGN METHOD FOR WRAP-AROUND GUSSET PLATES	
1 Horizontal brace connection at beam-to-column intersection	141
2 Force system for wrap-around gusset plates	141
3 Bending stresses in each leg	142
4 Elastic Stress contours for a typical model loaded in tension	142
5 Typical flexural stresses in gusset plate legs	143
6 Details of Specimens 8 and 10	144
7 Elastic Stress contours for a typical model loaded in tension	145
8 Typical buckled shape for the models loaded in tension	146
9 Typical buckled shape for the models loaded in compression	146

LIST OF FIGURES (Continued)

<i>Figure</i>	<i>Page</i>
10 Effective length of gusset legs	147
11 Load versus deflection plot for finite element model 9T	148
12 Connection for Example 1	148
13 Connection for Example 2	149

INTRODUCTION

Gusset plates are used in steel buildings to connect bracing members to other structural members in the lateral force resisting system. Horizontal bracing is commonly used to resist lateral loads in industrial structures and in commercial buildings where floor and roof diaphragms cannot carry the loads. Wrap-around gusset plates are L-shaped plates that are used where an opening is required at the corner of the plate. This typically occurs at horizontal bracing where the gusset plate is cut out around a column.

The purposes of this research were to gain a better understanding of the behavior of wrap-around gusset plates, identify potential failure modes, and formulate a design method for these connections. Ten experimental specimens were tested in compression and five were tested in tension. All of the specimens were modeled using the finite element method with material and geometric nonlinearities.

The project was separated into four phases: preliminary work, experimental testing, finite element modeling, and formulation of a design procedure. The first phase was the preliminary work. It consisted of a review of the available literature and a review of the current design methods for standard gusset plates and wrap-around gusset plates. The test frames and test specimens were designed and fabricated in the preliminary stage. The locations of the peak stresses within the gusset plates were determined with simple finite element models. This information was used to locate the strain gages on the experimental specimens. The preliminary finite element models were also used to

determine an approximate test load, so the proper ranges could be set on the testing machine.

The experimental phase was separated into two test programs because the specimens with compression loads required a different testing arrangement than the specimens with tension loads. Ten different specimens were tested in compression, and five different specimens were tested in tension.

The finite element models were built in the third phase. All 15 of the specimens and loading conditions from the experimental phase were modeled. Before the models were built, the modeling techniques were optimized using a parametric study. The effects of the following parameters were studied: mesh size, magnitude of the initial out-of-flatness, the effect of residual stresses, and the shape of the stress-strain curve. The accuracy of the finite element models was verified by comparing the results to the experimental results.

The fourth phase was the formulation of a design procedure. The experiments and finite element models indicated that wrap-around gusset plates are subject to limit states common to flexural members. The results were used to formulate a design method for wrap-around gusset plates, which is based on a cantilever beam model. The accuracy of the proposed design method was verified by comparing the calculated capacities to experimental and finite element results.

The findings of this research project will provide information on the design and behavior of wrap-around gusset plates. The results of this project are presented in a way that can be easily used by design engineers. It is expected that the findings will impact national specifications and will be used in design guides on steel connection design.

DESIGN CONSIDERATIONS FOR WRAP-AROUND GUSSET PLATES

by

BO DOWSWELL AND FOUAD FOUAD

Submitted to American Institute of Steel Construction Engineering Journal

Format adapted for dissertation

INTRODUCTION

Gusset plates are commonly used in steel buildings to connect bracing members to other structural members in the lateral force resisting system. Figure 1 shows a standard vertical bracing connection at a beam-to-column intersection. Horizontal bracing is used to resist lateral loads in industrial structures and in commercial buildings where floor and roof diaphragms have inadequate strength or stiffness. Figure 2 shows a typical horizontal bracing connection at a beam-to-beam intersection. Where a horizontal brace is located at a beam-to-column intersection, the gusset plate must be cut out around the column, as shown in Figure 3. These are called wrap-around gusset plates. At locations with large columns and heavy beam connection angles, a large area of the gusset plate is cut out, as shown in Figure 4.

Problem Statement

A large number of research projects have been dedicated to the analysis and design of standard gusset plates. Failure modes for standard gusset plates have been identified, and design procedures are well documented in the literature. However, failure modes unique to wrap-around gusset plates have not been studied, nor are guidelines for their design available in the literature.

Objectives

The purposes of this paper are to present potential failure modes associated with wrap-around gusset plates and to discuss design considerations for these connections.

Previous research and current design practice for standard gusset plates are reviewed.

Current design practice for wrap-around gusset plates is presented and discussed.

DESIGN PROCEDURES FOR STANDARD GUSSET PLATES

Effective Width

In design, gusset plates are treated as rectangular, axially loaded members with a cross section $L_e \times t$, where L_e is the effective width, and t is the gusset plate thickness.

The effective width is calculated by assuming that the stress spreads through the gusset plate at an angle of 30° . The effective width is shown in Figure 5 for various connection configurations.

Buckling Capacity

Thornton (1984) proposed a method to calculate the buckling capacity of gusset plates. He recommended that the gusset plate area between the brace end and the framing members be treated as a rectangular column with a cross section $L_e \times t$. For corner gusset plates, the column length, l_{avg} , is calculated as the average of l_1 , l_2 , and l_3 , as shown in Figure 6. The buckling capacity is then calculated using the column curve in the AISC Specification (AISC, 1999).

Normal and Shear Stresses

Gusset plates are designed so that the normal and shear stresses on any cross section of the plate do not exceed the design stresses. Traditionally, beam theory has

been used to determine the stresses at the critical sections. The normal stress and shear stress are considered separately. The elastic normal stress is:

$$f_a = \frac{P}{A} \pm \frac{Mc}{I} \quad (1)$$

The shear stress is calculated using a simplified average instead of the elastic parabolic distribution. The average shear stress is:

$$f_v = \frac{V}{A} \quad (2)$$

The selection of the most highly stressed section is at the discretion of the designer and is based on prior experience. Generally, for a standard vertical bracing gusset plate, the normal and shear stresses are checked at the gusset-to-beam interface and the gusset-to-column interface. Figure 7 shows the possible interface loads for a standard gusset plate.

EXISTING LITERATURE

A large number of research projects have been dedicated to the analysis and design of standard gusset plates. The research includes laboratory tests, finite element models, and theoretical studies. Many different failure modes have been identified.

Dowswell and Barber (2004) summarized previous experiments and finite element studies on gusset plates in compression. The research indicated that gusset plate buckling is concentrated at the end of the brace member and generally occurs in the inelastic range.

Effective Width Research

The first major experimental work on gusset plates was by Wyss (1926). The stress trajectories were plotted for gusset plate specimens representing a Warren truss joint. The maximum normal stress was at the end of the brace member. Wyss noted that the stress trajectories were along approximately 30 degree lines with the connected member, which defined the effective width of the gusset plate. The experimental investigations and finite element models of Sandel (1950), Whitmore (1952), Irvan (1957), Lavis (1967), Rabern (1983), and Bjorhovde and Chakrabarti (1985) confirmed Wyss' results.

Cheng and Grondin (1999) summarized the research on gusset plates at The University of Alberta. They noted that yielding in the specimens allowed the stress to redistribute and recommended that the effective width be calculated using a 45 degree dispersion angle instead of 30 degrees as noted by Wyss (1926). Using the Thornton method (Thornton, 1984) to calculate the buckling capacity with a 45 degree dispersion angle, the calculated capacities agreed well with the test results.

Research on Interface Stress Distribution

Rust (1938) published the results of a photoelastic study on the transfer of stress in gusset plates. He proposed a qualitative set of design rules and noted that a "generalized stress solution has not been found." In a discussion to the paper, Grinter (Rust, 1938) noted that a simple elastic analysis using beam theory overestimated the observed stress by 20 to 30 percent.

Perna (1941) tested a small-scale photoelastic model of a Pratt truss joint. He found that the stress distribution differed greatly from the stresses calculated using beam theory. The tests showed that the normal stresses at the edge of the plate were much smaller than the calculated stresses and the normal stresses at the interior of the plate were much greater than the calculated stresses. Although the maximum experimental stress did not occur in the same location as the maximum calculated stress, the author noted that beam theory appears to be conservative because the maximum calculated stress exceeded the maximum experimental stress.

Sandel (1950) conducted a photoelastic stress analysis of a 1/22-scale model of a Warren truss joint. The results showed that the use of beam theory to determine the stresses at critical sections in the gusset is “highly incorrect,” but conservative. The author suggested that the shear stress be calculated by using a plastic stress distribution instead of the theoretical parabolic distribution.

An experimental investigation was carried out by Whitmore (1952) to determine the stress distribution in gusset plates. The tests were conducted on 1/8-in. aluminum gusset plates with a yield strength of 39 ksi and a modulus of elasticity of 10,000 ksi. The specimen was a 1/4-scale model of a Warren truss joint with double gusset plates. Data from the strain gages was used to plot the bending and shear stresses at the critical section of the plate. He concluded that the use of simple beam formulas to calculate the stresses led to erroneous results. The maximum experimental bending stresses were slightly lower than the maximum calculated stresses, but they occurred in a different location. The maximum calculated elastic shear stress was about 20% higher than the maximum experimental stress.

Sheridan (1953) tested 21 rectangular plates loaded in tension. All of the plates were 0.507 in. thick and loaded only in the elastic range. The modulus of elasticity was 29,900 ksi and Poisson's ratio was 0.272. Some of the tests were loaded with eccentricity in the plane of the plate to determine the stress distribution with combined axial load and bending moment. Data from strain gages was used to plot the normal stress distribution in the plate. He concluded that, for the specimens with small eccentricity, the experimental stresses "differed greatly" from the stresses calculated using beam theory. The calculated stresses approached the experimental stresses as the eccentricity increased.

Irvan (1957) conducted tests on a model Pratt truss joint with double gusset plates. The plates were 1/8-in.-thick aluminum, with a yield strength of 35 ksi and a modulus of elasticity of 10,000 ksi. Data from strain gages was used to plot the normal and shear stresses in the gusset plate. Irvan came to a conclusion similar to Whitmore's with respect to the calculation of stresses at the critical sections: "The assumption that all of the beam formulas apply in calculating primary stress distribution on any cross-section (either vertical or horizontal) is considerably in error."

Hardin's test specimen (Hardin, 1958) was similar to Irvan's except that the chord was spliced within the joint. The gusset plate was used to carry tensile loads from the spliced chord members in addition to the loads from the truss web members. The plates were 3/16-in.-thick and had the same material properties as Irvan's test. As expected, a large tension stress developed in the gusset plate between the spliced chord members. The conclusions reached by Irvan were confirmed in Hardin's test.

Lavis (1967) used the finite element method to investigate the elastic stress distribution in gusset plates. He compared the finite element results to Whitmore's test and the results of a photoelastic model. His results compared well with Whitmore's. He noted that the use of beam theory "appears to be conservative."

Vasarhelyi (1971) published the results of experiments on a gusset plate model. The tests were conducted on 1/4-in.-thick gusset plates of A36 steel. The specimen was a Warren truss joint with double gusset plates. Data from strain gages was used to plot the stress distribution in the gusset plates. He also conducted photoelastic tests and analytical studies of the stress distribution. Vasarhelyi concluded that the maximum experimental stresses were "only slightly different" than the maximum stresses calculated using beam theory. He also wrote, "The present elementary analysis appears to be adequate for most cases."

Struik (1972) analyzed gusset plates using an elastic-plastic finite element program. The results of his studies indicated that current design procedures, which use beam theory, produced "substantial variations in the factor of safety." He wrote, "The finite element analysis differs significantly from beam theory. However, the difference is not necessarily an unsafe one. None of the stresses exceeded the maximum values predicted by beam theory by a significant amount."

Yamamoto et al. (1985) investigated the stress distribution of eight Warren and Pratt type truss joints with double gusset plates. Test specimens were made of 0.31-in.-thick plates. The researchers plotted the stress distribution using data from strain gages mounted on the gusset plates. The experimental results indicated that the maximum elastic shear stress in the plates could be closely approximated using beam theory.

FORCE DISTRIBUTION IN HORIZONTAL BRACE CONNECTIONS

The lower bound theorem of limit analysis states that a load calculated based on an assumed force distribution that satisfies equilibrium conditions with forces nowhere exceeding the capacity will be less than or equal to the true limit load. For a given connection, the strength calculated using the force path that gives the highest capacity is closest to the actual capacity. The designer can choose any force path that is convenient, if the following conditions are satisfied:

1. Equilibrium must be satisfied.
2. All components in the force path must be designed for the assumed force distribution.
3. All components in the joint must have adequate ductility to allow the stresses to redistribute so the assumed force distribution can be achieved.

A significant amount of judgement must be used to determine if the third condition is satisfied. In many cases a qualitative measure of the relative stiffness of the components in a joint gives a better indication of the force distribution. In addition to the technical aspects of the design, a reasonable force distribution must be assumed so the connection will be economical to fabricate and erect.

Figure 8a shows a plan view of a horizontal brace connection to two beams. The designer must assign a force path to distribute the axial load in the brace to the gusset plate-to-beam interfaces. The force path shown in Figure 8a is incorrect because the interface connections are much stiffer in the direction parallel to the beams than perpendicular to the beams. Even if deflection compatibility were not an issue, there are some practical problems with this force distribution. The connection angles on the gusset

plate will be designed for the component of the force perpendicular to the beam, which will require thicker angles due to the flexural stresses developed from the prying effect on the bolts. The beam webs will be subjected to the same force and will likely require stiffeners in the beam webs due to local out-of-plane bending stresses. Using this force distribution, the beams would be required to carry a weak-axis moment and weak-axis shear to satisfy equilibrium. Also, the beam-to-beam connection would need to be designed for an axial load of $F_E/2$ and a transverse force of $F_N/2$ to ensure a continuous load path. The correct force distribution is shown in Figure 8b.

CURRENT DESIGN PROCEDURES FOR WRAP-AROUND GUSSET PLATES

Effective Width

Wrap-around gusset plates in tension are designed the same as standard gusset plates for the effective width limit state. The method proposed by Thornton (1984) is probably not valid for wrap-around gusset plates in compression because the most highly stressed area has been cut out and it is unclear what effective buckling length should be used.

Bending of Gusset Plate Legs

Each leg of the gusset plate must be designed to resist flexural stresses. The force system in Figure 8b results in bending moments in each leg, as shown in Figure 9. Using a linear moment diagram, the bending moments at the critical sections of the plate are:

$$M_{1cr} = P_1 e_2 \quad (3a)$$

$$M_{2cr} = P_2 e_1 \quad (3b)$$

where P_1 and P_2 are the components of the factored brace load, P . e_1 and e_2 are the cutout dimensions at each leg, as shown in Figure 9. For design purposes, the elastic distribution is used to determine the bending stress in each leg. The elastic bending stresses are shown in Figure 10. The nominal moment capacity of each leg is:

$$M_{n1} = F_y \frac{td_1^2}{6} \quad (4a)$$

$$M_{n2} = F_y \frac{td_2^2}{6} \quad (4b)$$

where t is the gusset plate thickness, and F_y is the yield strength. d_1 and d_2 are the leg widths, as shown in Figure 9. For the design to be adequate, the following must be satisfied:

$$\phi M_{n1} \geq M_{1cr} \quad (5a)$$

$$\phi M_{n2} \geq M_{2cr} \quad (5b)$$

Shear at Gusset Plate Legs

Each leg of the gusset plate must be designed to resist shear. For design purposes, the plastic shear stress distribution is used. Using the plastic distribution, the nominal shear capacity of each leg is:

$$V_{n1} = 0.6F_y d_1 t \quad (6a)$$

$$V_{n2} = 0.6F_y d_2 t \quad (6b)$$

For the design to be adequate, the following must be satisfied:

$$\phi V_{n1} \geq P_1 \quad (7a)$$

$$\phi V_{n2} \geq P_2 \quad (7b)$$

OTHER CONSIDERATIONS

Stress Distribution

It is well-known that simple beam equations are not accurate when the length-to-depth ratio is small (Young, 1989); however, they are still used in design due to their simplicity and the lack of a better alternative. The use of the elastic bending stress appears to be conservative, based on the test results of Rust (1938), Perna (1941), Sandel (1950), Whitmore (1952), Vasarhelyi (1971), and the finite element results of Lavis (1967). Use of the plastic shear distribution appears to be valid, based on the test results of Sandel (1950).

Using an elastic finite element model, flexural stresses were plotted along the depth of a rectangular simply supported beam with a point load at the midspan. The results are shown in Figure 11a for a beam with a length-to-depth ratio of 2.0 and Figure 11b for a length-to-depth ratio of 1.0. The dashed lines show the bending stresses calculated using beam theory. The maximum stress from the finite element model exceeds the calculated stress by almost 50 percent for the beam, with a length-to-depth ratio of 2.0. For the beam with a length-to-depth ratio of 1.0, the finite element stress is almost double the calculated stress.

Bilinear Moment Diagram

The geometry of most wrap-around gusset plates dictates the linear moment diagrams in each leg, as shown in Figure 9. For unusual geometry, a bilinear moment diagram on one of the legs may be present, as shown in Figure 12. In this case, Equation 3a will give a conservative estimate of the moment in Leg 1.

Residual Stresses

Residual stresses have an influence on the stress distribution in wrap-around gusset plates. The equipment in most structural steel fabrication shops and the geometry of wrap-around gusset plates dictates that they are flame-cut. The residual stress pattern for plates with flame-cut edges is shown in Figure 13. According to Bjorhovde et al. (2001), the tensile residual stress at the plate edges is “generally around 60 to 70 ksi, regardless of the original material properties.”

Rao and Tall (1961), and Dwight and Ractliffe (1967) measured the residual stresses in edge-welded plates. Rao and Tall (1961) noted that plates with gas-cut edges have residual stress patterns very similar to edge-welded plates. Dwight and Ractliffe (1967) showed that the width of the tension portion of the residual stress pattern, x is “largely independent” of the plate width. Bjorhovde et al. (1972) measured the residual stresses in thick plates with flame-cut edges. Table 1 summarizes the residual stress measurements for these three projects. As shown in Figure 13, σ_r is the tension residual stress at the plate edge. σ_y is the yield strength of plate. The average x is 1.21 inches. Using the 29 results of Rao and Tall (1961) and Bjorhovde et al. (1972), the average σ_r/σ_y is 1.40. All but one of the specimens had residual stresses exceeding the yield strength of the plate.

Table 1. Experimental Residual Stress Patterns in Flame-cut Plates

Specimen	Width (in.)	Thickness (in.)	σ_x/σ_y	x (in.)
Dwight and Ractliffe (1967)				
1	11.0	0.25	NA	1.62
2	13.5	0.25	NA	1.58
3	16.5	0.25	NA	1.88
4	20.25	0.25	NA	1.60
Rao and Tall (1961)				
T-7	6	0.5	1.12	0.95
T-8	8	0.25	1.33	1.00
T-8	8	0.25	1.39	0.80
T-8	8	0.25	1.36	0.90
T-8	8	0.25	1.42	0.90
T-3	8	0.5	1.70	1.10
T-3	8	0.5	1.66	1.30
T-3	8	0.5	1.82	1.30
T-2	10	0.5	1.97	1.05
T-2	10	0.5	1.97	1.10
T-2	10	0.5	1.94	1.00
T-5	12	0.75	1.45	1.45
T-18	12	1.0	1.09	1.09
T-13	16	0.5	1.21	1.15
T-10	16	1.0	1.15	1.01
T-16	18	0.75	1.36	1.75
T-14	20	0.5	1.21	1.40
T-6	20	1.0	1.18	1.36
T-6	20	1.0	1.33	1.20
T-6	20	1.0	1.27	1.16
T-6	20	1.0	1.15	1.00
Bjorhovde et al. (1972)				
1	9	1.5	1.33	1.08
2	12	2.0	1.75	0.84
3	12	3.5	1.43	1.20
4	16	1.5	1.40	1.05
5	20	1.5	0.85	0.80
6	20	2.0	1.38	1.40
7	24	2.0	1.22	1.20
8	24	6.0	1.29	1.68

Biaxial Stress

The interior corner of a wrap-around gusset plate where the two legs meet is subjected to flexural stress from each leg, as shown in Figure 14. Several theories have been proposed to predict the behavior of materials under multiaxial states of stress. Von Mises' criterion is the most common for predicting the initiation of yield in ductile metals when loaded by various combinations of normal and shear stresses. For plane stress, von Mises' equation reduces to:

$$\sigma_e = \sqrt{\sigma_x^2 + \sigma_y^2 - \sigma_x \sigma_y + 3\tau^2} \quad (8)$$

where σ_e is the effective stress, σ_x is the applied normal stress in the x-direction, σ_y is the applied normal stress in the y-direction, and τ is the applied shear stress as shown in Figure 15. The material is assumed to yield if σ_e exceeds the yield strength of the plate. At the interior corner of a wrap-around gusset plate, σ_x and σ_y will always be of the same sense. Using Equation 8, it can be shown that this condition always produces an effective stress less than the largest normal stress if the shear stress is excluded from the calculation. Because shear stresses are relatively small for wrap-around gusset plates typically encountered in practice, it can be concluded that yielding due to biaxial stress is not likely to be a controlling factor in the design of wrap-around gusset plates.

Although wrap-around gusset plates are not likely to yield at the interior corner, there are some potential problems created by the stress condition there. When the brace member is in tension, the biaxial stresses will be compressive, which could make the plate more susceptible to buckling. When the brace member is in compression, the biaxial stresses will be tensile, which will decrease the plate's ductility at the corner.

Plastic Moment Capacity

von Mises criterion is a good predictor of first yield, but is not necessarily a good predictor of the strength of a member. Due to the questionable applicability of the beam equations to the geometry of wrap-around gusset plates and the residual stresses due to flame cutting, a better approach may be to determine the gusset strength based on the plastic capacity of each leg. The plastic capacity of a rectangular cross section subjected to moment and shear can be predicted with (ASCE-WRC, 1971):

$$\frac{M_u}{M_p} + \left(\frac{V_u}{V_p} \right)^4 \leq 1.0 \quad (9)$$

where M_u is the applied moment, M_p is the plastic moment capacity, V_u is the applied shear, and V_p is the plastic shear capacity. The plastic bending stress distribution is shown in Figure 16. At this time, it is not known if the gusset plate legs can reach their full plastic capacity without buckling.

Lateral-Torsional Buckling

Due to the flexural stresses within the gusset plate, the legs are subject to lateral-torsional buckling. It is interesting to note that the gusset legs can buckle when the brace is in tension. Dowswell and Fouad (2005) have verified this behavior with tests and finite element models. The legs can be modeled as cantilever beams to determine the critical load, but it is doubtful that buckling equations derived for beams will be accurate for gusset plates. Most of the published literature on rectangular cantilever beams is based on elastic analysis without consideration of residual stresses or geometric

imperfections. The problem is further complicated by stress concentrations and unknown boundary conditions with respect to rotation and translation at the root of the cantilever.

Geometric Imperfections

It is well-known that geometric imperfections have a detrimental effect on the capacity of beams and columns. Walbridge et al. (1998) studied the effect of initial imperfections on the stability of standard gusset plates. The study revealed that the magnitude of the imperfections had a significant effect on the capacity, but the shape of the imperfections was much less critical. With an imperfection magnitude of 0.0787 in. (2 mm), the finite element models behaved similar to the test results of Rabinovitch and Cheng (1993).

ASTM A6 (2004) specifies a permissible camber of 0.025-in. per foot and a permissible variation from flat of 0.25 in. for carbon steel plates less than 36 in. long. The ASTM Standard specifies manufacturing tolerances and does not address the tolerances for plates after fabrication is complete. Some deformations can be expected from the shop operations. Fouad et al. (2003) surveyed state departments of transportation, manufacturers, and engineers to determine the current state of practice regarding flatness tolerances for connection plates and base plates. They recommended using the flatness requirements of ASTM A6 after fabrication is complete. Measurements of wrap-around gusset plate specimens by Dowswell and Fouad (2005) determined the maximum out-of-plane imperfection to be 0.028-inches, which was within the ASTM A6 tolerances.

CONCLUSIONS

Some potential failure modes and important design considerations associated with wrap-around gusset plates have been presented. Previous research and current design procedures for standard gusset plates were reviewed, but no treatment of wrap-around gusset plates was found. Common design practice for wrap-around gusset plates was presented and discussed. It was shown that the existing literature and design procedures do not address all of the potential failure modes. Experimental and analytical research projects are being conducted by the authors with the goal of understanding the behavior of these gusset plates.

REFERENCES

- AISC (2001), "Manual of Steel Construction, Load and Resistance Factor Design," 3rd ed., American Institute of Steel Construction, Inc., Chicago, Illinois.
- AISC (1999), Load and Resistance Factor Design Specification for Structural Steel Buildings, American Institute of Steel Construction, Inc., Chicago, Illinois.
- ASCE-WRC (1971), "Plastic Design in Steel, A Guide and Commentary," 2nd ed., American Society of Civil Engineers, New York, pp. 130.
- Astaneh, A. (1992), "Cyclic Behavior of Gusset Plate Connections in V-Braced Steel Frames," *Stability and Ductility of Steel Structures Under Cyclic Loading*, Fukumoto, Y. and Lee, G. C., eds., CRC Press, Ann Arbor, pp. 63-84.
- ASTM A6 (2004), "Standard Specification for General Requirements for Rolled Structural Steel Bars, Plates, Shapes, and Sheet Piling," ASTM International, West Conshohocken, PA.
- Bjorhovde, R., Engstrom, M. F., Griffis, L. G., Kloiber, L. A., and Malley, J. O. (2001), "Structural Steel Selection Considerations-A Guide for Students, Educators, Designers, and Builders," American Society of Civil Engineers, Reston, VA.
- Bjorhovde, R. and Chakrabarti, S. K. (1985), "Tests of Full-size Gusset Plate Connections," *Journal of Structural Engineering*, ASCE, Vol. 111, No. 3, March, pp. 667-683.

Bjorhovde, R., Brozzetti, J., Alpsten, G. A., and Tall, L. (1972), "Residual Stresses in Thick Welded Plates," *Welding Research Supplement*, August, pp. 392-s through 405-s.

Brown, V. L. (1988), "Stability of Gusseted Connections in Steel Structures," Doctoral Dissertation, University of Delaware.

Chakrabarti, S. K. and Richard, R. M. (1990), "Inelastic Buckling of Gusset Plates," *Structural Engineering Review*, Vol. 2, pp. 13-29.

Cheng, J. J. R., and Grondin, G. Y. (1999), "Recent Development in the Behavior of Cyclically Loaded Gusset Plate Connections," *Proceedings, North America Steel Construction Conference*. American Institute of Steel Construction, Chicago, pp. 8-1 through 8-22.

Cheng, J. J. R. and Hu, S. Z. (1987), "Comprehensive Tests of Gusset Plate Connections," *Proceedings, 1987 Annual Technical Session*, Structural Stability Research Council, pp. 191-205.

Dowswell, B. and Fouad, F. (2005), "Wrap-Around Gusset Plates in Tension," Page 33 of this document.

Dowswell, B. (2004), "Lateral-Torsional Buckling of Wide Flange Cantilever Beams," *AISC Engineering Journal*, Third Quarter, pp. 135-147.

Dowswell, B. and Barber, S. (2004), "Buckling of Gusset Plates: A Comparison of Design Equations to Test Data," *Proceedings, 2004 Annual Stability Conference*, Structural Stability Research Council, pp. 199-221.

Dwight, J. B. and Ractliffe, A. T. (1967), "The Strength of Thin Plates in Compression," *Thin Walled Steel Structures: Their Design and Use in Building*, Crosby Lockwood & Son, Ltd., London, pp. 3-34.

Fouad, F. H., Davidson, J. S., Delatte, N., Calvert, E. A., Chen, S., Nunez, E., and Abdalla, R. (2003), "Structural Supports for Highway Signs, Luminaries, and Traffic Signals," NCHRP Report 494, Transportation Research Board, Washington, D. C.

Gross, J. L. and Cheok, G. (1988), "Experimental Study of Gusseted Connections for Laterally Braced Steel Buildings," National Institute of Standards and Technology, Gaithersburg, Maryland, November.

Hardin, B. O. (1958), "Experimental Investigation of the Primary Stress Distribution in the Gusset Plates of a Double Plane Pratt Truss Joint with Chord Splice at the Joint," University of Kentucky Engineering Experiment Station Bulletin No. 49, September.

Irvan, W. G. (1957), "Experimental Study of Primary Stresses in Gusset Plates of a Double Plane Pratt Truss," University of Kentucky Engineering Research Station Bulletin No. 46, December.

Lavis, C. S. (1967), "Computer Analysis of the Stresses in a Gusset Plate," Master's Thesis, University of Washington.

Nast, T. E., Grondin, G. Y., and Cheng, J. J. R. (1999), "Cyclic Behavior of Stiffened Gusset Plate Brace Member Assemblies," University of Alberta Department of Civil and Environmental Engineering Structural Engineering Report No. 229, December.

Perna, F. J. (1941), "Photoelastic Stress Analysis, with Special Reference to Stresses in Gusset Plates," Master's Thesis, University of Tennessee, August.

Rabinovitch, Jeffrey and Cheng, J. J. R. (1993), "Cyclic Behavior of Steel Gusset Plate Connections," University of Alberta Department of Civil Engineering Structural Engineering Report No. 191, August.

Rabern, D. A. (1983), "Stress, Strain and Force Distributions in Gusset Plate Connections," Master's Thesis, University of Arizona.

Rao, N. and Tall, L. (1961), "Residual Stresses in Welded Plates," *Welding Research Supplement*, October, pp. 468-s through 480-s.

Rust, T. H. (1938), "Specification and Design of Steel Gusset-Plates," *Proceedings, American Society of Civil Engineers*, November, pp. 142-167.

Sandel, J. A. (1950), "Photoelastic Analysis of Gusset Plates," Master's Thesis, University of Tennessee, December.

Sheng, N., Yam, C. H., and Iu, V. P. (2002), "Analytical Investigation and the Design of the Compressive Strength of Steel Gusset Plate Connections," *Journal of Constructional Steel Research*, Vol. 58, pp. 1473-1493.

Sheridan, M. L. (1953), *An Experimental Study of the Stress and Strain Distribution in Steel Gusset Plates*, Doctoral Dissertation, University of Michigan.

Struik, J. H. A. (1972), *Applications of Finite Element Analysis to Non-linear Plane Stress Problems*. Doctoral Dissertation, Lehigh University.

Thornton, W. A. (1984), "Bracing Connections for Heavy Construction," *Engineering Journal*, American Institute of Steel Construction, Third Quarter, pp. 139-148.

Vasarhelyi, D. D. (1971), "Tests of Gusset Plate Models," *Journal of the Structural Division, Proceedings of the American Society of Civil Engineers*, Vol. 97, No. ST2, February, pp. 665-679.

Walbridge, S. S., Grondin, G. Y., and Cheng, J. J. R. (1998), "An Analysis of the Cyclic Behavior of Steel Gusset Plate Connections," University of Alberta Department of Civil and Environmental Engineering Structural Engineering Report No. 225, September.

Whitmore, R. E. (1952), "Experimental Investigation of Stresses in Gusset Plates," University of Tennessee Engineering Experiment Station Bulletin No. 16, May.

Wyss, T. (1926), "Die Kraftfelder in Festen Elastischen Korpern und ihre Praktischen Anwendungen," Berlin.

Yam, M. C. H. and Cheng, J. J. R. (1993), "Experimental Investigation of the Compressive Behavior of Gusset Plate Connections," University of Alberta Department of Civil Engineering Structural Engineering Report No. 194, September.

Yamamoto, K., Akiyama, N., and Okumara, T. (1985), "Elastic Analysis of Gusseted Truss Joints," *Journal of Structural Engineering*, ASCE, Vol. 111, No. 12, December, pp. 2545-2564.

Young, W. C. (1989), *Roark's Formulas for Stress and Strain*, 6th ed., McGraw-Hill, New York.

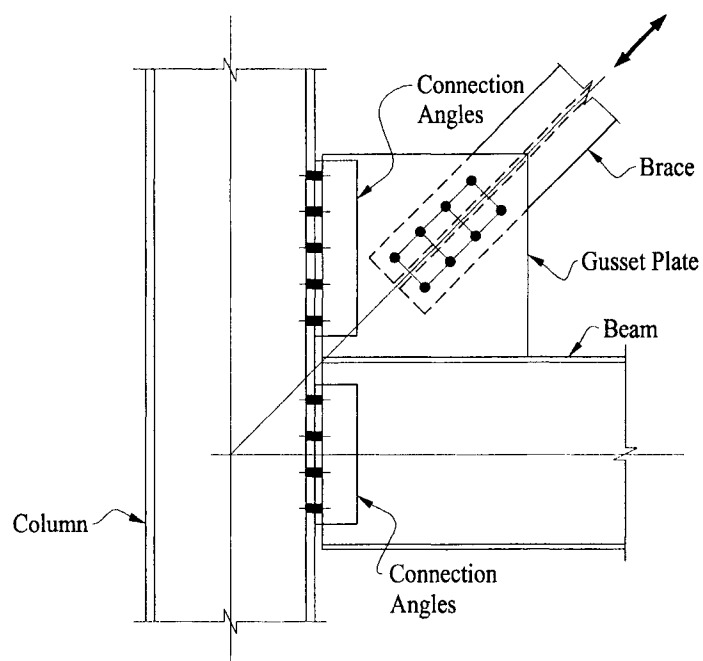


Fig. 1. Standard vertical brace connection.

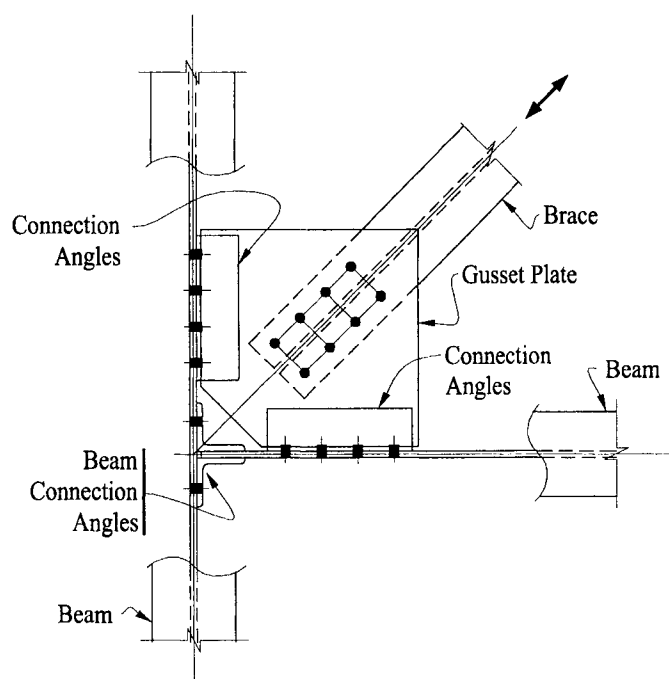


Fig. 2. Horizontal brace connection at beam-to-beam intersection.

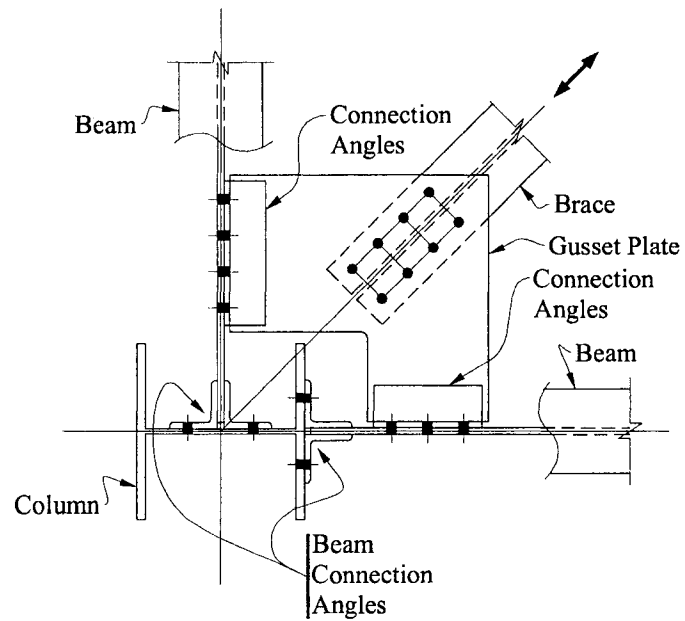


Fig. 3. Wrap-around gusset plate connection.

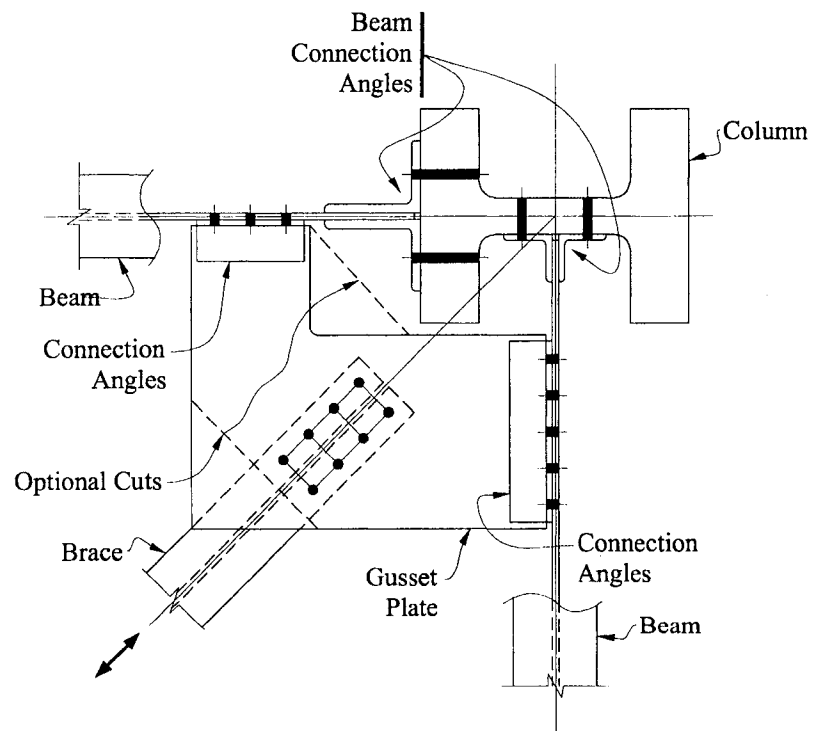


Fig. 4. Wrap-around gusset plate connection at a large column.

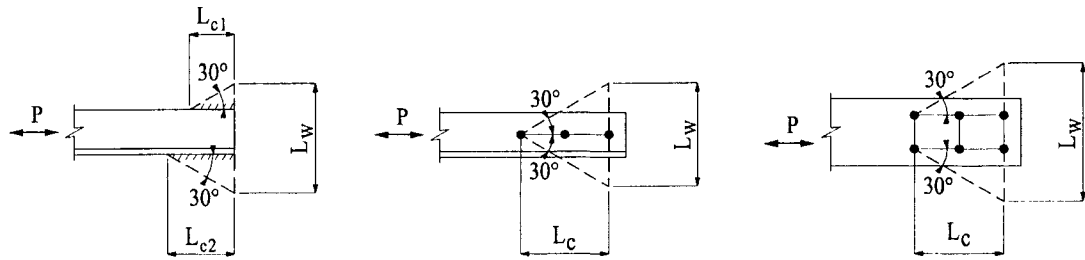


Fig. 5. Effective width for various connection configurations.

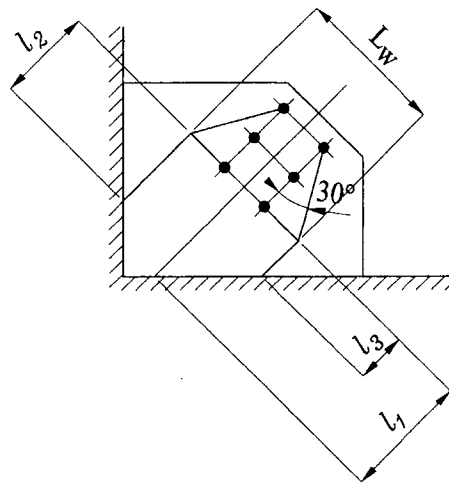


Fig. 6. Geometry of effective column.

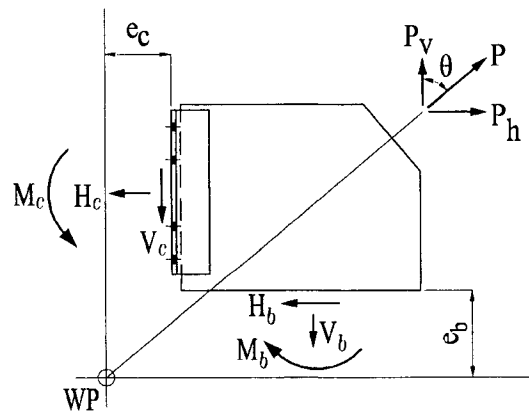


Fig. 7. Interface loads for a standard gusset plate.

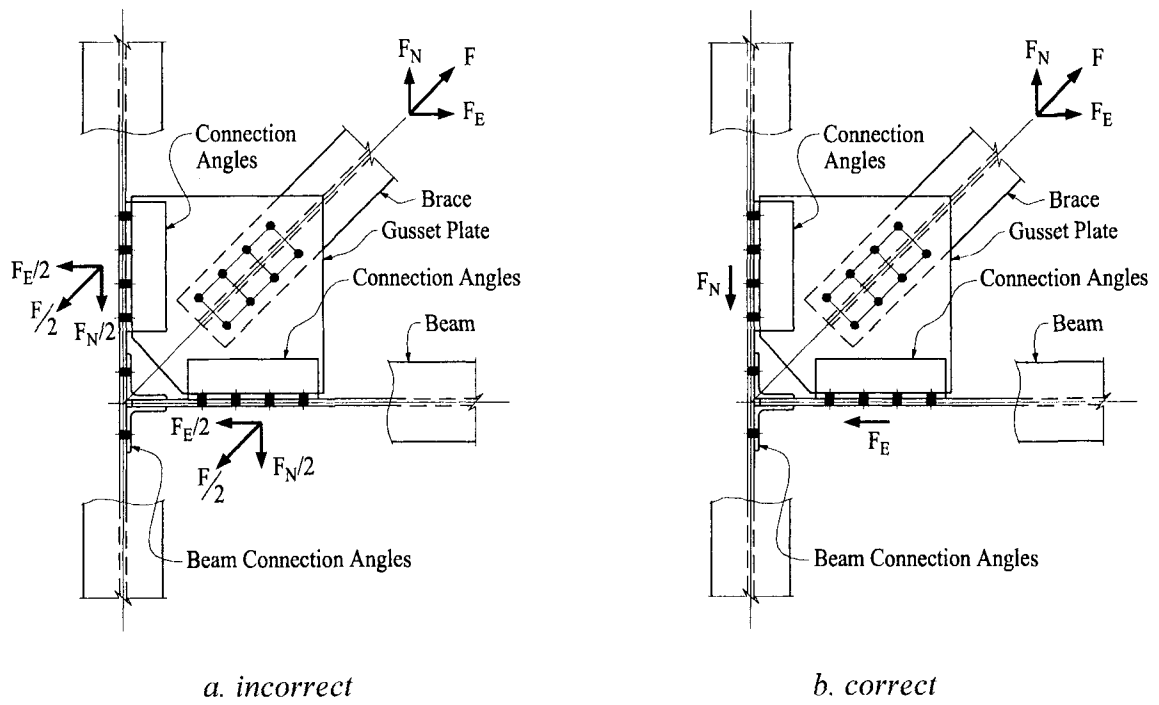


Fig. 8. Various force distributions for horizontal brace connections.

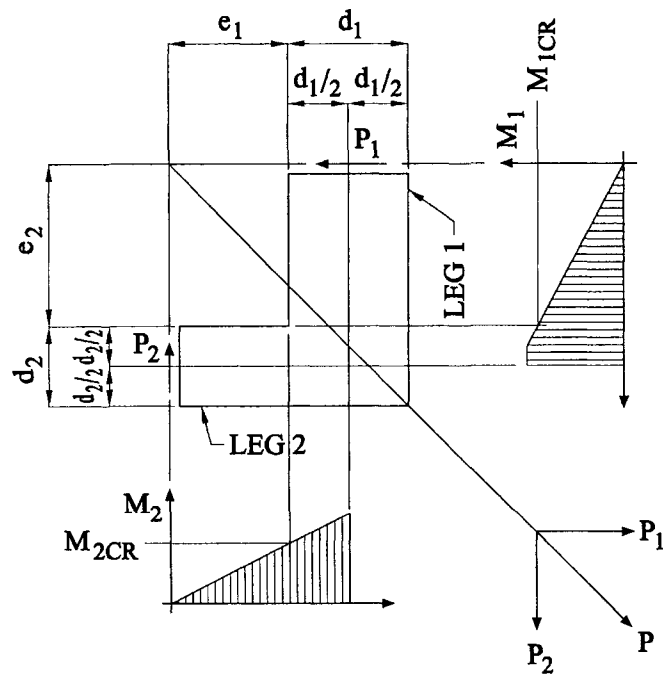


Fig. 9. Force system for wrap-around gusset plates.

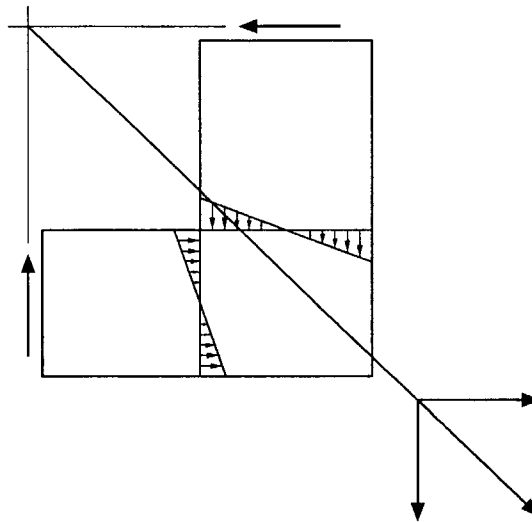
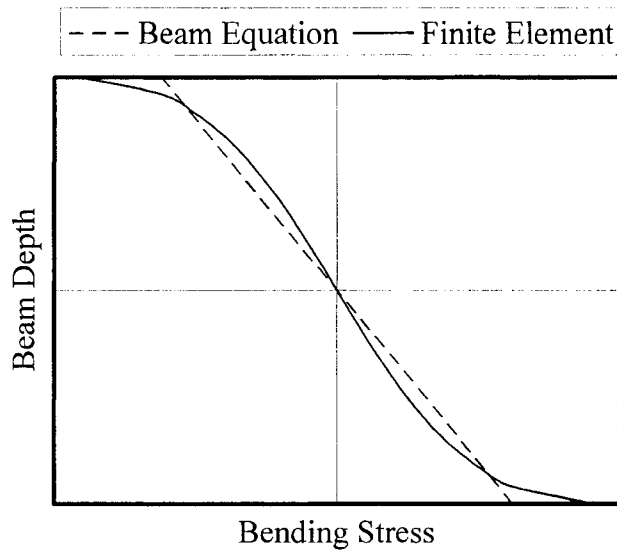
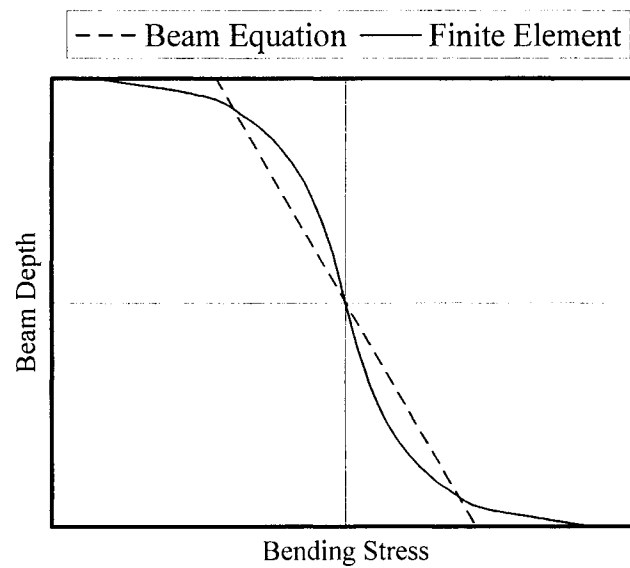


Fig. 10. Elastic bending stresses in gusset plate legs.



a. length-to-depth ratio of 2.0



b. length-to-depth ratio of 1.0

Fig. 11. Flexural stresses for rectangular beams.

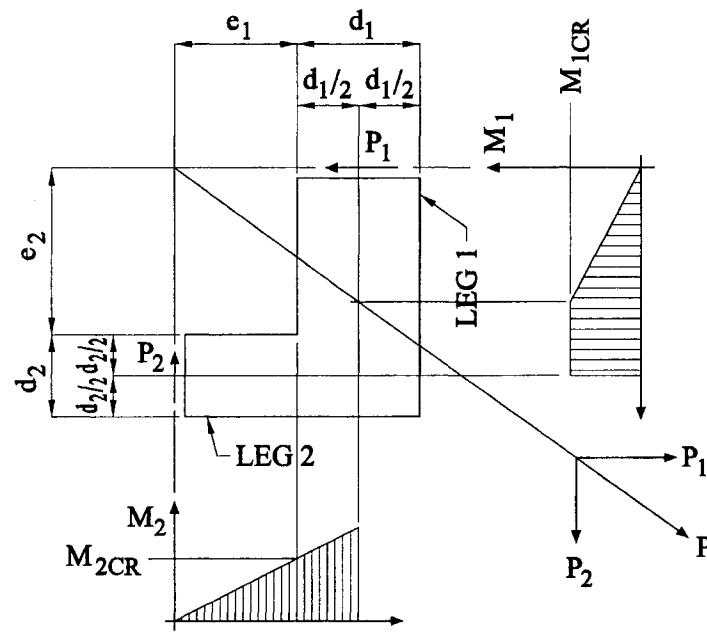


Fig. 12. Force system with bilinear moment diagram at Leg 1.

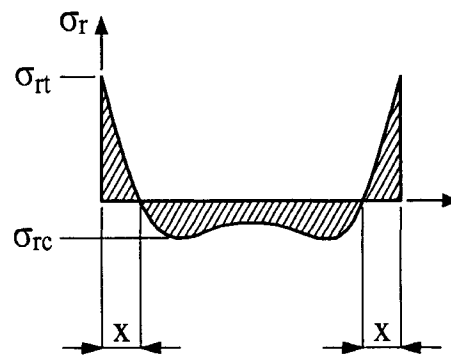


Fig. 13. Residual stress pattern in a flame-cut plate.

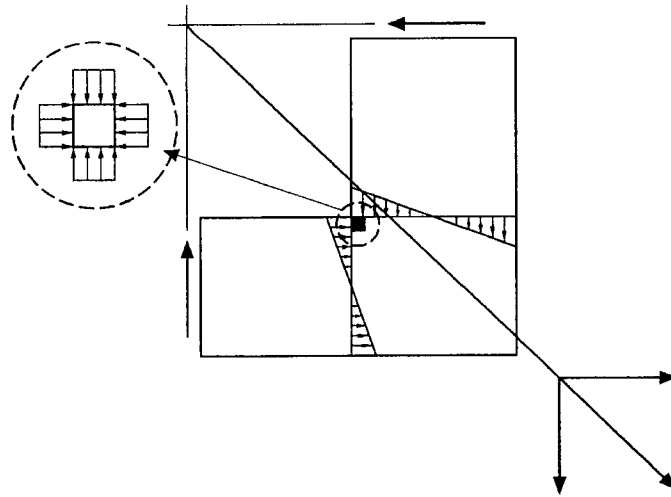


Fig. 14. Biaxial stress at the interior corner.

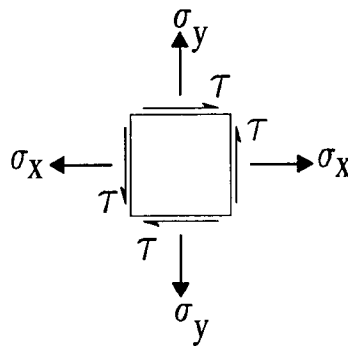


Fig. 15. Plane stress element.

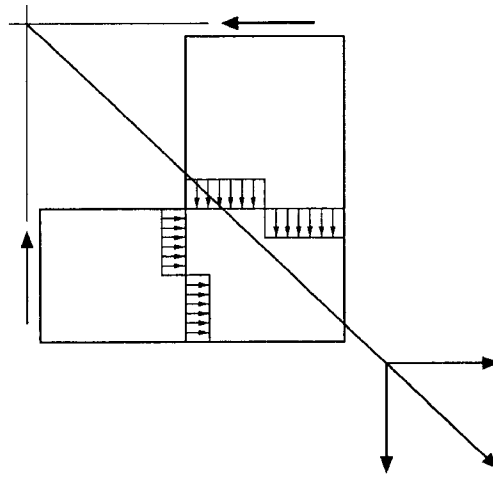


Fig. 16. Plastic bending stresses in each leg.

WRAP-AROUND GUSSET PLATES IN TENSION

by

BO DOWSWELL AND FOUAD FOUAD

Submitted to American Institute of Steel Construction Engineering Journal

Format adapted for dissertation

INTRODUCTION

Gusset plates are used in steel buildings to connect bracing members to other structural members in the lateral force resisting system. Horizontal bracing is commonly used to resist lateral loads in industrial structures and in commercial buildings where floor and roof diaphragms cannot carry the loads. Figure 1 shows a typical horizontal bracing connection at a beam-to-beam intersection. Where a horizontal brace is located at a beam-to-column intersection, the gusset plate must be cut out around the column, as shown in Figure 2. These are known as wrap-around gusset plates.

Problem Statement

Due to the increasing complexity of building designs, horizontal bracing members are being used to resist very large forces. A large number of research projects have been dedicated to the analysis and design of standard gusset plates; however, there are no published methods for designing wrap-around gusset plates. Dowswell and Fouad (2005a) presented a review of the factors affecting the design of wrap-around gusset plates, including modes of failure that are unique to such gusset plates. These issues need to be addressed so engineers can provide safe and economical designs.

Objectives

The purpose of this research was to gain a better understanding of the behavior of wrap-around gusset plates in tension.

EXISTING LITERATURE

A large number of research projects have been dedicated to the analysis and design of standard gusset plates. Failure modes for standard gusset plates have been identified, and design procedures are well-documented in the literature. However, failure modes unique to wrap-around gusset plates have not been studied, nor are guidelines for their design available in the literature. Dowswell and Fouad (2005a) summarized the existing research on the stress distribution in standard gusset plates. Dowswell and Barber (2004) summarized previous experiments and finite element studies on gusset plates in compression. Dowswell and Fouad (2005b) reviewed the existing experimental research on statically loaded gusset plates.

EXPERIMENTAL PROGRAM

Five wrap-around gusset plates were tested monotonically in tension. The specimens were loaded until the load versus deflection curve started to level off due to the decreasing stiffness of the specimen. The load versus deflection data was recorded and plotted. The specimens had strain gages installed in the areas of the highest stresses. The strain gage data was recorded and plotted versus the load. The specimens were loaded slowly, so the behavior could be observed during the tests.

Specimens

The specimens were fabricated by a shop experienced in steel structures and certified by AISC for complex steel buildings. They were flame-cut to shape and had a reentrant corner radius of 1 in. Five different gusset plates were fabricated of A36

material, with dimensions shown in Figure 3. By fabricating the specimens with short slots in each leg and using finger-tight bolts, the in-plane moment restraint was released.

To determine the actual mechanical properties of the material, tension coupons were taken from the same parent plate as the specimens. The coupons were tested in accordance with ASTM A370 (2003). The 1/4-in. plates had a yield strength of 56.7 ksi, an ultimate strength of 71.2 ksi, and a modulus of elasticity of 30,000 ksi. The 3/8-in. plates had a yield strength of 48.8 ksi, an ultimate strength of 70.6 ksi, and a modulus of elasticity of 29,000 ksi. The thickness of each specimen was measured using a SONAGAGE II ultrasonic thickness meter by SONATEST. The results are shown in Table 1.

Table 1. Measured Plate Thickness

Specimen	Nominal Thickness (in.)	Measured Thickness (in.)
2T	3/8	0.391
6T	1/4	0.235
8T	3/8	0.384
9T	3/8	0.380
10T	3/8	0.387

In order to measure the geometric imperfections in the plates, photographs were taken of each specimen showing the two longest edges. The out-of-flatness was measured graphically in the computer program photo editor relative to the plate thickness. The actual out-of-flatness was then determined by scaling the dimensions based on the actual plate thickness. The typical out-of-flatness resembled a half sine wave. The maximum out-of-flatness for all specimens was 0.028 in.

Instrumentation, Testing Machine, and Test Frame

Electrical strain gages were bonded to each specimen in the areas of the highest stresses. Elastic finite element models were used to locate the most highly stressed regions on the plate. The models showed that the highest stresses were longitudinal flexural stresses at the critical section of each leg. The critical section is at the reentrant corner, perpendicular to the length of each leg. The gages were mounted according to Figure 4. The strain gage data was recorded using a MEGADAK data acquisition system.

A test frame fabricated specifically for testing the gusset plates is shown in Figure 5. Generally, the frame consisted of two parts: a brace member, and a frame simulating the beams shown in Figure 2. The channels marked M2, shown in Figure 5b, acted as the brace member. To provide a knife-edge connection between the brace and the specimen, the channels had 1/4-in. square bars tilted at 45° welded between the bolt holes. The angles marked M3 acted as the beams and were fabricated from 4 x 4 x 1/2 angles welded together at a right angle, as shown in Figure 5c. To provide a pinned boundary condition, the frame was required to pivot about the work point in the plane of the specimen. To accomplish this, a single 1½-in. diameter A490 bolt was used at the corner where the angles were welded together. The bolt was tightened to a finger-tight condition. This also allowed the same frame to be used with all of the specimens without adjusting the angle of the test frame. To provide a knife-edge connection, 1/4-in. square bars were welded to the angles similar to member M2. M1 and M4 were plates that attached the test frame members to the grips of the testing machine.

The loads were applied to the specimens using a 600-kip Tinius Olsen Super-L Universal Testing Machine with a Model CMH 289 Controller and a Model 290 Display. The test configuration with a specimen and the test frame mounted in the testing machine is shown in Figure 6.

RESULTS

Load vs. Deflection

All of the specimens behaved in a ductile manner, and none of the specimens fractured. Load vs. deflection plots for Specimens 2T and 9T are shown in Figure 7. The plots for the remaining specimens were similar in shape. The tests were generally characterized by a load-deflection curve divided into three parts. The first stage was dominated by bolt slippage and slippage of the loading grips. The second stage was the linear range, and the third stage was the nonlinear range. All of the specimens had a permanent in-plane deformation, which can be seen in Figure 8 for Specimen 2T. The tests were stopped when significant nonlinear deformations were observed.

Out-of-Plane Deformations

All of the specimens had a permanent out-of-plane deformation, which was at its maximum at the reentrant corner where the two legs met. Figure 9 shows the out-of-plane deformation for Specimen 2T. The lateral deformation was accompanied by twisting, indicating a lateral-torsional buckling type of failure. The maximum out-of-plane deformation for Specimen 10T occurred at approximately the mid-length of the diagonal cut at the reentrant corner. The maximum permanent deformation was

measured, with the following results: 1.2 in. for Specimen 2T, 1.2 in. for Specimen 6T, 0.6 in. for Specimen 8T, 0.7 in. for Specimen 9T, and 0.4 in. for Specimen 10T.

Strain Measurements

The strain gage data was plotted in terms of stress instead of strain so the yield point could be easily identified. Hooke's law was used to convert the strain gage readings to stresses. The disadvantage of this method is that the stresses displayed beyond the yield point of the material are not accurate and only give a qualitative measure of the strain. The term "apparent stress" is used in this paper to signify that the displayed stresses are not accurate over the full range of data.

The strain gage data for Specimens 9T and 10T are shown in Figure 10. The strain versus load behavior was similar for all of the specimens. From the strain gage data, it was determined that there were generally three stages of behavior. In the first stage, the material behaved elastically. In the second stage, the material still appeared to be approximately linear; however, it is clear from the data that much of the material is above the yield point. This behavior is due to a combination of residual stresses, strain hardening, biaxial stresses at the reentrant corner, and stress redistribution due to yielding. When a substantial portion of the specimen had yielded, stiffness was lost, and the specimen buckled. The third stage is post-buckling. All of the specimens carried more load after buckling occurred.

In the early stages of loading the strain gage readings for all of the specimens were linear. The readings for gages located at each edge of a particular gusset plate leg

were approximately equal in magnitude, but were of opposite sense, indicating that the legs were in almost pure flexure.

Experimental Loads

Because the load versus deflection curves did not have a well-defined yield point, the experimental yield loads, P_{ey} , were determined using a 1/64-in. offset relative to the linear portion of the load versus deflection plots, as shown in Figure 7. The yield load is where the load versus deflection curve crosses the 1/64-in. offset line. The results are shown in Table 2.

Table 2. Test Loads

Spec. No.	Test Loads (k)	
	P_{ey}	P_{eu}
2T	69.0	89.9
6T	42.3	53.6
8T	85.3	91.2
9T	51.5	63.6
10T	96.2	109.8

P_{ey} test yield load determined using a 1/64-in. offset.

P_{eu} maximum test load

CONCLUSIONS

Five wrap-around gusset plates were tested in tension. The results of the tests will help to provide a better understanding of the behavior of these gusset plates. The experiments indicated that wrap-around gusset plates are subject to limit states common to flexural members. In the early stages of loading the strain gage readings were linear.

The readings for gages located at each edge of a particular gusset plate leg were approximately equal in magnitude, but were of opposite sense, indicating that the legs were in almost pure flexure. All of the plates had a permanent out-of-plane deformation due to inelastic buckling in the vicinity of the re-entrant corner. The out-of-plane deformation was accompanied by the twisting of the gusset plate legs, indicating a lateral-torsional buckling failure.

ACKNOWLEDGEMENTS

The test frame and specimens were fabricated and donated to the project by Gipson Steel, Inc. Bell Steel Company supplied the bolts. The technical assistance of Elton Hogan and Mark Gipson of Gipson Steel, George Reed and Kane Combs of Structural Steel Services, and Curtis Smith of Bell Steel is greatly appreciated. The testing was performed in the structures laboratory at the Department of Civil and Environmental Engineering at The University of Alabama at Birmingham.

REFERENCES

- ASTM A370-03a (2003), "Standard Test Method and Definitions for Mechanical Testing of Steel Products," ASTM International, West Conshohocken, PA.
- Dowswell, B. and Barber, S. (2004), "Buckling of Gusset Plates: A Comparison of Design Equations to Test Data," *Proceedings, 2004 Annual Stability Conference*, Structural Stability Research Council, pp. 199-221.
- Dowswell, B. and Fouad, F. H. (2005a), "Design Considerations for Wrap-Around Gusset Plates," Page 3 of this document.
- Dowswell, B. and Fouad, F. H. (2005b), "Wrap-Around Gusset Plates in Compression," Page 50 of this document.

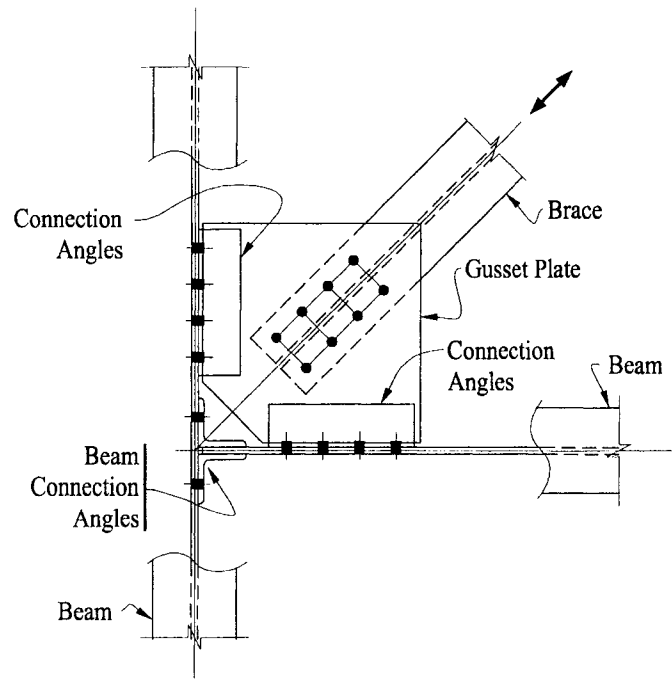


Fig. 1. Horizontal brace connection at beam-to-beam intersection.

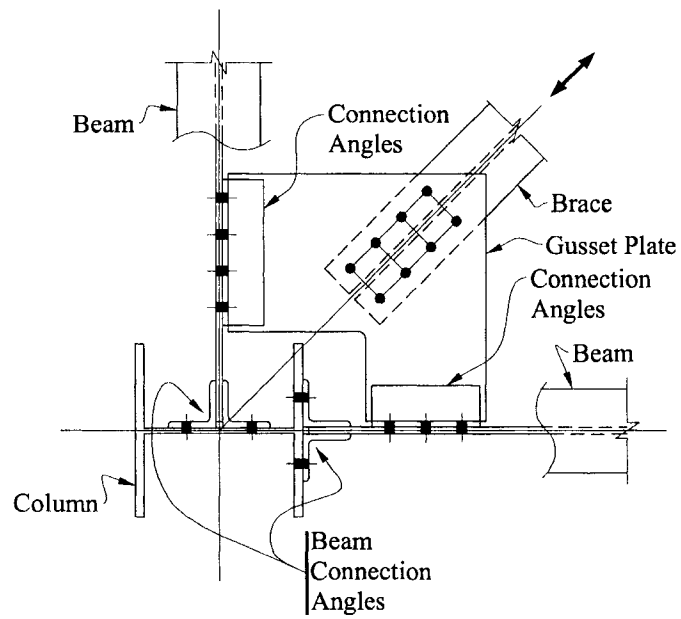
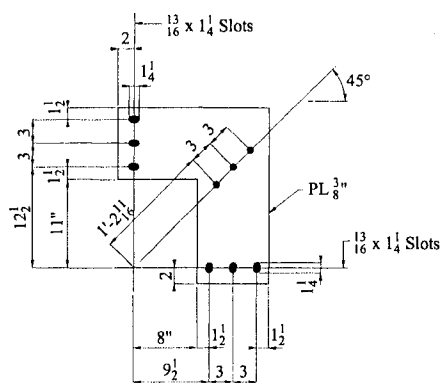
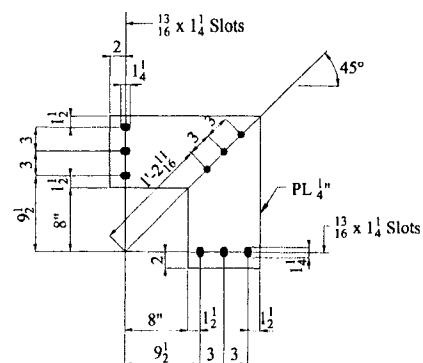


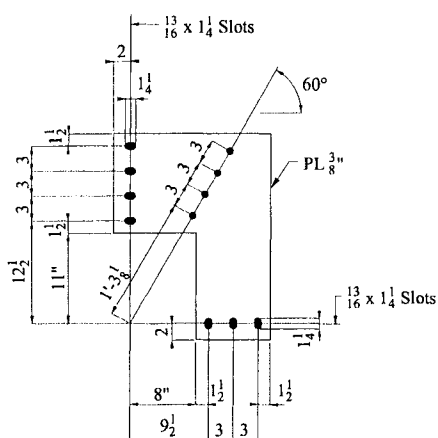
Fig. 2. Horizontal brace connection at beam-to-column intersection.



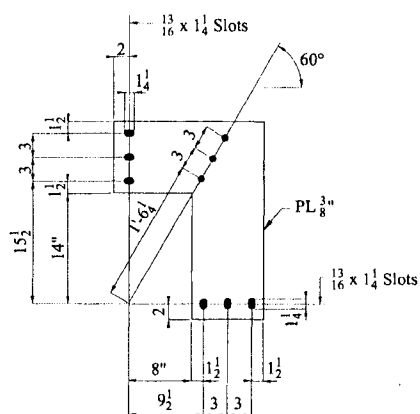
Specimen 2T



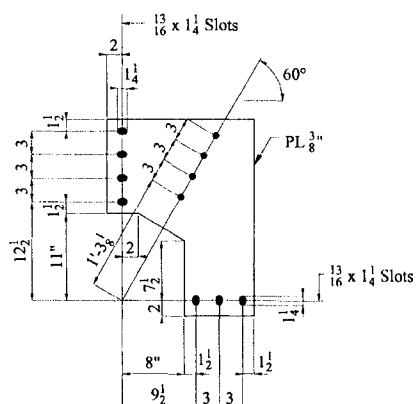
Specimen 6T



Specimen 8T

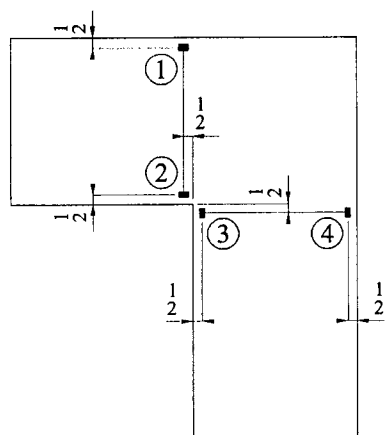


Specimen 9T

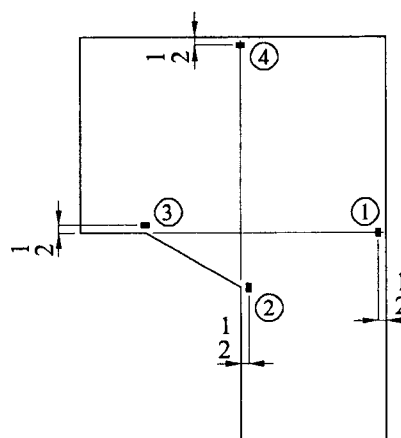


Specimen 10T

Fig. 3. Fabrication drawings.



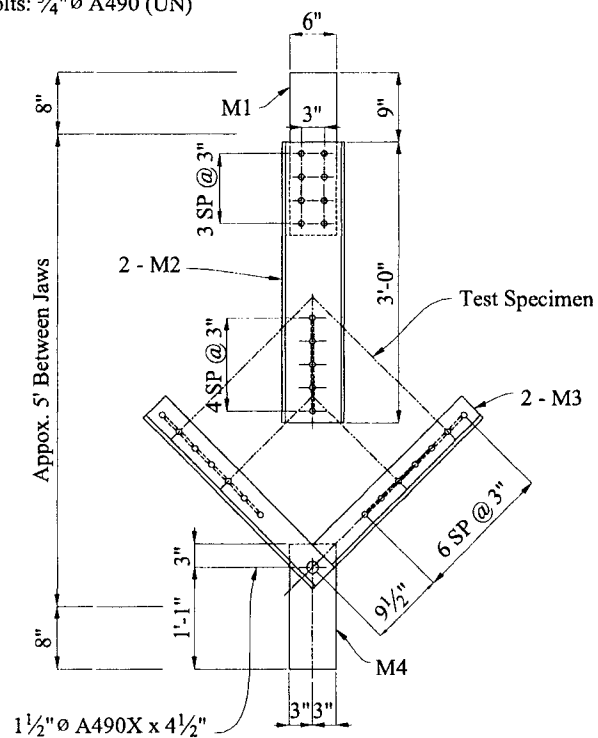
Specimens 2T, 6T, 8T, and 9T



Specimen 10T

Fig. 4. Strain gage locations.

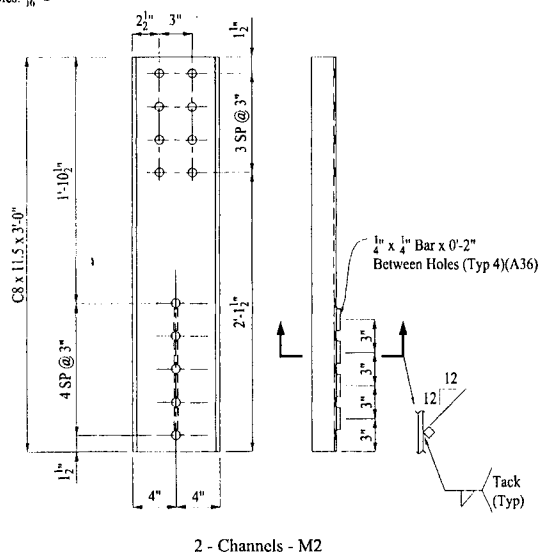
Bolts: $\frac{3}{4}$ " \emptyset A490 (UN)



a. Assembled test frame

Mat'l: A992 or A572 GR. 50 (UN)

Holes: $\frac{13}{16} \text{ } \phi$

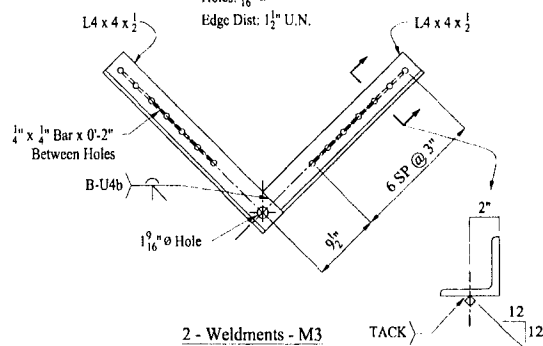


b. Fabrication drawing for M2

Mat'l: A992 or A572 Gr. 50

Holes: $\frac{13}{16}$ " \varnothing

Edge Dist: $1\frac{1}{2}$ " U.N.



c. Fabrication drawing for M3

Fig. 5. Test frame drawings.

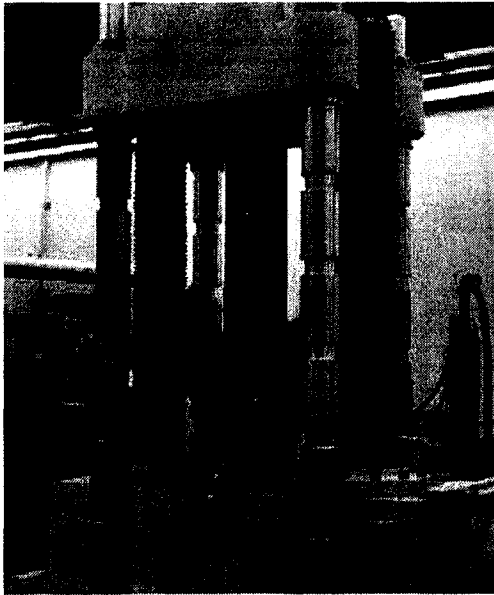
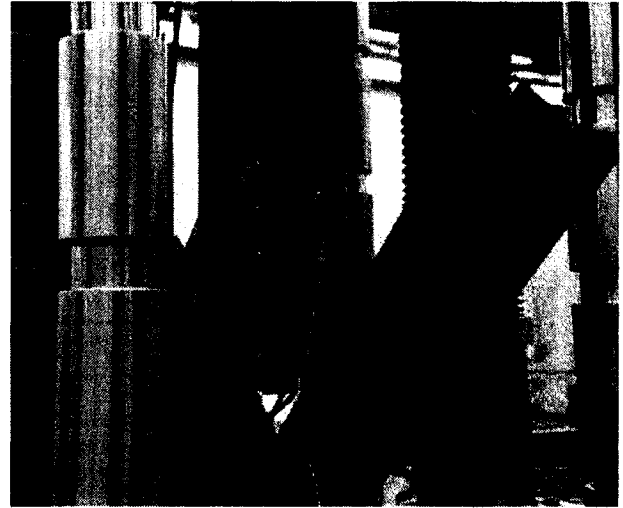
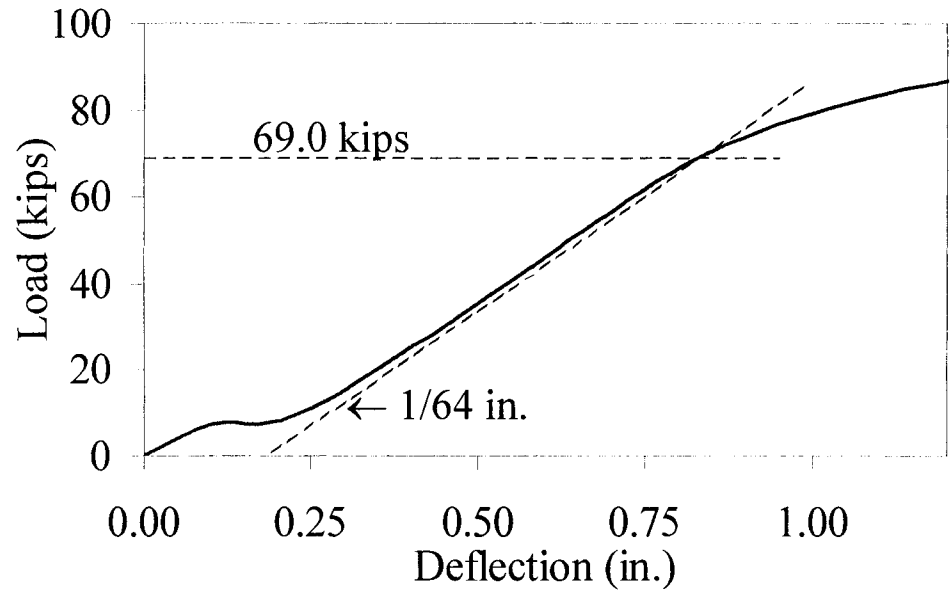
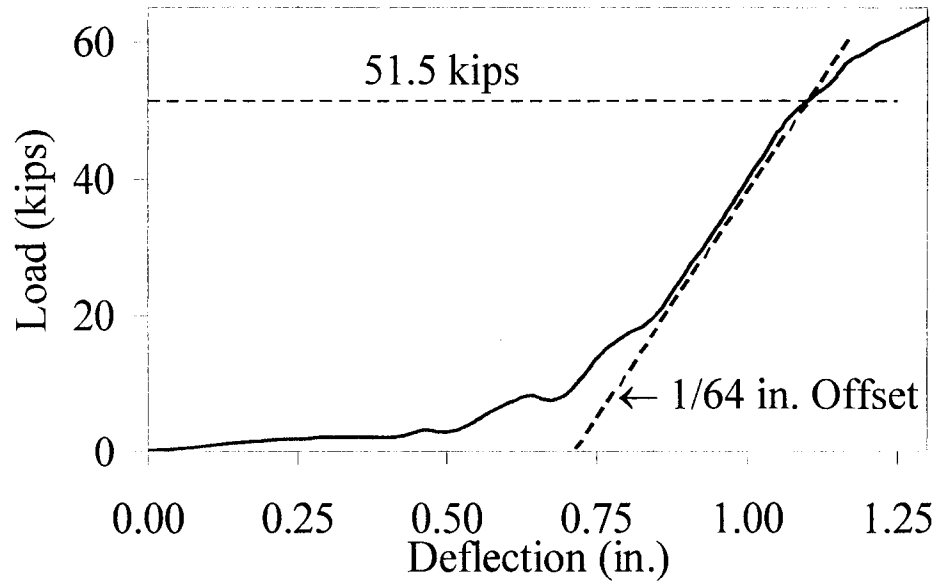
*a.**b.*

Fig. 6. Pictures of testing machine and test frame.



a. Specimen 2T



b. Specimen 9T

Fig. 7. Load versus deflection plots.

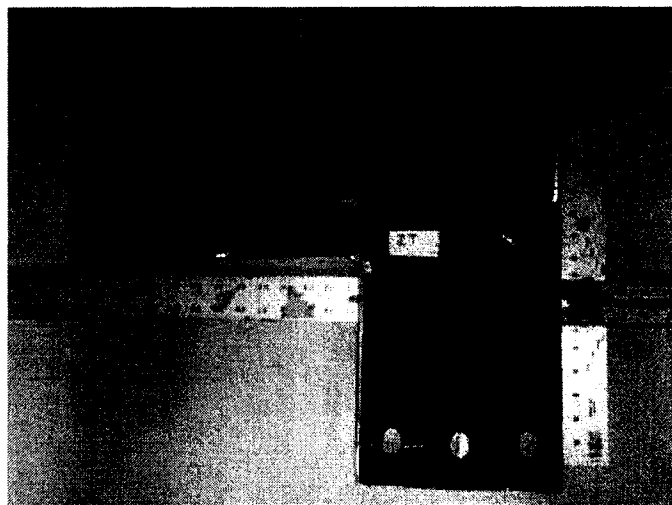
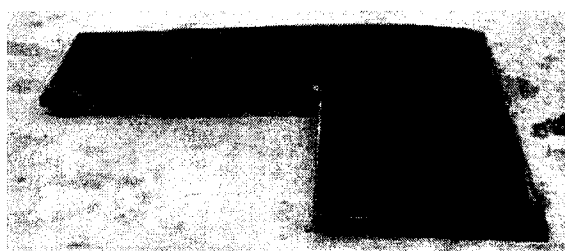
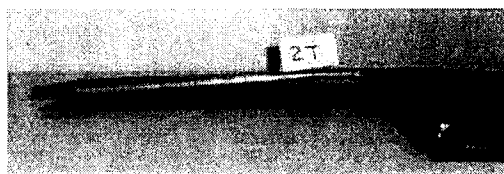


Fig. 8. In-plane deformation of Specimen 2T after test.

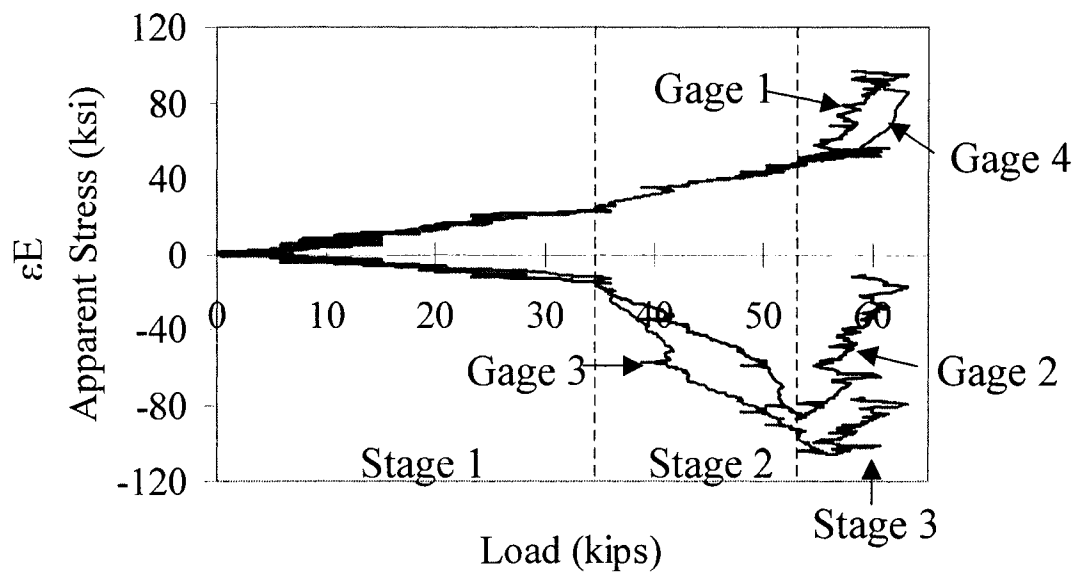


a. Top view.

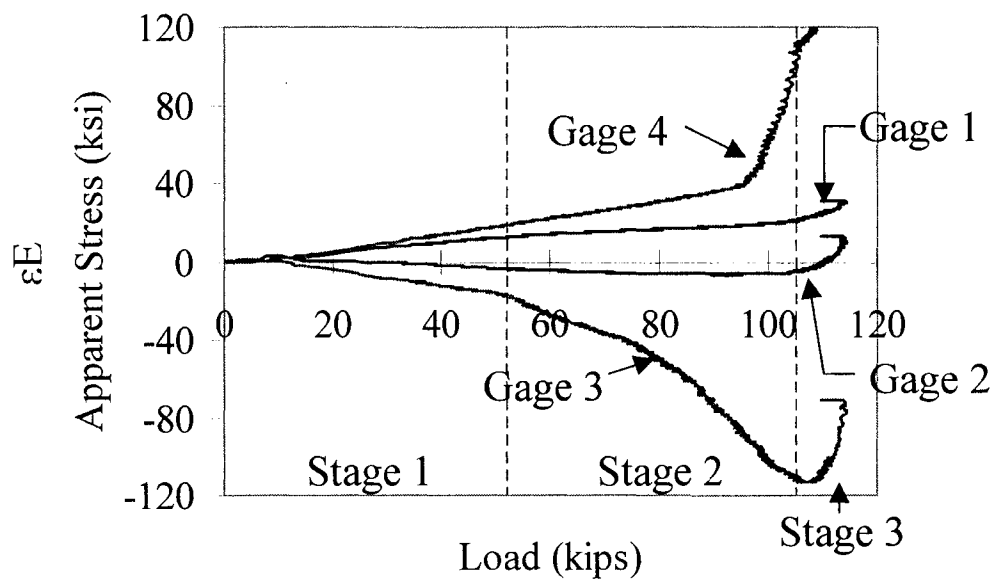


b. Side view of longer edge.

Fig. 9. Out-of-plane deformation of Specimen 2T after test.



a. Specimen 9T



b. Specimen 10T

Fig. 10. Apparent stress versus load plot for Specimens 9T and 10T.

WRAP-AROUND GUSSET PLATES IN COMPRESSION

by

BO DOWSWELL AND FOUAD FOUAD

Submitted to American Institute of Steel Construction Engineering Journal

Format adapted for dissertation

INTRODUCTION

Gusset plates are used in steel buildings to connect bracing members to other structural members in the lateral force resisting system. Horizontal bracing is commonly used to resist lateral loads in industrial structures and in commercial buildings where floor and roof diaphragms cannot carry the loads. Figure 1 shows a typical horizontal bracing connection at a beam-to-beam intersection. Where horizontal bracing is located at a beam-to-column intersection, the gusset plate must be cut out around the column as shown in Figure 2. These plates are called wrap-around gusset plates.

Problem Statement

Due to the increasing complexity of building designs, horizontal bracing members are being used to resist very large forces. A large number of research projects have been dedicated to the analysis and design of standard gusset plates; however, there are no published methods for designing wrap-around gusset plates. Dowswell and Fouad (2005) presented a review of the factors affecting the design of wrap-around gusset plates including modes of failure that are unique to such gusset plates. These issues need to be addressed so engineers can provide safe and economical designs.

Objectives

The purpose of this research was to gain a better understanding of the behavior of wrap-around gusset plates in compression.

EXISTING LITERATURE

A large number of research projects have been dedicated to the analysis and design of standard gusset plates. Failure modes for standard gusset plates have been identified, and design procedures are well-documented in the literature. However, failure modes unique to wrap-around gusset plates have not been studied, nor are guidelines for their design available in the literature. Dowswell and Fouad (2005) summarized the existing research on the stress distribution in standard gusset plates. Dowswell and Barber (2004) summarized previous experiments and finite element studies on gusset plates in compression. This literature review will briefly present the experimental research on statically loaded gusset plates.

The first major experimental work on gusset plates was by Wyss (1926). The stress trajectories were plotted for gusset plate specimens representing a Warren truss joint. The normal and shear stresses were also plotted at the vertical section of the joint where the vertical web member was riveted to the gusset plate.

Rust (1938) published the results of a photoelastic study on the transfer of stress in gusset plates. He wrote, "If an unsupported edge is stressed in compression, the edge will buckle before failure, throwing more moment and direct stress into the interior of the plate." Perna (1941) and Sandel (1950) also used photoelastic studies to study small-scale models of truss joints. They found that the stress distribution differed greatly from the stresses calculated using beam theory, but they both noted that the beam equations appear to be conservative.

Whitmore (1952), Sheridan (1953), Irvan (1957), and Hardin (1958) tested standard truss joints, using strain gages to measure the stresses within the gusset plates.

All of these researchers concluded that beam theory is not a good predictor of stresses within gusset plates. Vasarhelyi (1971) conducted similar experiments, but concluded, “The various analytical methods indicate that the maximums of stress found in a gusset by various simplified methods are only slightly different; the major deviations are in the locations of those maximums.” He also wrote, “The present elementary analysis appears to be adequate for most cases.”

Chakrabarti (1983) and Bjorhovde and Chakrabarti (1985) tested six full-scale diagonal bracing connections. The test specimens were typical of vertical bracing connections found in commercial and industrial structures. The gusset plate was welded to the beam flange and bolted to the column flange using double clip angles. The plates were fabricated from 1/8-in.- and 1/4-in.-thick mild steel. Bjorhovde and Chakrabarti (1985) came to the following conclusions: “The type and location of the gusset plate boundaries, combined with the load transfer pattern into the plate, have important secondary effects of plate buckling and associated out-of-plane bending.” Although the brace was subjected to tensile loading only, “Plate buckling as a result of secondary effects appears to be a significant factor in the development of design criteria for such plates.”

Yamamoto et al. (1985) investigated the stress distribution of eight Warren and Pratt truss joints with double gusset plates. Test specimens were made of 0.31-in.-thick gusset plates. The researchers plotted the stress distribution using data from strain gauges mounted on the gusset plates. The experimental results indicated that the maximum elastic shear stress in the plates could be closely approximated using beam theory. Based on an elastic finite element analysis of a triangular shaped plate, the researchers proposed

an equation to determine the critical gusset plate thickness to prevent buckling of the unsupported edges of the plate.

Yamamoto et al. (1988) investigated the buckling strength of eight Warren and Pratt truss joint specimens with double gusset plates. Strain gauges and photoelastic coatings were used to measure strain distribution in the plates. All of the specimens yielded before reaching the buckling load. The test results showed that the ratio of ultimate load to initial buckling load varied from 1.2 to 1.7 due to the post-buckling strength of the gusset plate. Using the experimental results and elastic finite element analyses, the researchers developed equations for calculating the gusset plate thickness based on an edge buckling model.

Brown (1988) tested 24 half-scale vertical brace connections with corner gusset plates. The plates were 15 in. square and fabricated from A36 steel. They were 3/16 in., 1/4 in., and 3/8 in. thick. The brace angles varied from 26° to 55°. Two bracing members with different bolt patterns were used. Most of the tests failed by buckling of the free edges. Brown wrote, “The buckling pattern of the free edge overwhelmingly exhibited the behavior of a column which was restrained against both translation and rotation on the test fixture side and restrained against rotation only on the bracing member’s side.” The gusset plates were able to carry additional load after buckling occurred, but the post-buckling capacity was accompanied by large lateral deflections. The writer proposed a method to calculate the allowable load on gusset plates based on the plate edge acting as a column with an effective length factor of 1.2.

Gross and Cheok (1988) tested three nearly full-scale braced frame subassemblies. The specimens were loaded monotonically in tension and compression.

The main parameters of the study were the gusset geometry, eccentricity of forces in the connection, and orientation of the column. All but one of the gusset plates failed by buckling. All specimens exhibited yielding before reaching the ultimate load.

Cheng and Hu (1987) investigated the behavior of 14 full-scale gusset plates in compression. The test variables were plate thickness, plate size, boundary conditions, out-of-plane eccentricity, and reinforcement. The primary failure mode was the buckling of the gusset plates. The specimens that were free to move laterally out of plane buckled in an overall sidesway mode. The specimens that were fixed against out-of-plane translation failed by local buckling of the longer free edge of the plate.

Yam and Cheng (1993) tested 19 gusset plate specimens in compression. The primary failure mode was the buckling of the gusset plates. Yielding was observed in most of the specimens prior to buckling.

EXPERIMENTAL PROGRAM

Ten wrap-around gusset plates were tested monotonically in compression. The specimens were loaded until buckling occurred or the load versus deflection curve started to level off due to the decreasing stiffness of the specimen. The load versus deflection data was recorded and plotted. The specimens had strain gages installed in the areas of the highest stresses. The strain gage data was recorded and plotted versus the load. The specimens were loaded slowly, so the behavior could be observed during the tests.

Specimens

The specimens were fabricated by a shop experienced in steel structures and certified by AISC for complex steel buildings. The specimens were flame-cut to shape and had a reentrant corner radius of 1 in. Ten different gusset plates were fabricated. The dimensions are shown in Figure 3. By fabricating the specimens with short slots in each leg and using finger-tight bolts, the in-plane moment restraint was released.

The plate material was A36. To determine the actual mechanical properties of the material, tension coupons were taken from the same parent plate as the specimens. The coupons were tested in accordance with ASTM A370 (2003). The 1/4-in. plates had a yield strength of 56.7 ksi, an ultimate strength of 71.2 ksi, and a modulus of elasticity of 30,000 ksi. The 3/8-in. plates had a yield strength of 48.8 ksi, an ultimate strength of 70.6 ksi, and a modulus of elasticity of 29,000 ksi. The thickness of each specimen was measured using a SONAGAGE II ultrasonic thickness meter by SONATEST. The results are shown in Table 1.

Table 1. Measured Plate Thickness

Specimen	Nominal Thickness (in.)	Measured Thickness (in.)
1C	3/8	0.381
2C	3/8	0.388
3C	3/8	0.380
4C	1/4	0.235
5C	1/4	0.234
6C	1/4	0.235
7C	3/8	0.387
8C	3/8	0.388
9C	3/8	0.390
10C	3/8	0.384

In order to measure the geometric imperfections in the plates, photographs were taken of each specimen showing the two longest edges. The out-of-flatness was measured graphically in the computer program photo editor relative to the plate thickness. The actual out-of-flatness was then determined by scaling the dimensions based on the actual plate thickness. The typical out-of-flatness resembled a half sine wave. The maximum out-of-flatness for all specimens was 0.026 in.

Instrumentation, Testing Machine, and Test Frame

Electrical strain gages were bonded to each specimen in the areas of the highest stresses. Elastic finite element models were used to locate the most highly stressed regions on the plate. The models showed that the highest stresses were longitudinal flexural stresses at the critical section of each leg. The critical section is at the reentrant corner, perpendicular to the length of each leg. The gages were mounted according to Figure 4. The strain gage data was recorded using a MEGADAK data acquisition system.

A test frame fabricated specifically for testing the gusset plates is shown in Figure 5. Generally, the frame consisted of two parts: a brace member, and a frame simulating the beams shown in Figure 2. The channels marked M2, shown in Figure 5b, acted as the brace member. To provide a knife-edge connection between the brace and the specimen, the channels had 1/4-in. square bars tilted at 45° welded between the bolt holes. M3 acted as the beams and was fabricated from 4 x 4 x 1/2 angles welded together at a right angle as shown in Figure 5c. To provide a pinned boundary condition, the frame was required to pivot about the work point in the plane of the specimen. To accomplish this,

a single bolt was used at the corner where the angles were welded together. This also allowed the same frame to be used with all of the specimens without adjusting the angle of the test frame. To provide a knife-edge connection, 1/4-in.-square bars were welded to the angles, as with member M2. M1-C is made of two plates welded together and was used to connect the bracing member, M2, to the testing machine. M4-C is made of two plates welded together. M3 was bolted to M4-C with a single 1½-in. diameter A490 bolt and tightened to a finger-tight condition. The horizontal plate of weldment M4-C was then placed in a roller bearing assembly that allowed lateral movement only in the direction perpendicular to the plane of the specimen. The bearings were ½ inch diameter rods spaced 1-in. center-to-center, and the assembly had stays at each side to prevent in-plane movement. It was very important that this detail allowed almost frictionless movement in the out-of-plane direction in order to simulate sidesway buckling. The bearing assembly can be seen in Figure 6.

The loads were applied to the specimens using a 600-kip Tinius Olsen Super-L Universal Testing Machine with a Model CMH 289 Controller and a Model 290 Display. The test configuration with a specimen and the test frame mounted in the testing machine is shown in Figure 6.

RESULTS

Load vs. Deflection

After the initial slip of the bolts and test frame, the first part of the curve for all of the specimens was linear. Generally, the nonlinear part of the load-deflection curves can be separated into three distinct behaviors: bilinear, nonlinear buckling, and linear

buckling. Load-deflection plots illustrating the three different behaviors are shown in Figure 7.

Specimens 2C and 8C behaved in a bilinear manner. The load-deflection plots were linear up to a point, where the curve became flatter, but was still almost linear. After a large inelastic deflection, the curves became highly nonlinear for a small interval, then buckling occurred. The bilinear behavior is illustrated in Figure 7a, which shows the load-deflection plot for Specimen 8C.

Nonlinear buckling was observed in Specimens 1C, 3C, 5C, 7C, 9C, and 10C. Beyond the linear portion of the curves, the behavior became slightly nonlinear and the specimens became less stiff. Buckling occurred after a relatively small inelastic deflection interval. The behavior is illustrated in Figure 7b, which shows the load-deflection plot for Specimen 1C.

Linear buckling occurred in Specimens 4C and 6C. The behavior was almost linear for each of the specimens until they reached the buckling load. The load-deflection plot for Specimen 6C is shown in Figure 7c.

Out-of-Plane Deformations

Each specimen had a permanent out-of-plane deformation, which was at its maximum at the outer edge of one of the legs, as shown in Figure 8. The lateral deformation was accompanied by twisting, indicating a lateral-torsional buckling type of failure. Specimen 7 was the only plate that buckled in a symmetric mode with both legs buckling simultaneously. Specimen 6 failed in an anti symmetric mode, with each leg buckling in a different direction. All of the specimens with unequal leg lengths buckled

on the longest leg except Specimen 4C, which buckled on its short leg. It appears that the bracing member provided restraint to the long leg, preventing it from buckling. All of the specimens except Specimen 4C buckled without causing lateral movement of the bearing assembly, indicating a non sway type of buckling. Specimen 4C buckled in a sidesway manner.

Stress Measurements

The strain gage data was plotted in terms of stress instead of strain so the yield point could be easily identified. Hooke's law was used to convert the strain gage readings to stresses. The disadvantage of this method is that the stresses displayed beyond the yield point of the material are not accurate and only give a qualitative measure of the strain. The term "apparent stress" is used in this paper to signify that the displayed stresses are not accurate over the full range of data.

The stresses for Specimens 4C and 6C, which failed by linear buckling, were essentially linear until buckling occurred. This behavior is illustrated in Figure 9, which shows the stress versus load plot for specimen 6C.

The plots for the remaining specimens were similar and could be separated into three stages of behavior. In the first stage, the material behaved elastically. In the second stage, the material still appeared to be approximately linear; however, it is clear from the data that much of the material is above the yield point. This behavior is due to a combination of residual stresses, strain hardening, biaxial stresses at the reentrant corner, and stress redistribution due to yielding. The third stage is post-buckling. All of the specimens except 4C and 6C carried additional load after buckling occurred. This

behavior is illustrated in Figures 10 and 11, which show the stress versus load plots for specimens 7C and 9C, respectively.

In the early stages of loading, the strain gage readings for all of the specimens were linear. The readings for gages located at each edge of a particular gusset plate leg were approximately equal in magnitude, but were of opposite sense, indicating that the legs were in almost pure flexure.

Experimental Loads

The yield loads, P_{ey} , and maximum test loads, P_{eu} , are shown in Table 2. For the specimens that failed by linear buckling, the recorded load was the load at which buckling occurred. The load-deflection curves for the remaining specimens did not have a well-defined yield point; therefore, the yield loads were determined using a 1/64-in. offset relative to the linear portion of the load versus deflection plots, as shown in Figures 7a and 7b. The yield load is where the load versus deflection curve crosses the 1/64-in. offset line.

Table 2. Test Data

Spec. No.	Test Loads (k)		Load-Deflection Behavior
	P_{ey}	P_{eu}	
1C	33.3	45.8	Nonlinear Buckling
2C	47.3	63.9	Bilinear
3C	46.6	64.2	Nonlinear Buckling
4C	32.0	32.0	Linear Buckling
5C	28.7	46.8	Nonlinear Buckling
6C	25.3	25.3	Linear Buckling
7C	46.4	46.5	Nonlinear Buckling
8C	38.4	60.8	Bilinear
9C	44.4	51.5	Nonlinear Buckling
10C	57.0	66.5	Nonlinear Buckling

P_{ey} test yield load determined using a 1/64-in. offset.

P_{eu} maximum test load

CONCLUSIONS

Ten wrap-around gusset plates were tested in compression. The results of the tests will help to provide a better understanding of the behavior of these gusset plates. The experiments indicated that wrap-around gusset plates are subject to limit states common to flexural members. In the early stages of loading the strain gage readings were linear. The readings for gages located at each edge of a particular gusset plate leg were approximately equal in magnitude, but were of opposite sense, indicating that the legs were in almost pure flexure. All of the specimens had a permanent out-of-plane deformation at the plate edges that carried flexural compression stresses. The out-of-plane deformation was accompanied by twisting of the gusset plate legs, indicating a lateral-torsional buckling failure.

ACKNOWLEDGEMENTS

The test frame and specimens were fabricated and donated to the project by Gipson Steel, Inc. Structural Steel Services, Inc., also fabricated parts of the test frame. Bell Steel Company supplied the bolts. The technical assistance of Elton Hogan and Mark Gipson of Gipson Steel, George Reed and Kane Combs of Structural Steel Services, and Curtis Smith of Bell Steel is greatly appreciated. The testing was performed in the structures laboratory at the Department of Civil and Environmental Engineering at The University of Alabama at Birmingham. The assistance of lab supervisor Richard Hawkins was invaluable and is appreciated.

REFERENCES

- ASTM A370 (2003), "Standard Test Method and Definitions for Mechanical Testing of Steel Products," ASTM International, West Conshohocken, PA.
- Bjorhovde, R. and Chakrabarti, S. K. (1985), "Tests of Full-size Gusset Plate Connections," *Journal of Structural Engineering*, ASCE, Vol. 111, No. 3, March, pp. 667-683.
- Brown, V. L. (1988), "Stability of Gusseted Connections in Steel Structures," Ph.D. Dissertation, University of Delaware.
- Chakrabarti, S. K. (1983), "Tests of Gusset Plate Connections," Masters Thesis, University of Arizona.
- Cheng, J. J. R. and Hu, S. Z. (1987), "Comprehensive Tests of Gusset Plate Connections," *Proceedings, 1987 Annual Technical Session*, Structural Stability Research Council, pp. 191-205.
- Dowswell, B. and Fouad, F. H. (2005), "Design Considerations for Wrap-Around Gusset Plates," Page 3 of this document.
- Dowswell, B. and Barber, S. (2004), "Buckling of Gusset Plates: A Comparison of Design Equations to Test Data," *Proceedings, 2004 Annual Stability Conference*, Structural Stability Research Council, pp. 199-221.

Gross, J. L. and Cheok, G. (1988), "Experimental Study of Gusseted Connections for Laterally Braced Steel Buildings," National Institute of Standards and Technology, Gaithersburg, Maryland, November.

Hardin, B. O. (1958), "Experimental Investigation of the Primary Stress Distribution in the Gusset Plates of a Double Plane Pratt Truss Joint with Chord Splice at the Joint," University of Kentucky Engineering Experiment Station Bulletin No. 49, September.

Irvan, W. G. (1957), "Experimental Study of Primary Stresses in Gusset Plates of a Double Plane Pratt Truss," University of Kentucky Engineering Research Station Bulletin No. 46, December.

Perna, F. J. (1941), *Photoelastic Stress Analysis, with Special Reference to Stresses in Gusset Plates*, Master's Thesis, University of Tennessee, August.

Rust, T. H. (1938), "Specification and Design of Steel Gusset-Plates," *Proceedings, American Society of Civil Engineers*, November, pp. 142-167.

Sandel, J. A. (1950), "Photoelastic Analysis of Gusset Plates," Master's Thesis, University of Tennessee, December.

Sheridan, M. L. (1953), "An Experimental Study of the Stress and Strain Distribution in Steel Gusset Plates," Doctoral Dissertation, University of Michigan.

Vasarhelyi, D. D. (1971), "Tests of Gusset Plate Models," *Journal of the Structural Division, Proceedings of the American Society of Civil Engineers*, Vol. 97, No. ST2, February, pp. 665-679.

Whitmore, R. E. (1952), "Experimental Investigation of Stresses in Gusset Plates," University of Tennessee Engineering Experiment Station Bulletin No. 16, May.

Wyss, T. (1926), "Die Kraftfelder in Festen Elastischen Korpern und ihre Praktischen Anwendungen," Berlin.

Yam, M. C. H. and Cheng, J. J. R. (1993), "Experimental Investigation of the Compressive Behavior of Gusset Plate Connections," University of Alberta Department of Civil Engineering Structural Engineering Report No. 194, September.

Yamamoto, K., Akiyama, N. and Okumura, T. (1988), "Buckling Strengths of Gusseted Truss Joints," *Journal of Structural Engineering, ASCE*, Vol. 114, No. 3, March, pp. 575-591.

Yamamoto, K., Akiyama, N., and Okumara, T. (1985), "Elastic Analysis of Gusseted Truss Joints," *Journal of Structural Engineering, ASCE*, Vol. 111, No. 12, December, pp. 2545-2564.

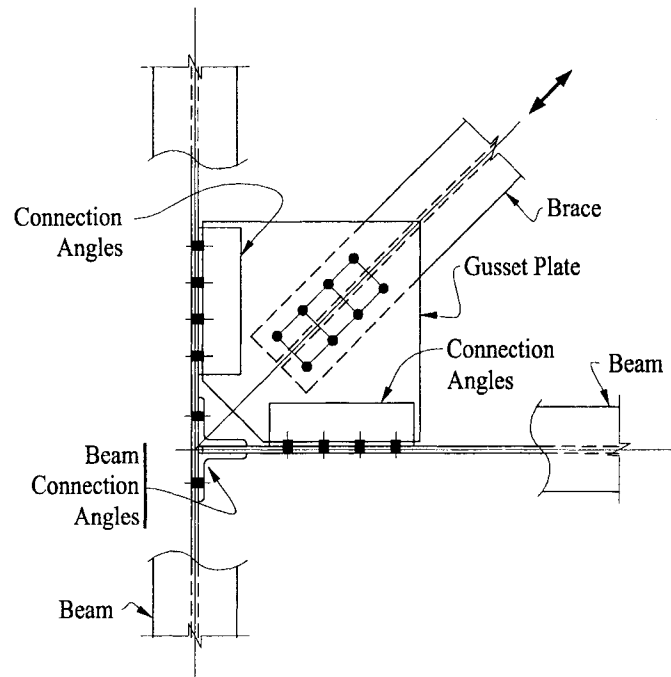


Fig. 1. Horizontal brace connection at beam-to-beam intersection.

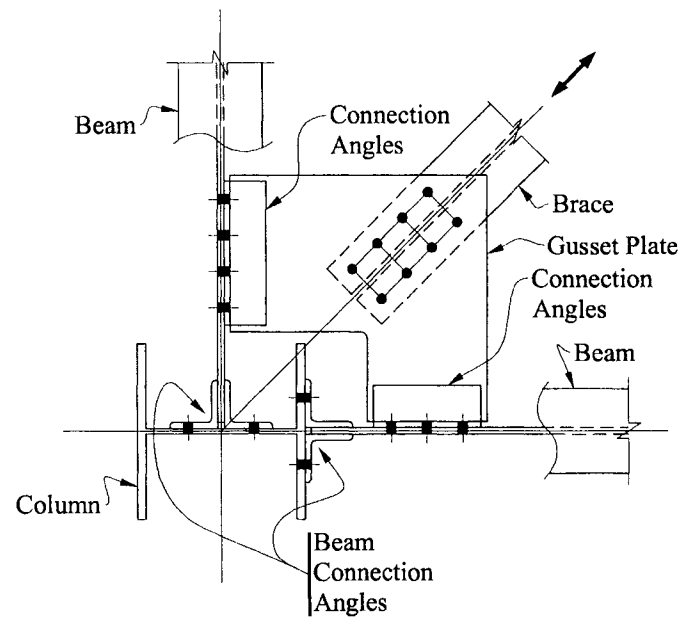
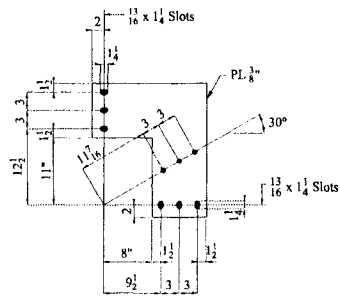
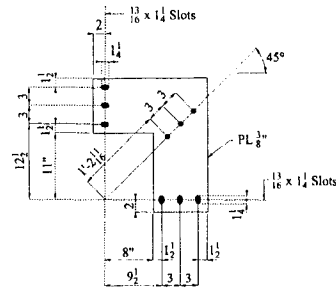


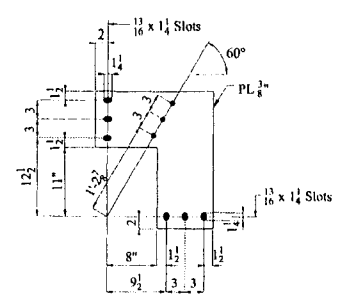
Fig. 2. Horizontal brace connection at beam-to-column intersection.



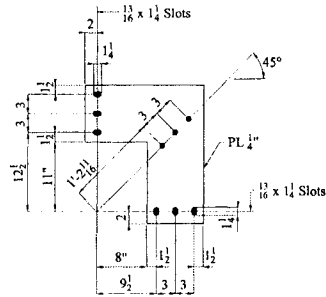
Specimen 1C



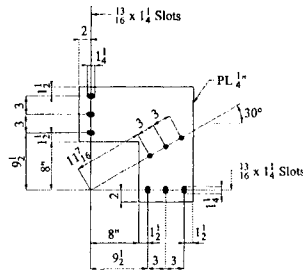
Specimen 2C



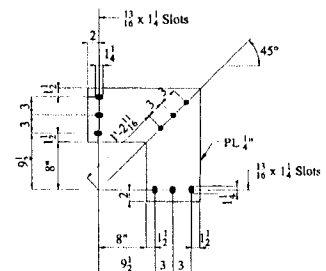
Specimen 3C



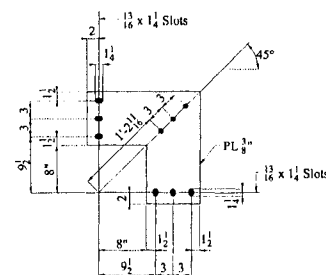
Specimen 4C



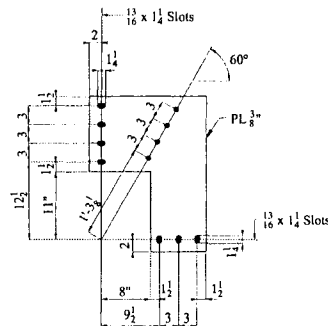
Specimen 5C



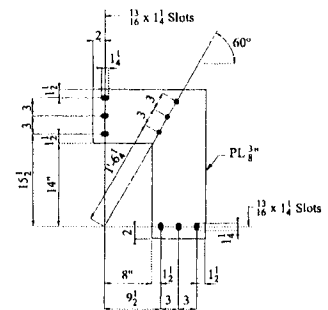
Specimen 6C



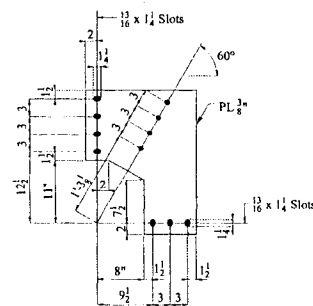
Specimen 7C



Specimen 8C

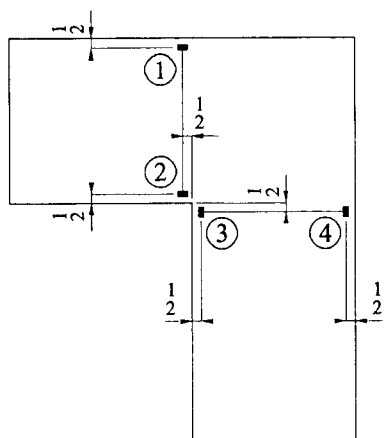


Specimen 9C

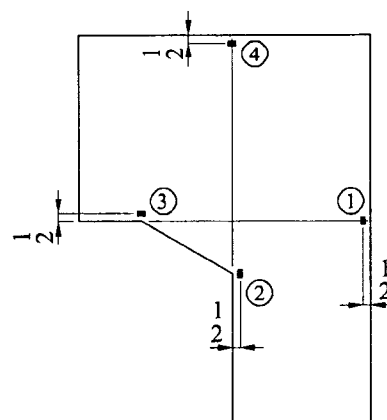


Specimen 10C

Fig. 3. Fabrication drawings.

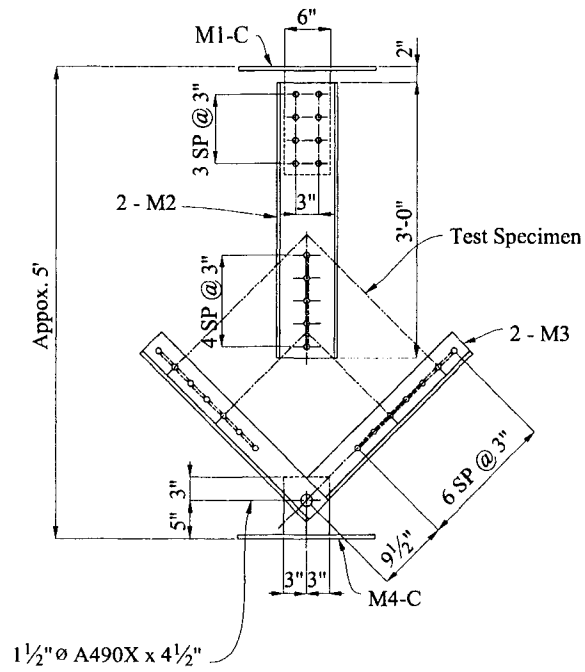


Specimens 1C through 9C



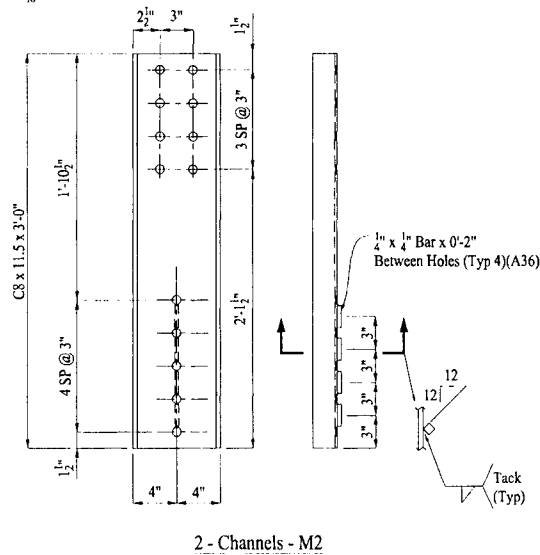
Specimen 10C

Fig. 4. Strain gage locations.

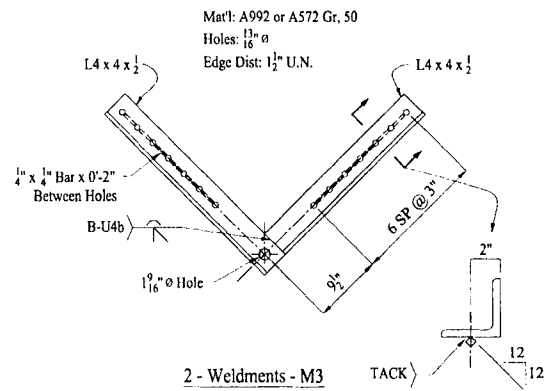


a. Assembled test frame

Mat'l: A992 or A572 GR. 50 (UN)
Holes: $\frac{11}{16}$ " ϕ

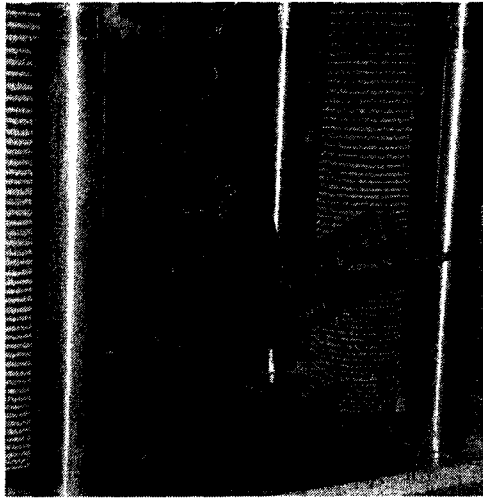
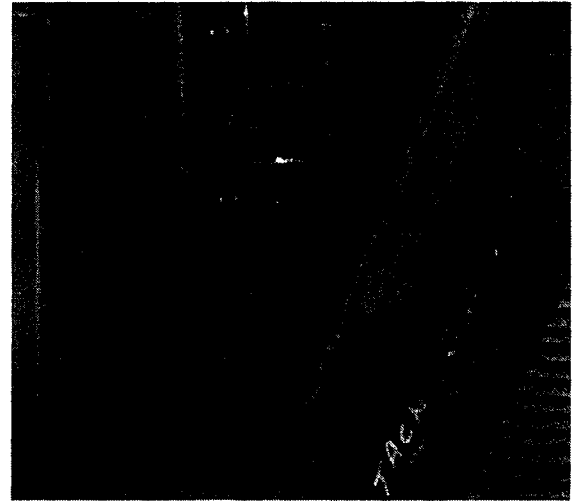
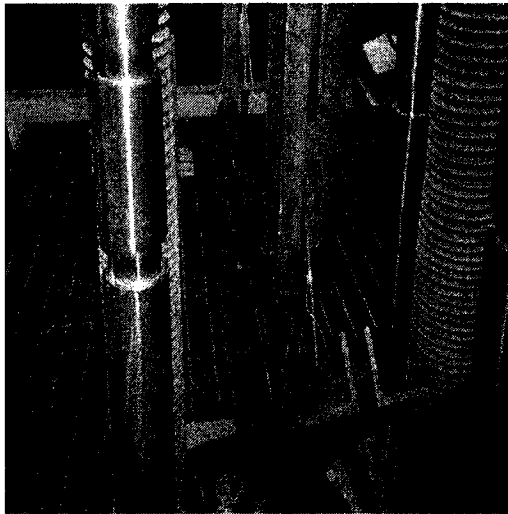
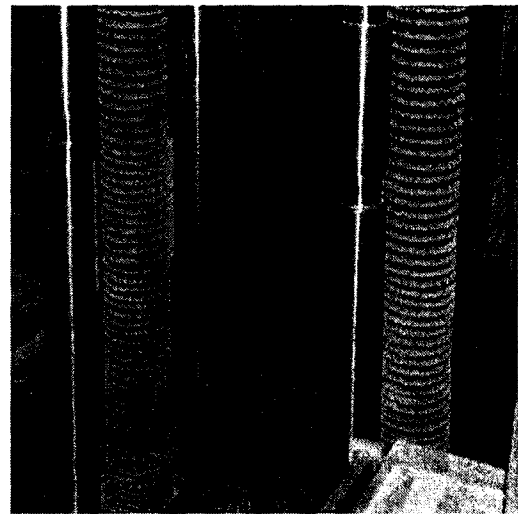


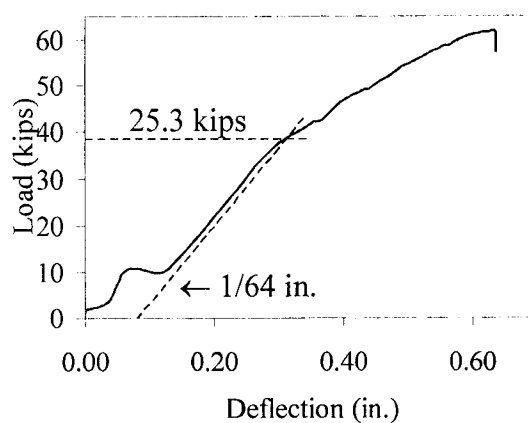
b. Fabrication drawing for M2



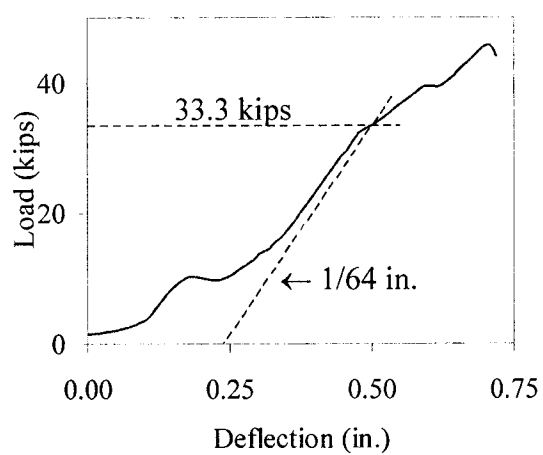
c. Fabrication drawing for M3

Fig. 5. Test frame drawings.

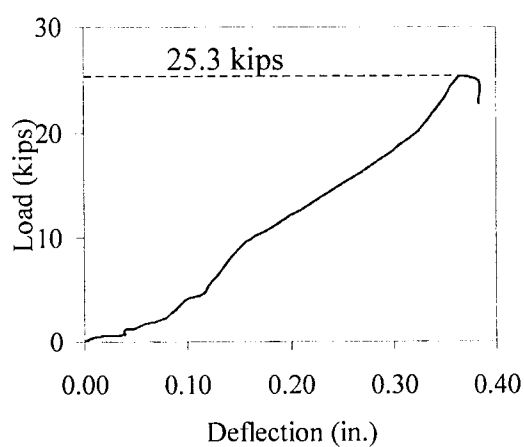
*a.**b.**c.**d.**Fig. 6. Photographs of test frame.*



a. Specimen 8C

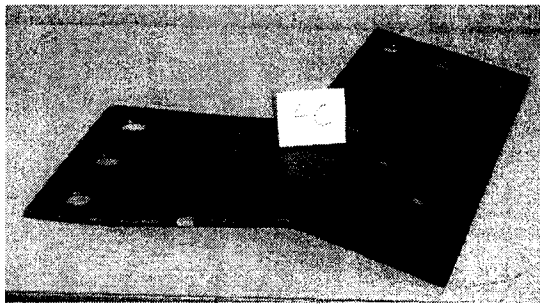


b. Specimen 1C

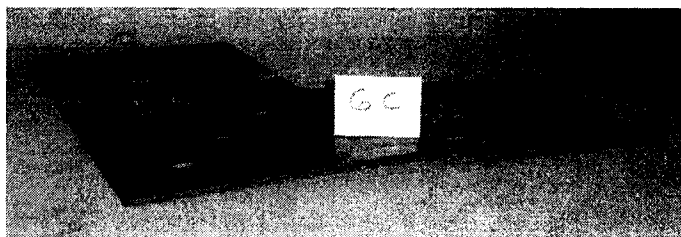


c. Specimen 6C

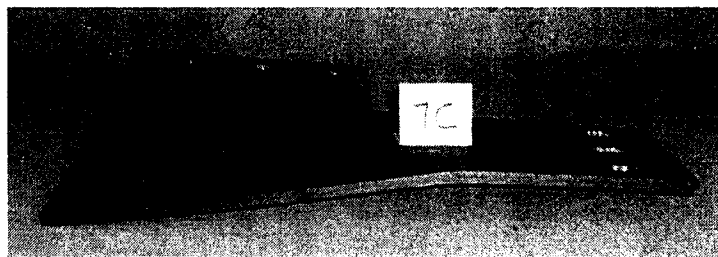
Fig. 7. Load versus deflection plots.



a. Specimen 4C



b. Specimen 6C



c. Specimen 7C

Fig. 8. Specimens 4C, 6C and 7C, after test.

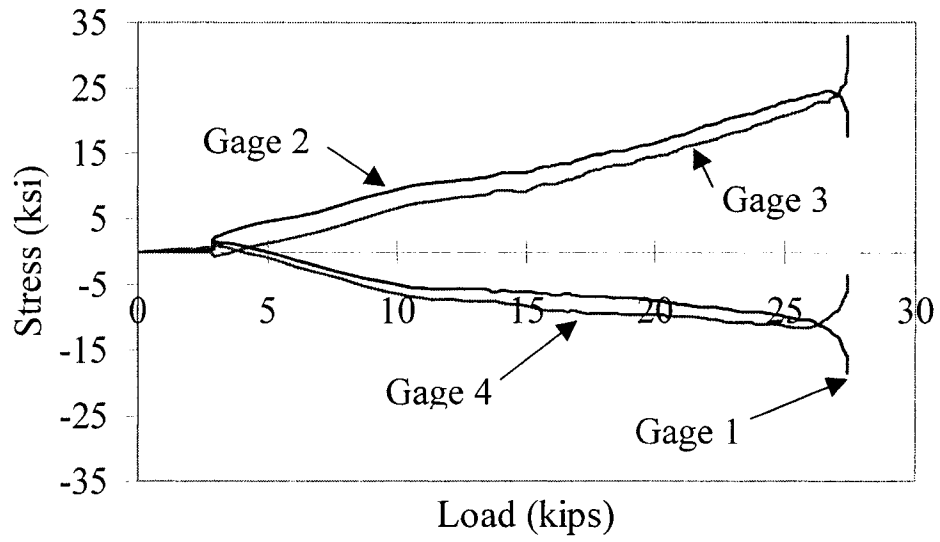


Fig. 9. Stress versus load plot for Specimen 6C.

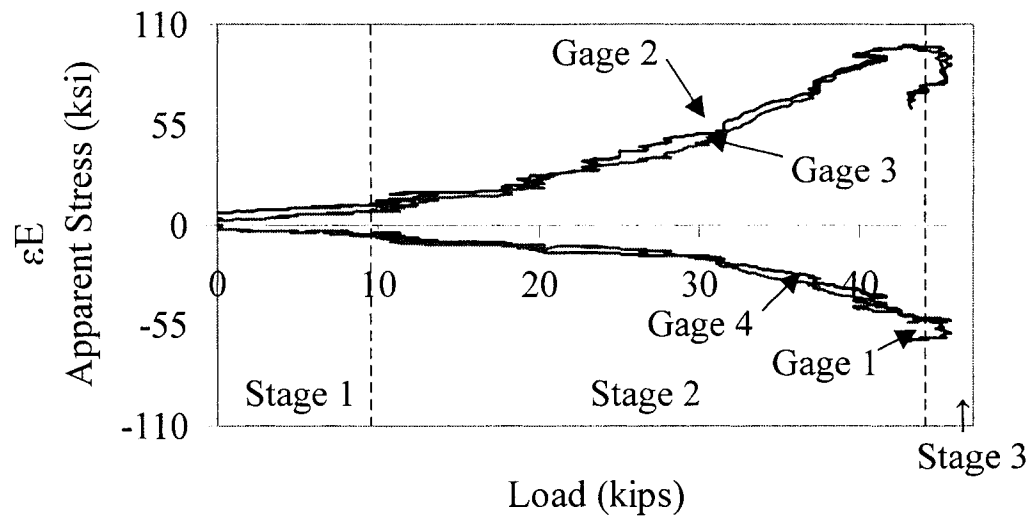


Fig. 10. Apparent stress versus load plot for Specimen 7C.

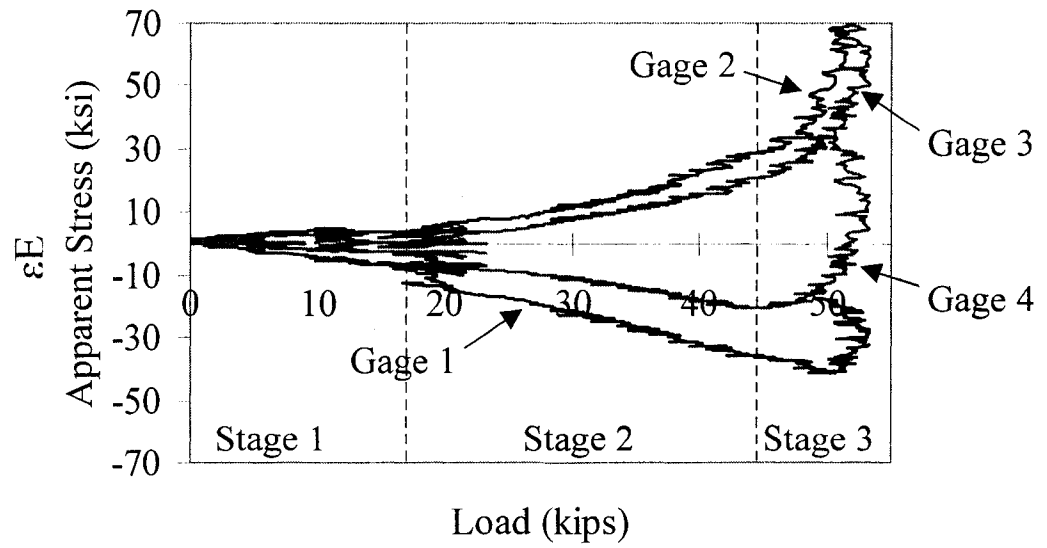


Fig. 11. Apparent stress versus load plot for Specimen 9C.

MODELING TECHNIQUES FOR WRAP-AROUND GUSSET PLATES

by

BO DOWSWELL, ROBERT WHYTE, JIM DAVIDSON, AND FOUAD FOUAD

Submitted to Computers and Structures

Format adapted for dissertation

INTRODUCTION

Gusset plates are used in steel buildings to connect bracing members to other structural members in the lateral force resisting system. Figure 1 shows a standard vertical bracing connection at a beam-to-column intersection. Horizontal bracing is used to resist lateral loads in industrial structures and in commercial buildings where floor and roof diaphragms cannot carry the loads. Where a horizontal brace is located at a beam-to-column intersection, the gusset plate must be cut out around the column as shown in Figure 2. These plates are known as wrap-around gusset plates.

Problem Statement

Several research projects have documented the finite element analysis of standard gusset plates; however, published research on wrap-around gusset plates is not available. Experiments by Dowswell and Fouad (2005) showed that the behavior of wrap-around gusset plates is complex. Previous research on finite element modeling of standard gusset plates has shown that the models can closely represent the behavior of real gusset plates if the proper modeling techniques are used. The accuracy of finite element models of wrap-around gusset plates must be verified before the results can be used with confidence.

Objective

The purpose of this research was to determine an accurate method to model the behavior of wrap-around gusset plates using the finite element method.

Procedure

A parametric study was conducted which included material and geometric nonlinearities. The effects of the following parameters were studied: mesh size, magnitude of the initial out-of-flatness, the effect of residual stresses, and the shape of the stress-strain curve. A linear analysis was performed first, to determine the locations within the gusset plate with the highest stresses. A mesh study was used to establish an adequate mesh refinement scheme that would be used for the remainder of the project. The finite element modeling software program ALGOR was used.

LITERATURE REVIEW

Lavis (1967) used the finite element method to investigate the elastic stress distribution in gusset plates. His results compared well with the experimental results of Whitmore (1952). Desai (1970) discussed finite elements as a method to determine the capacity of arbitrarily loaded gusset plates. Nonlinear material behavior was modeled by successive modification of constants used for element stiffness. A rectangular compound element with a hole in the center was developed for use on gusset plates and other problems with similar stress gradients. Struik (1972) analyzed gusset plates using an elastic-plastic finite element program.

Rabern (1983) carried out 12 inelastic finite element analyses on gusset plate connections. The connections were modeled to represent typical vertical bracing connections in buildings with the gusset plate welded to the beam and bolted to the column with clip angles. Load-deformation properties for the interface connections were obtained from physical tests and integrated into the model in the form of nonlinear spring

elements. The loads on the plate interfaces were plotted, showing the magnitude and direction of the load at each element. The internal gusset plate stresses were also plotted. The results were compared to experiments that verified the accuracy of the finite element models. The results also agreed well with the Whitmore (1952) model for stress distribution at the end of the bracing members.

Williams (1986) and Richard (1986) generated 51 inelastic finite element models of standard vertical brace connections to determine the force distributions at the gusset-to-beam and gusset-to-column interfaces. He used the same modeling techniques as Rabern (1983), but the entire frame was included in the model to determine the effect of frame deformations on the gusset interface forces. Williams (1986) also conducted a linear-elastic buckling analysis on 17 gusset plate models. 11 of the models represented standard vertical bracing connections with the brace intersecting at a beam-to-column connection. Six of the models represented “V” bracing connections where a tension brace and a compression brace frames to the top flange of a beam. The gusset plate at the brace-to-gusset connection was restrained from out-of-plane translation.

Chakrabarti (1987), and Chakrabarti and Richard (1990) used elastic and inelastic finite element models to determine the buckling capacity of gusset plates in Warren truss joints and typical vertical brace joints. They modeled four of the eight specimens that were tested experimentally by Yamamoto et al. (1988). The interface between the gusset plate and the chord was fixed against translation and rotation. The plate was held from out-of-plane translation where the diagonal members connected to the plate. The test results, as well as the finite element models, indicated that the gusset plates buckled inelastically. The buckling loads from the elastic finite element models were much

higher than the experimental loads, but the loads from the inelastic models compared well with the experiments. The inelastic models more closely resembled the buckled shapes of the test specimens, where the out-of-plane deformation extended from the end of the compression brace to the free edges of the plate.

Cheng et al. (1994) analyzed the experimental results of Cheng and Hu (1987). The finite element program ANSYS was employed to perform the analysis. The models provided reasonably accurate predictions of the elastic buckling strength. A large deflection analysis performed on one of the specimens indicated that the plate had significant post-buckling capacity. The analytical load deflection curves agreed well with that of the tests.

Walbridge et al. (1998) developed finite element models of gusset plates using ABAQUS. They were validated with the experimental results of Yam and Cheng (1993) and Rabinovitch and Cheng (1993). The researchers found that the capacity of the gusset plates could be accurately predicted using a linear elastic-perfectly plastic material model, a 2-mm initial imperfection in the shape of a quarter sine wave, and full restraint at the splice member.

DESCRIPTION OF MODELS

Geometry

The models were created to match the dimensions of a laboratory specimen tested by Dowswell and Fouad (2005), as seen in Figure 3. The actual thickness of the plate from the laboratory specimen was 9.93-mm.

Loading

The brace load was applied at the diagonal bolts using a rigid frame to equally distribute the load to each bolt. The rigid frame was modeled with stiff beam elements.

Boundary Conditions

The boundary conditions at the brace bolts were set to simulate a typical bracing member connected to the gusset plate. Rotations in the in-plane (x and y) directions were fixed, and the other four degrees of freedom were released. These boundary conditions provided a simulated bending restraint from the brace member but allowed the plate to buckle in a sidesway mode

The bolt lines parallel to the x-axis and the y-axis represent the gusset plate to beam interface. The nodes along the bolt lines were fixed against out-of-plane translation. At the bolts in the line parallel to the y-axis, translation was fixed in the y direction. At the bolts in the line parallel to the x-axis, translation was fixed in the x direction. Table 1 and Figure 4 summarize the boundary conditions adopted for the analysis.

MESH STUDY

A mesh study was conducted using a linear elastic analysis to determine the level of mesh refinement required for the nonlinear inelastic analysis model. An initial mesh was created using predominantly quadrilateral shell elements, and a linear analysis was performed to determine the regions of high stress. These highly stressed regions were concentrated around the reentrant corner and on the free edge of the gusset plate legs, as

shown in Figure 5. The mesh was refined in these areas, as shown in Figure 6. The initial mesh was called Mesh 1, and the refined mesh was called Mesh 2. Another mesh, called Mesh 3, was refined further. Mesh 1 had 319 elements, Mesh 2 had 414 elements, and Mesh 3 had 519 elements.

Table 1. Summary of Boundary Conditions

Location	Fixed	Free
At brace connection	Rx, Ry	Tx, Ty, Tz, Rz
At bolts in the gusset plate leg perpendicular to the y direction	Ty, Tz	Tx, Rx, Ry, Rz
At bolts in the gusset plate leg perpendicular to the x direction	Tx, Tz	Ty, Rx, Ry, Rz
At first bolt in the gusset plate leg perpendicular to the x direction	Tx, Ty, Tz	Rx, Ry, Rz
Nodes along line of bolt holes in the gusset plate legs	Tz	Tx, Ty, Rx, Ry, Rz

Rx Ry Rz: Rotations in the x, y, and z directions

Tx Ty Tz: Translations in the x, y, and z directions

Three parameters were compared from the linear analysis of the three mesh schemes: critical buckling load, maximum von Mises stress, and in-plane deflection in the direction of the applied load. Table 2 shows the results of these comparisons. The difference between Mesh 1 and Mesh 3 for any of the three parameters was 3 percent or less; therefore, Mesh 1 was selected for the remainder of this investigation.

Table 2. Summary of Linear Elastic Mesh Study

Mesh Scheme	Number of Elements	Maximum Stress (MPa)	In-plane Displacement (mm)	Buckling Load (kN)
Mesh 1	319	24.00	0.02997	387.9
Mesh 2	414	24.75	0.03023	386.1
Mesh 3	519	24.14	0.03073	385.7

PARAMETRIC STUDY

A parametric study was conducted, which included material and geometric nonlinearities. The effects of the following parameters were studied: magnitude of the initial out-of-flatness, the effect of residual stresses, and the shape of the stress-strain curve. A total of 24 models were analyzed. 12 were loaded in tension and 12 in compression.

General Description of Nonlinear Models

The updated lagrangian analysis method was used because the behavior was expected to be highly dependent on the out-of-plane deformations. Because this study focuses on the global behavior of the models rather than the local behavior near the bolts, the elements at the bolt locations were modeled with thick elastic elements. This made the gusset plate models more efficient because the bearing areas between the bolts and the plate become inelastic at early stages of loading, which greatly increased the computation time on preliminary models. Using a preliminary run, it was determined that the local behavior at the bolts has an insignificant effect on the global behavior of the

plate. Additionally, the mesh size was approximately the same size as a bolt head or nut that would exert a clamping force to restrain the plate in an actual structure.

Initial Out-of-Flatness

For the nonlinear analysis, the shape and magnitude of the initial out-of-flatness of the plate had to be determined. Walbridge et al. (1998) found that the shape of the initial imperfection is much less critical than the magnitude; therefore, the shape was held constant, so the effect of varying the magnitude could be studied.

The buckled shape was determined using a linear buckling analysis. The eigenvector was scaled to give three different magnitudes of initial out-of-flatness. The buckled shape from the linear buckling analysis is shown in Figure 7. Figure 8 shows the residual deformation of Specimen 2 from Dowswell and Fouad (2005) after it was tested in tension. It can be observed that the buckled shape of the specimen is similar to the shape of the eigenvector for the linear buckling analysis. The highest point of out-of-plane deformation on the eigenvector is consistent with that of the laboratory specimen.

A survey of the gusset plate specimens tested by Dowswell and Fouad (2005) determined the maximum out-of-plane deformation to be 0.71-mm. Therefore, three maximum out-of-plane displacement magnitudes were selected for the inelastic analysis: 0.20-mm, 0.79-mm, and 3.18-mm.

Stress–Strain Relationships

The two material models studied were the linear elastic-perfectly plastic model and the experimental material curve from the tensile coupon tests of Dowswell and Fouad

(2005). The yield strength of Specimen 2 tested by Dowswell and Fouad (2005) was 337 MPa. This value was used in both material models. The experimental curve is shown in Figure 9.

Residual Stresses

Residual stresses will have an influence on the stress distribution in wrap-around gusset plates. The equipment in most structural steel fabrication shops and the geometry of wrap-around gusset plates dictates that they are flame-cut. The residual stress pattern for plates with flame-cut edges is shown in Figure 10. According to Bjorhovde et al. (2001), the tensile residual stress at the plate edges is generally around 414 to 483 MPa, “regardless of the original material properties.”

Rao and Tall (1961) and Dwight and Ractliffe (1967) measured the residual stresses in edge-welded plates. Rao and Tall (1961) noted that plates with gas-cut edges have residual stress patterns very similar to edge-welded plates. Dwight and Ractliffe (1967) showed that dimension x is “largely independent” of the plate width. Bjorhovde et al. (1972) measured the residual stresses in thick plates with flame-cut plates. A summary of the residual stress measurements is shown in Table 3. As shown in Figure 10, σ_r is the tension residual stress at the plate edge, and x is the width of the tension portion of the residual stress pattern. σ_y is the yield strength of plate. The average x is 30.7 mm. Using the 29 results of Rao and Tall (1961) and Bjorhovde et al. (1972), the average σ_r/σ_y is 1.40.

Table 3. Experimental Residual Stress Patterns in Flame-cut Plates

Specimen	Width (mm)	Thickness (mm)	σ_x/σ_y	x (mm)
Dwight and Ractliffe (1967)				
1	279	6.35	NA	41.1
2	343	6.35	NA	40.1
3	419	6.35	NA	47.7
4	514	6.35	NA	40.6
Rao and Tall (1961)				
T-7	152	12.7	1.12	24.1
T-8	203	6.35	1.33	25.4
T-8	203	6.35	1.39	20.3
T-8	203	6.35	1.36	22.9
T-8	203	6.35	1.42	22.9
T-3	203	12.7	1.70	27.9
T-3	203	12.7	1.66	33.0
T-3	203	12.7	1.82	33.0
T-2	254	12.7	1.97	26.7
T-2	254	12.7	1.97	27.9
T-2	254	12.7	1.94	25.4
T-5	305	19.0	1.45	36.8
T-18	305	25.4	1.09	27.7
T-13	406	12.7	1.21	29.2
T-10	406	25.4	1.15	25.6
T-16	457	19.0	1.36	44.4
T-14	508	12.7	1.21	35.6
T-6	508	25.4	1.18	34.5
T-6	508	25.4	1.33	30.5
T-6	508	25.4	1.27	29.5
T-6	508	25.4	1.15	25.4
Bjorhovde et al. (1972)				
1	229	38.1	1.33	27.4
2	305	50.8	1.75	21.3
3	305	88.9	1.43	30.5
4	406	38.1	1.40	26.7
5	508	38.1	0.85	20.3
6	508	50.8	1.38	35.6
7	610	50.8	1.22	30.5
8	610	152	1.29	42.7

Dwight and Ractliffe (1967) and Dwight and Moxham (1977) used a simplified residual stress pattern in their studies where the curved pattern was replaced with rectangular stress blocks, as shown in Figure 11. To use the simplified residual stress pattern, x_s must be defined. The value of x_s can be determined by approximating the actual stress pattern as linear and setting the tension force from the simplified model equal to the average force from the experiments.

Using the average value of σ_{rt} from the experiments,

$$\sigma_{rt} = 1.4\sigma_y$$

The tension residual stress for the simplified pattern is set equal to the yield stress of the plate,

$$\sigma_{rts} = \sigma_y$$

The tensile force generated by the actual pattern is,

$$F_{rt} = (1/2)(1.4\sigma_y)(x)$$

The tensile force generated by the simplified pattern is,

$$F_{rts} = \sigma_y x_s$$

Set $F_{rt} = F_{rts}$ and solve for x_s ,

$$x_s = 0.70x$$

using the average value of x from the experimental measurements,

$$x_s = (0.70)(30.7 \text{ mm}) = 21.5 \text{ mm}$$

The residual stresses were considered to affect a 21.5-mm-wide strip along the edges of the gusset plate, as shown in Figure 12. From the elastic models, it was determined that

the stresses on the outer edges were always of the same sense as the applied load, and the stresses on the inner edges were always of the opposite sense as the applied load.

Because the residual stresses used in the model were equal to the material yield stress, the elements on the tension edges were modeled with a yield stress of zero. The yield stress was doubled for the elements on the compression edges.

Summary of Models

Table 4 summarizes the parameters that were considered for each model. All parameters of the model can be identified in the name. The first three numbers identify the initial out-of-flatness. The fourth and fifth characters identify the stress-strain relationship. EP designates the elastic-plastic material model, and LC indicates that the experimental curve was used. The sixth character is T if the brace load was in tension and C if the brace load was in compression. If the model included residual stresses, an R was added to the end.

RESULTS

The load versus in-plane deflection was plotted to determine how each parameter studied affects the stiffness, yield load, and ultimate capacity. Each condition was plotted for brace loads in tension and compression. In part a of Figures 13, 14, and 15, the brace load is in tension. In part b, the brace load is in compression.

Table 4. Summary of Models Analyzed for Nonlinear Inelastic Analysis

Model	Initial Out-of-Flatness (mm)	Residual Stresses	Stress-Strain Relationship	Direction of Load
008EPT	0.20	No	Elastic-Plastic	Tension
032EPT	0.79	No	Elastic-Plastic	Tension
128EPT	3.18	No	Elastic-Plastic	Tension
008EPC	0.20	No	Elastic-Plastic	Compression
032EPC	0.79	No	Elastic-Plastic	Compression
128EPC	3.18	No	Elastic-Plastic	Compression
008LCT	0.20	No	Test Curve	Tension
032LCT	0.79	No	Test Curve	Tension
128LCT	3.18	No	Test Curve	Tension
008LCC	0.20	No	Test Curve	Compression
032LCC	0.79	No	Test Curve	Compression
128LCC	3.18	No	Test Curve	Compression
008EPTR	0.20	Yes	Elastic-Plastic	Tension
032EPTR	0.79	Yes	Elastic-Plastic	Tension
128EPTR	3.18	Yes	Elastic-Plastic	Tension
008EPCR	0.20	Yes	Elastic-Plastic	Compression
032EPCR	0.79	Yes	Elastic-Plastic	Compression
128EPCR	3.18	Yes	Elastic-Plastic	Compression
008LCTR	0.20	Yes	Test Curve	Tension
032LCTR	0.79	Yes	Test Curve	Tension
128LCTR	3.18	Yes	Test Curve	Tension
008LCCR	0.20	Yes	Test Curve	Compression
032LCCR	0.79	Yes	Test Curve	Compression
128LCCR	3.18	Yes	Test Curve	Compression

Effect of Initial Out-of-Flatness

Figure 13 shows the load versus deflection plot for the models with the experimental stress-strain curve and residual stresses included. The magnitude of the out-of-flatness has a minor effect on the stiffness and yield load, but the effect on the ultimate capacity is not significant. The initial out-of-flatness for all remaining models in

this study was 0.79 mm because this was closest to the maximum measured imperfection by Dowswell and Fouad (2005).

Effect of Residual Stresses

Figure 14 shows the effect of residual stresses on the behavior of the models. The models with compressive brace loads showed a significant reduction in capacity when residual stresses were included. The tension models showed a slight stiffening effect caused by the residual stresses. This is because the most highly stressed region of the plate is at the inner edges near the reentrant corner, where the applied stress acts in compression and the residual stress acts in tension. The applied stress must overcome the residual stress before the material yields.

Effect of Stress–Strain Relationship

Figure 15 shows the difference between the elastic-plastic stress-strain curves and the experimental curves for the models without residual stresses. The difference in the stiffness and yield strength is insignificant between the two material models. For the elastic-plastic models, the plates were not able to carry additional loading after they were fully yielded, and the yield loads equaled the ultimate loads. For the models with the experimental curve, the plates were able to take on more load after they yielded, due to strain hardening.

CONCLUSIONS

A parametric study was conducted, which included material and geometric nonlinearities. The effects of the following parameters were studied: mesh size, magnitude of the initial out-of-flatness, the effect of residual stresses, and the shape of the stress-strain curve. A linear mesh study was performed, and it was determined that Mesh 1 is adequate.

The magnitude of the out-of-flatness has a minor effect on the stiffness and yield load, but the effect on the ultimate capacity is not significant. An initial out-of-flatness of 0.79 mm can be used, based on the measured imperfections by Dowswell and Fouad (2005). The models with compressive brace loads showed a significant reduction in capacity when residual stresses were included; therefore, it is recommended that the effect of residual stresses be accounted for. At yield loads, the elastic-plastic model and the model with the experimental stress-strain curve behaved almost identically. The strain hardening portion of the curve provides useful information about the behavior of wrap-around gusset plates; however, the large in-plane deformations at this level of loading make the use of this extra strength impractical in design.

REFERENCES

- Bjorhovde, R., Brozetti, J., Alpsten, G.A., and Tall, L. (1972), "Residual Stresses in Thick Welded Plates," *Welding Research Supplement*, August, 392s-405s.
- Bjorhovde, R., Engstrom, M.F., Griffis, L.G., Kloiber, L.A., and Malley, J.O. (2001), *Structural Selection Considerations: A Guide for Students, Educators, Designers, and Builders*, American Society of Civil Engineers, New York, New York.
- Chakrabarti, S. K. and Richard, R. M. (1990), "Inelastic Buckling of Gusset Plates," *Structural Engineering Review*, Vol. 2, pp. 13-29.

Chakrabarti, S. K. (1987), "Inelastic Buckling of Gusset Plates," Doctoral Dissertation, University of Arizona.

Cheng, J. J. R., Yam, M. C. H., and Hu, S. Z. (1994), "Elastic Buckling Strength of Gusset Plate Connections," *Journal of Structural Engineering*, ASCE, Vol. 120, No. 2, February, pp. 538-559.

Cheng, J. J. R. and Hu, S. Z. (1987), "Comprehensive Tests of Gusset Plate Connections," *Proceedings, 1987 Annual Technical Session*, Structural Stability Research Council, pp. 191-205.

Desai, S. (1970), "Application of Finite Element Method to the Problem of Gusseted Connections," Civil Engineering Report to Dr. J. W. Fisher, Lehigh University, January.

Dowswell, B. and Fouad, F. (2005), "Wrap-Around Gusset Plates in Tension," Page 33 of this document.

Dwight, J.B. and Moxham, K.E. (1977), "Comprehensive Strength of Welded Plates," *Stability of Structures Under Static and Dynamic Loads*, American Society of Civil Engineers, 463-480.

Dwight, J.B. and Ractliffe, A.T. (1967), "The Strength of Thin Plates in Compression," *Thin Walled Steel Structures: Their Design and Use in Building*, Crosby Lockwood & Son, Ltd., pp. 3-34.

Lavis, C. S. (1967), "Computer Analysis of the Stresses in a Gusset Plate," Master's Thesis, University of Washington.

Rabern, D. A. (1983), "Stress, Strain and Force Distributions in Gusset Plate Connections," Master's Thesis, University of Arizona.

Rabinovitch, Jeffrey and Cheng, J. J. R. (1993), "Cyclic Behavior of Steel Gusset Plate Connections," University of Alberta Department of Civil Engineering Structural Engineering Report No. 191, August.

Rao, N. and Tall, L. (1961), "Residual Stresses in Welded Plates," *Welding Research Supplement*, October, 468s-480s.

Richard, R. M. (1986), "Analysis of Large Bracing Connection Designs for Heavy Construction," *National Steel Construction Conference Proceedings*, AISC, Chicago, IL, pp. 31.1-31.24.

Struik, J. H. A. (1972), "Applications of Finite Element Analysis to Non-linear Plane Stress Problems," Doctoral Dissertation, Lehigh University.

Walbridge, S. S., Grondin, G. Y., and Cheng, J. J. R. (1998), "An Analysis of the Cyclic Behavior of Steel Gusset Plate Connections," University of Alberta Department of Civil and Environmental Engineering Structural Engineering Report No. 225, September.

Whitmore, R. E. (1952), "Experimental Investigation of Stresses in Gusset Plates," University of Tennessee Engineering Experiment Station Bulletin No. 16, May.

Williams, G. C. (1986), "Steel Connection Designs Based on Inelastic Finite Element Analysis," Doctoral Dissertation, The University of Arizona.

Yam, M. C. H. and Cheng, J. J. R. (1993), "Experimental Investigation of the Compressive Behavior of Gusset Plate Connections," University of Alberta Department of Civil Engineering Structural Engineering Report No. 194, September.

Yamamoto, K., Akiyama, N. and Okumura, T. (1988), "Buckling Strengths of Gusseted Truss Joints," *Journal of Structural Engineering*, ASCE, Vol. 114, No. 3, March, pp. 575-591.

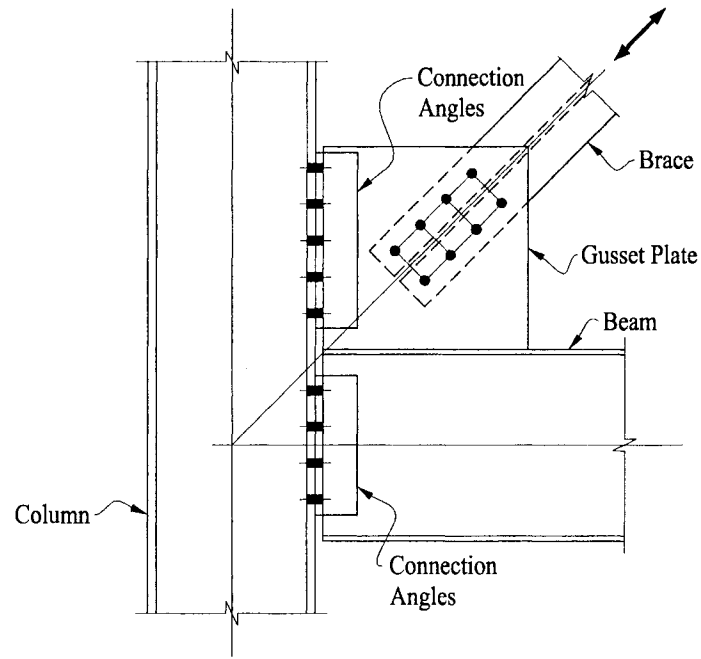


Fig. 1. Standard vertical brace connection.

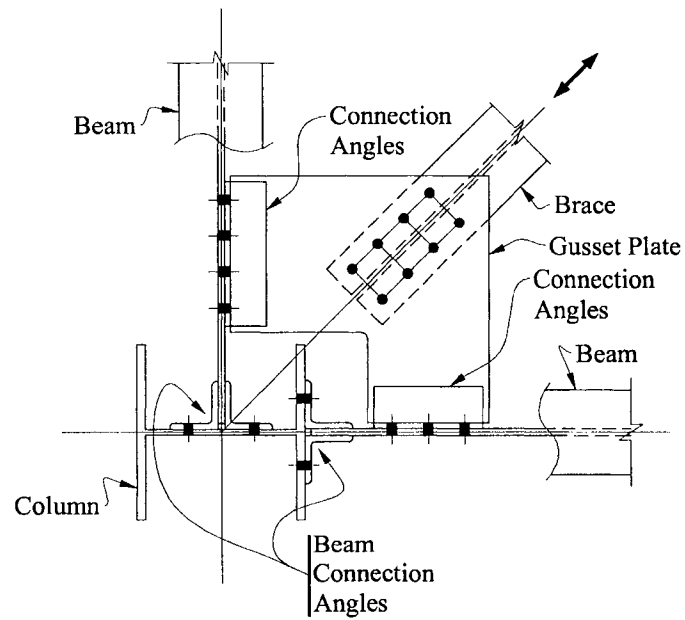


Fig. 2. Horizontal brace connection at beam-to-column intersection.

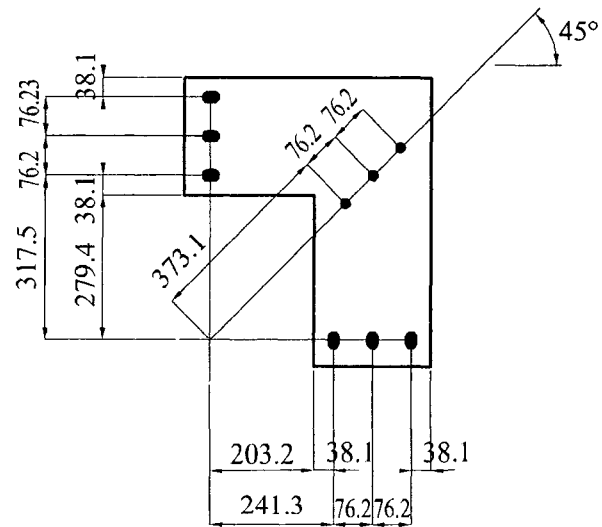


Fig. 3. Dimensions of the plate modeled.

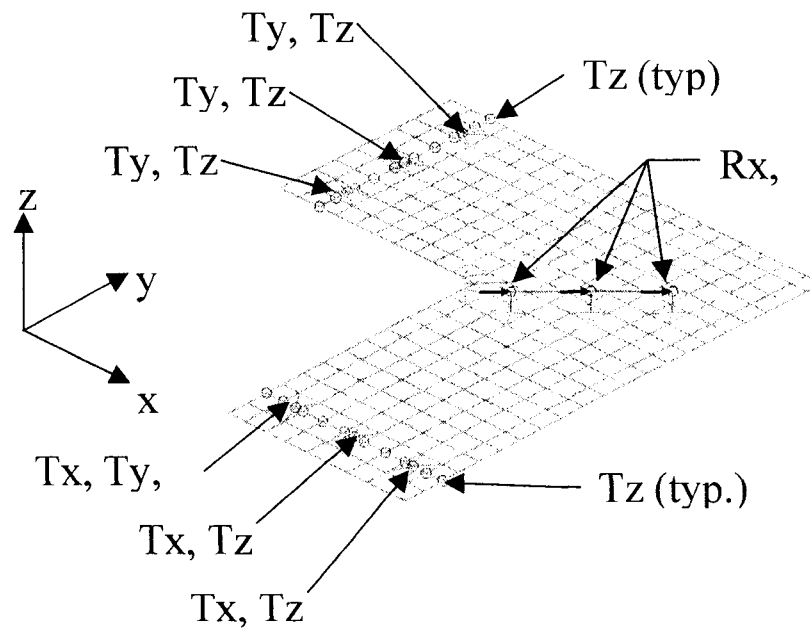


Fig. 4. Boundary conditions.

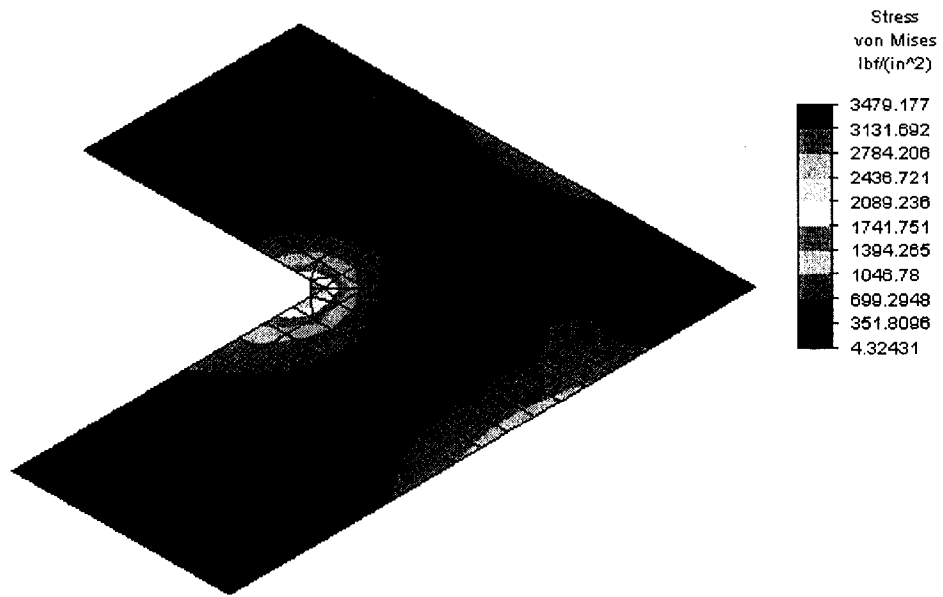
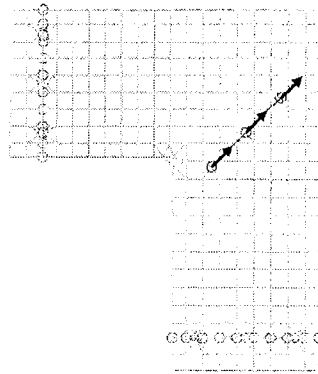
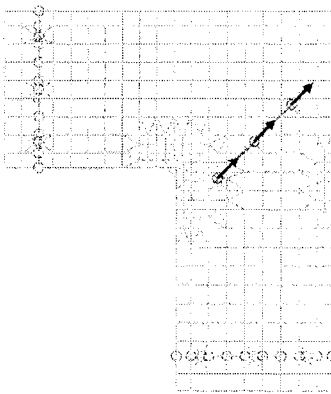


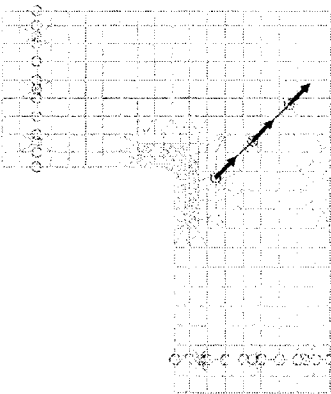
Fig. 5. Von Mises stress contour for Mesh 1.



a. Mesh 1

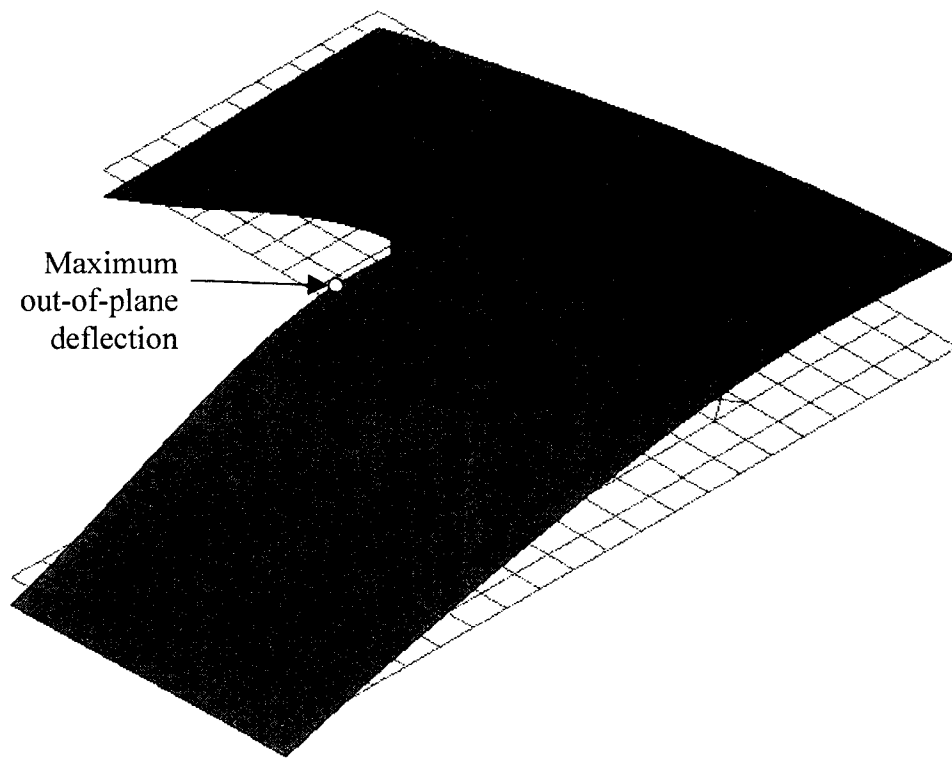


b. Mesh 2

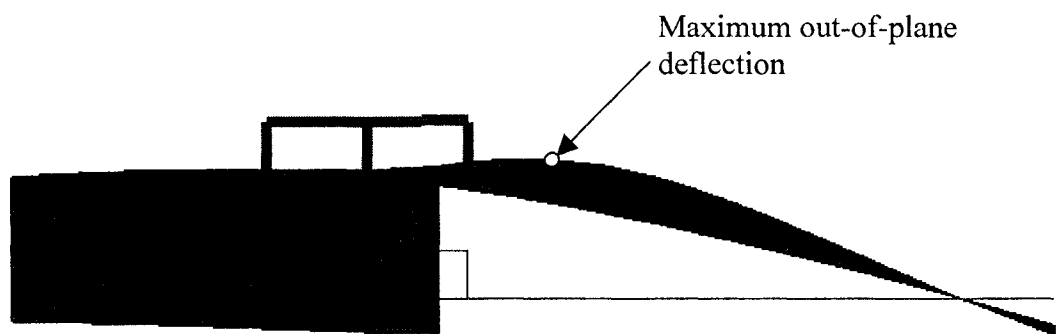


c. Mesh 3

Fig. 6. Mesh Schemes Studied.

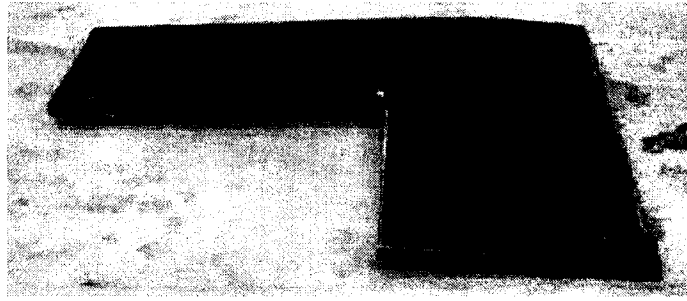


a. Top view.

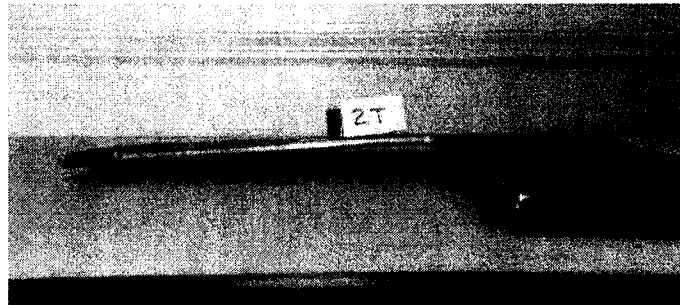


b. Side View.

Fig. 7. Buckled shape for elastic buckling analysis.



a. Top view



b. Side view

Fig. 8. Residual deformation of Specimen 2 from Dowswell and Fouad (2005).

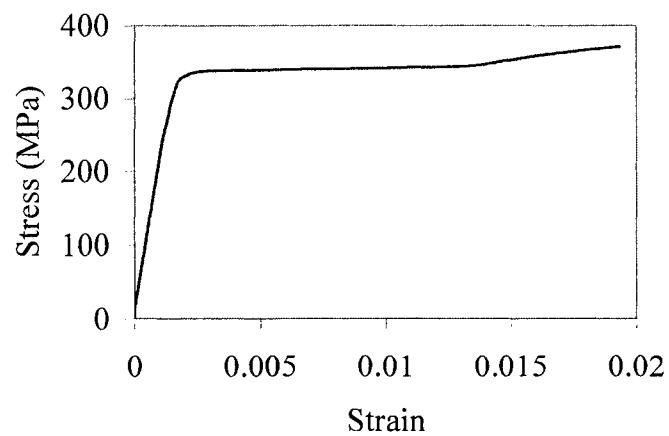


Fig. 9. Experimental stress-strain curve by Dowswell and Fouad (2005).

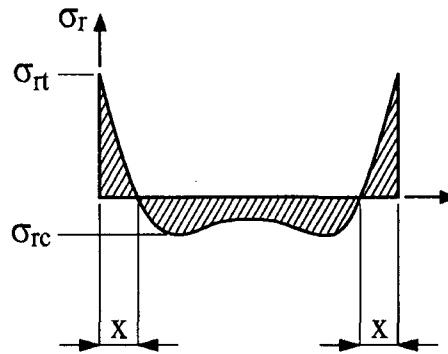


Fig. 10. Residual stress pattern in a flame-cut plate.

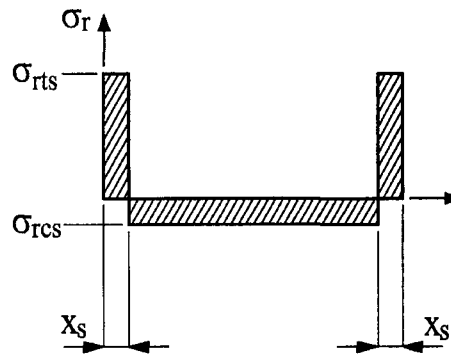


Fig. 11. Simplified residual stress pattern.

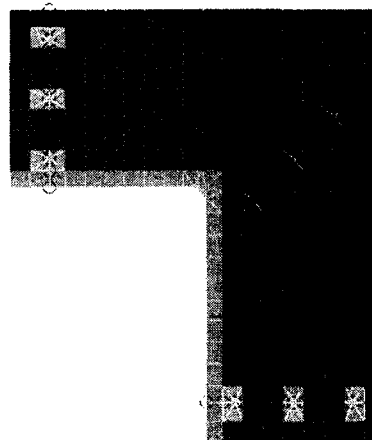
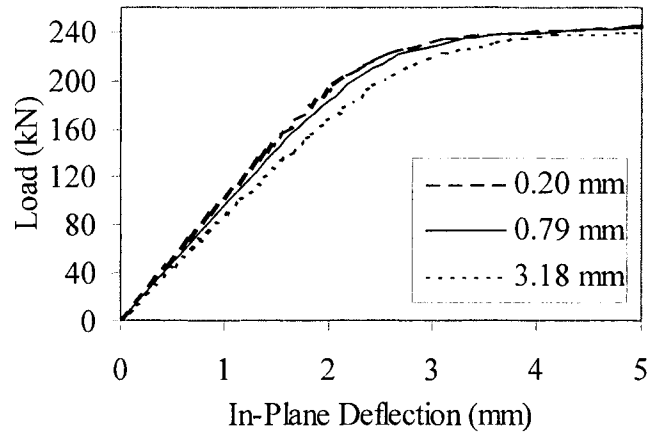
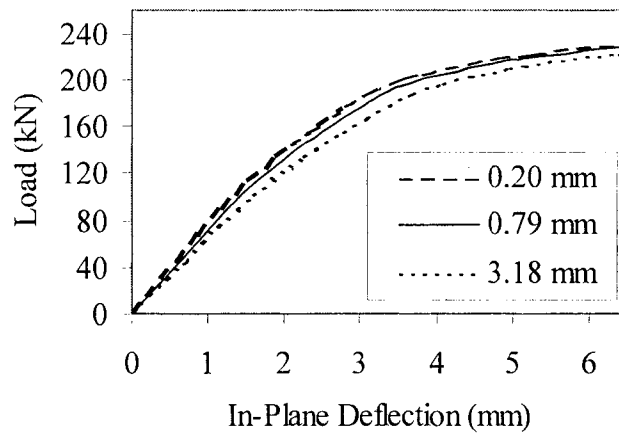


Fig. 12. Model with residual stresses at edges.

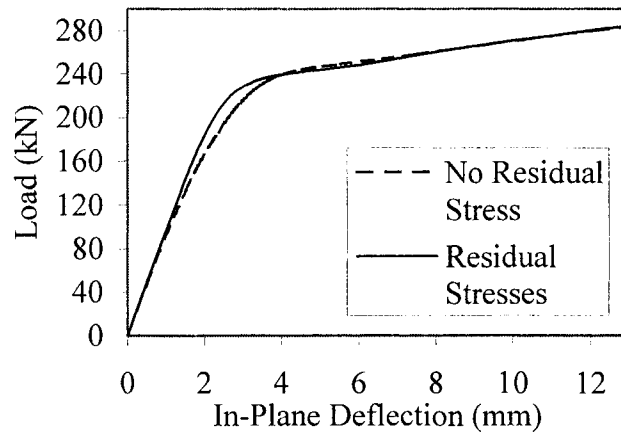


a. Tension load

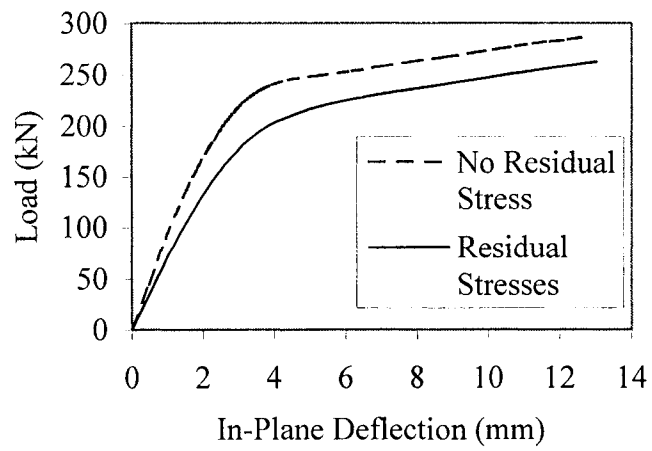


b. Compression load

Fig. 13. Load versus in-plane deflection for models with residual stresses and experimental stress strain curve.

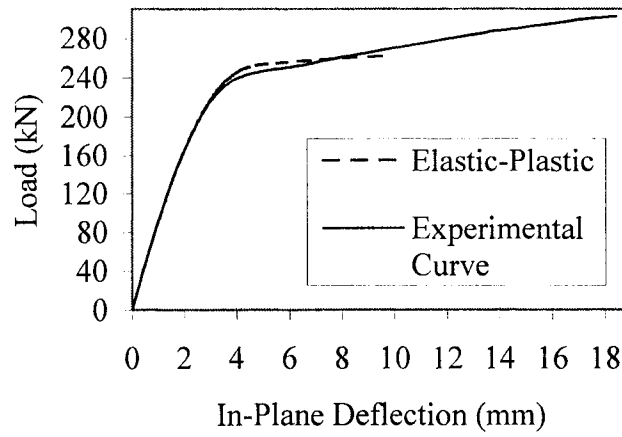


a. Tension load

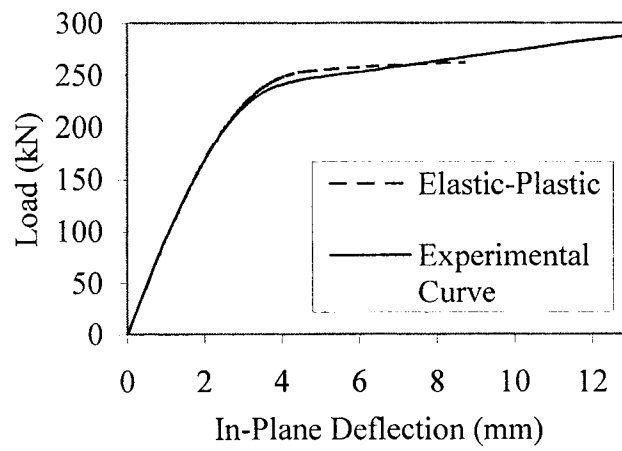


b. Compression load

Fig. 14. Load versus in-plane deflection for model with residual stresses and without residual stresses incorporated. Experimental curve.



a. Tension load



b. Compression load

Fig. 15. Load versus in-plane deflection for model with elastic-plastic curve and experimental curve. No residual stresses.

FINITE ELEMENT ANALYSIS OF WRAP-AROUND GUSSET PLATES

by

BO DOWSWELL, ROBERT WHYTE, JIM DAVIDSON, AND FOUAD FOUAD

In preparation for American Institute of Steel Construction Engineering Journal

Format adapted for dissertation

INTRODUCTION

Gusset plates are used in steel buildings to connect bracing members to other structural members in the lateral force resisting system. Horizontal bracing is commonly used to resist lateral loads in industrial structures and in commercial buildings where floor and roof diaphragms cannot carry the loads. Wrap-around gusset plates are L-shaped plates that are used where an opening is required at the corner of the plate. This typically occurs at horizontal bracing where the gusset plate is cut out around a column, as shown in Figure 1.

Finite element models were used to determine the behavior of wrap-around gusset plates. The plates were modeled using material and geometric nonlinearities. Ten different gusset plates were modeled with geometry and material properties matching the experimental specimens of Dowswell and Fouad (2005b). All 10 of the models were loaded in compression and 5 were loaded in tension. The loads from the finite element models were compared to the experimental loads.

Problem Statement

Due to the increasing complexity of building designs, horizontal bracing members are being used to resist very large forces. A large number of research projects have been dedicated to the analysis and design of standard gusset plates; however, there are no published methods for designing wrap-around gusset plates. There are a number of possible failure modes unique to wrap-around gusset plates. These need to be addressed so that design engineers can provide safe and economical designs.

Objectives

The purpose of this research was to study the behavior of wrap-around gusset plates using the finite element method.

EXISTING LITERATURE

A large number of research projects have been dedicated to the analysis and design of standard gusset plates. Failure modes for standard gusset plates have been identified, and design procedures are well-documented in the literature. However, failure modes unique to wrap-around gusset plates have not been studied nor are guidelines for their design available in the literature. Dowswell and Fouad (2005a) summarized the existing research on the stress distribution in standard gusset plates. Dowswell and Barber (2004) summarized previous experiments and finite element studies on gusset plates in compression. Dowswell and Fouad (2005b) reviewed the existing experimental research on statically loaded gusset plates, and Dowswell et al. (2005) reviewed the research on finite element modeling of gusset plates.

PROCEDURE

Specimens Tested by Dowswell and Fouad

Ten different gusset plates were modeled with geometry and material properties matching the experimental specimens of Dowswell and Fouad (2005b). The details of each plate are shown in Figure 2. The plate material was A36. To determine the actual mechanical properties of the material, tension coupons were taken from the same parent plate as the specimens. The 1/4-in. plates had a yield strength of 56.7 ksi, an ultimate

strength of 71.2 ksi, and a modulus of elasticity of 30,000 ksi. The 3/8-in. plates had a yield strength of 48.8 ksi, an ultimate strength of 70.6 ksi, and a modulus of elasticity of 29,000 ksi. The actual thickness of each specimen was measured, and the results are shown in Table 1. The measured thicknesses and material properties were used in the finite element models.

Table 1. Measured Plate Thickness

Specimen	Nominal Thickness (in.)	Measured Thickness (in.)
2T	3/8	0.391
6T	1/4	0.235
8T	3/8	0.384
9T	3/8	0.380
10T	3/8	0.387
1C	3/8	0.381
2C	3/8	0.388
3C	3/8	0.380
4C	1/4	0.235
5C	1/4	0.234
6C	1/4	0.235
7C	3/8	0.387
8C	3/8	0.388
9C	3/8	0.390
10C	3/8	0.384

General Description of Models

A finite element modeling procedure was developed by Dowswell et al. (2005), which accounts for material and geometric nonlinearities. To develop the procedure, the effects of the following parameters were studied: mesh size, magnitude of the initial out-of-flatness, residual stresses, and the shape of the stress-strain curve. It was determined that the mesh scheme shown in Figure 3 is adequate, based on a linear mesh study. The

parametric study also showed that a linear elastic-perfectly plastic material model provided accurate results. The recommendations developed by Dowswell et al. (2005) were used to model the plates in this research.

All 10 of the models were loaded in compression. Only specimens 2, 6, 8, 9, and 10 were loaded in tension. The brace load was applied at the nodes representing the diagonal bolts using a rigid frame to equally distribute the load to each bolt. The rigid frame was modeled with stiff beam elements. The updated lagrangian analysis method was used because the behavior was expected to be highly dependent on the out-of-plane deformations. The finite element modeling software program ALGOR was used.

Because this study focuses on the global behavior of the models rather than the local behavior near the bolts, the elements at the bolt locations were modeled with thick elastic elements. This made the gusset plate models more efficient because the bearing areas between the bolts and the plate become inelastic at early stages of loading, which greatly increased the computation time on preliminary models. Using a preliminary run, it was determined that the local behavior at the bolts has an insignificant effect on the global behavior of the plate. Additionally, the mesh size was approximately the same size as a bolt head or nut that would exert a clamping force to restrain the plate in an actual structure.

Boundary Conditions

The boundary conditions at the brace bolts were set to simulate a typical bracing member connected to the gusset plate. Rotations in the in-plane (x and y) directions were fixed, and the other four degrees of freedom were released. These boundary conditions

provided a simulated bending restraint from the brace member, but allowed the plate to buckle in a sidesway mode

The bolt lines parallel to the x-axis and the y-axis represent the gusset plate to beam interface. The nodes along the bolt lines were fixed against out-of-plane translation. At the bolts in the line parallel to the y-axis, translation was fixed in the y direction. At the bolts in the line parallel to the x-axis, translation was fixed in the x direction. Table 2 and Figure 4 summarize the boundary conditions adopted for the analysis.

Table 2. Summary of Boundary Conditions

Location	Fixed	Free
At brace connection	Rx, Ry	Tx, Ty, Tz, Rz
At bolts in the gusset plate leg perpendicular to the y direction	Ty, Tz	Tx, Rx, Ry, Rz
At bolts in the gusset plate leg perpendicular to the x direction	Tx, Tz	Ty, Rx, Ry, Rz
At first bolt in the gusset plate leg perpendicular to the x direction	Tx, Ty, Tz	Rx, Ry, Rz
Nodes along line of bolt holes in the gusset plate legs	Tz	Tx, Ty, Rx, Ry, Rz

Rx Ry Rz: Rotations in the x, y, and z directions

Tx Ty Tz: Translations in the x, y, and z directions

Initial Out-of-Flatness

Walbridge et al. (1998) found that the shape of the initial imperfection is much less critical than the magnitude. The buckled shape from a linear buckling analysis was

used as the shape of the initial imperfection. The maximum out-of-flatness for all of the specimens tested by Dowswell and Fouad (2005b) was 0.028 in.; therefore, the eigenvector was scaled to give an initial out-of-flatness of 1/32 in.

Residual Stresses

The equipment in most structural steel fabrication shops and the geometry of wrap-around gusset plates dictates that they be flame-cut. The residual stress pattern for plates with flame-cut edges is shown in Figure 5. Dowswell et al. (2005) showed that gusset plates with compressive brace loads had a significant reduction in capacity when residual stresses were included in the models; therefore, the effect of residual stresses are included in this study. Dowswell et al. (2005) modeled the residual stresses with the simplified pattern shown in Figure 6. According to their research, the tension residual stress, σ_{rx} , can be set equal to the yield strength of the plate, and the tension width in the pattern, x_s , is 0.85-in.

The residual stresses were modeled using a 0.85-in.-wide strip along each edge of the gusset plate. From preliminary models, it was determined that the stresses on the outer edges were always of the same sense as the applied load, and the stresses on the inner edges were always of the opposite sense as the applied load. Because the residual stresses used in the model were equal to the material yield stress, the elements on the tension edges were modeled with a yield stress of zero. The yield stress was doubled for the elements on the compression edges.

RESULTS

Out-of-Plane Deformations

The buckled shape of Model 2T from the linear buckling analysis is shown in Figure 7. The out-of-plane deformation for all of the tension models was at its maximum near the reentrant corner where the two legs met. The buckled shapes are similar to the specimens tested in tension by Dowswell and Fouad (2005c). The compression models had an out-of-plane deformation, which was at its maximum at the outer edge of the legs, as shown in Figure 8. The location of the maximum deformation is consistent with the test specimens of Dowswell and Fouad (2005b). Both the tests and finite element models showed twisting in the legs in addition to the lateral deformation, indicating a lateral-torsional buckling type of failure.

Flexural Stresses

Figure 9 shows the theoretical bending stress in each leg of a gusset plate. The elastic stress distribution is shown in Figure 9a, and the plastic distribution is shown in Figure 9b. As discussed by Dowswell and Fouad (2005a), it is unclear which stress distribution is closest to the actual stresses within a gusset plate.

Figure 10 shows the elastic stress contours for Model 2T. In Figure 10a, it can be seen that the highest von Mises stresses are concentrated at the reentrant corner where the two legs meet. Figure 10b shows the normal stresses in the x-direction. The highest stresses are at the edges of the gusset leg. The stresses on opposite edges of each leg are similar in magnitude and of opposite sense, indicating flexure in the leg. Figure 10c shows the normal stresses in the y-direction. The stress pattern is similar to that of the

adjacent leg; however, the stresses in the y-direction are higher than the stresses in the x-direction because of the larger cutout dimension in the y-direction.

The flexural stresses along Section a-a in Figure 10b are shown in Figure 11 for a brace load of 65 k. The stresses from the elastic model are plotted, but it is clear that much of the cross-section is stressed beyond the yield strength of 48.8 ksi. The inelastic stresses are also plotted, as are the theoretical stresses that were calculated using elastic beam theory. The maximum elastic stresses in the plates are reasonably close to the stresses calculated using simple beam theory. As the material begins to yield, the stresses redistribute, and the stresses move closer to the plastic distribution. None of the models reached a fully plastic distribution before the maximum load was reached.

The inelastic behavior and the existence of flexural stresses in the gusset legs confirms the experimental findings of Dowswell and Fouad (2005b) and Dowswell and Fouad (2005c), where strain gage readings showed similar behavior. The stress patterns and stress versus load behavior were similar for all of the models.

Load Versus In-Plane Deflection

All of the models had load versus in-plane deflection plots that were linear for most of the load range. The nonlinear load range is relatively small due to the linear elastic-perfectly plastic material model that was used. Dowswell et al. (2005) showed that a strain-hardening curve is more accurate in the inelastic range, but the two models produce almost identical results in the elastic range. Load vs. deflection plots for Models 2T and 9T are shown in Figure 12. The plots for the remaining models were similar in shape.

The yield loads, P_{fy} , were determined using a 1/64-in. offset relative to the linear portion of the load versus deflection plots. The yield load is where the load vs. deflection curve crosses the 1/64-in. offset line. The ultimate loads, P_{fu} , are the maximum loads reached by the models. The yield and ultimate loads are shown in Table 3, along with the experimental loads of Dowswell and Fouad (2005b) and Dowswell and Fouad (2005c). The average experimental-to-finite element ratio for yield is 0.96. The standard deviation is 0.22. The average experimental-to-finite element ratio for ultimate is 1.00, with a standard deviation of 0.21.

The deflected shape of Model 2T is shown in Figure 13b. It is similar to Specimen 2T tested by Dowswell et al. (2005), shown in Figure 13a. The angle between the gusset legs decreased for the models loaded in tension and increased for the models loaded in compression.

The load versus deflection data for model 2C is plotted with the experimental results in Figure 14. The finite element models had a steeper curve than the experiments, indicating a higher stiffness. This may be due to the flexibility of the testing setup. The finite element models generally had a lower ultimate strength than the tests due to the elastic-plastic material model.

Table 3. Loads from Finite Element Models and Experiments

Spec. No.	Experimental Load (k)		Finite Element Load (k)		Experimental/ Finite Element	
	P_{ey}	P_{eu}	P_{fy}	P_{fu}	P_{ey}/P_{fy}	P_{eu}/P_{fu}
2T	69.0	89.9	50.7	65.0	1.36	1.38
6T	42.3	53.6	39.9	52.5	1.06	1.02
8T	85.3	91.2	73.8	78.5	1.16	1.16
9T	51.5	63.6	46.9	60.0	1.10	1.06
10T	96.2	109.8	84.8	104	1.13	1.06
1C	33.3	45.8	51.6	58.0	0.64	0.79
2C	47.3	63.9	44.7	51.5	1.06	1.24
3C	46.6	64.2	45.0	52.5	1.03	1.22
4C	32.0	32.0	30.2	35.0	1.06	0.91
5C	28.7	46.8	36.3	41.5	0.79	1.12
6C	25.3	25.3	34.5	41.0	0.73	0.61
7C	46.4	46.5	51.3	60.0	0.90	0.78
8C	38.4	60.8	67.6	73.5	0.57	0.82
9C	44.4	51.5	38.7	50.0	1.15	1.03
10C	57.0	66.5	76.6	84.5	0.74	0.80

P_{ey} experimental yield load determined using a 1/64-in. offset.

P_{eu} maximum experimental load

P_{fy} finite element yield load determined using a 1/64-in. offset.

P_{fu} maximum load from finite element model

CONCLUSIONS

Ten wrap-around gusset plates were modeled to determine their behavior under tension and compression loads. The gusset plates were modeled with geometry and material properties matching experimental specimens tested previously. The behavior of the finite element models closely resembled that of the specimens. The stresses within the plates indicated that the brace load is resisted primarily by flexure in the gusset legs. The flexural stresses were largest at the edges of the gusset legs near the reentrant corner. In the early stages of loading the load versus in-plane deflection behavior was linear. The

maximum out-of-plane deformation was at the reentrant corner for the models loaded in tension. The compression models had an out-of-plane deformation, which was at its maximum at the outer edge of the legs. The out-of-plane deformations were accompanied by twist of the gusset plate legs, indicating a lateral-torsional buckling failure. The deformed shapes as well as the yield and ultimate loads compared well with the experimental results.

REFERENCES

Dowswell, B., and Barber, S. (2004), "Buckling of Gusset Plates: A Comparison of Design Equations to Test Data," *Proceedings, 2004 Annual Stability Conference*, Structural Stability Research Council, pp. 199-221.

Dowswell, B., Whyte, R., Davidson, J., and Fouad, F. (2005), "Modeling Techniques for Wrap-Around Gusset Plates," Page 74 of this document.

Dowswell, B. and Fouad, F. H. (2005a), "Design Considerations for Wrap-Around Gusset Plates," Page 3 of this document.

Dowswell, B. and Fouad, F. H. (2005b), "Wrap-Around Gusset Plates in Compression," Page 50 of this document.

Dowswell, B. and Fouad, F. H. (2005c), "Wrap-Around Gusset Plates in Tension," Page 33 of this document.

Walbridge, S. S., Grondin, G. Y., and Cheng, J. J. R. (1998), "An Analysis of the Cyclic Behavior of Steel Gusset Plate Connections," University of Alberta Department of Civil and Environmental Engineering Structural Engineering Report No. 225, September.

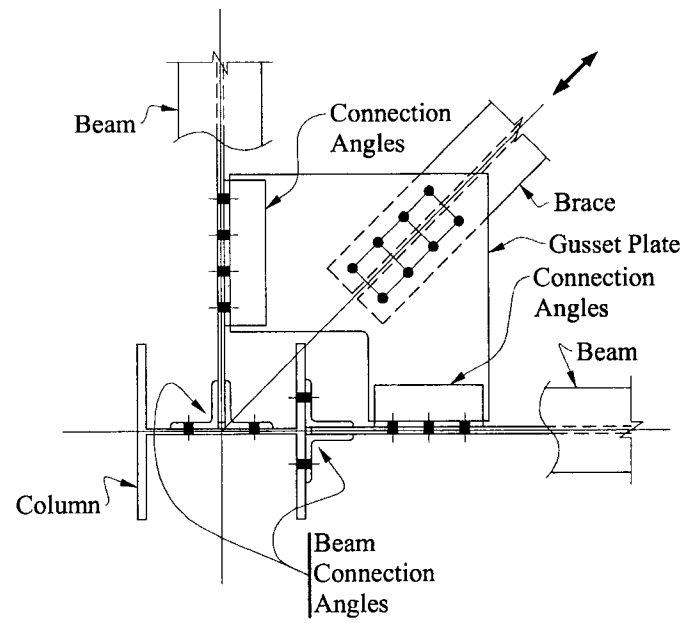


Fig. 1. Wrap-around gusset plate connection.

[illegible][illegible][illegible]

Reproduced with permission of the copyright owner. Further reproduction prohibited without permission.

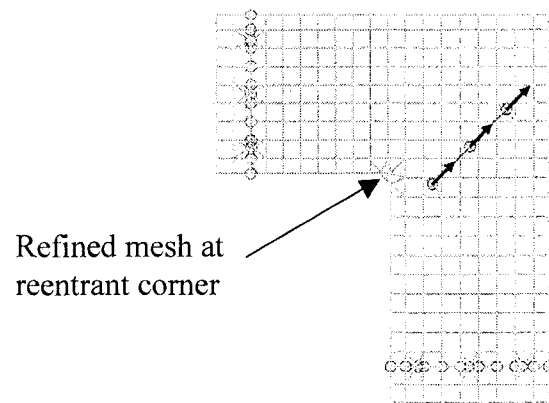


Fig. 3. Mesh Scheme.

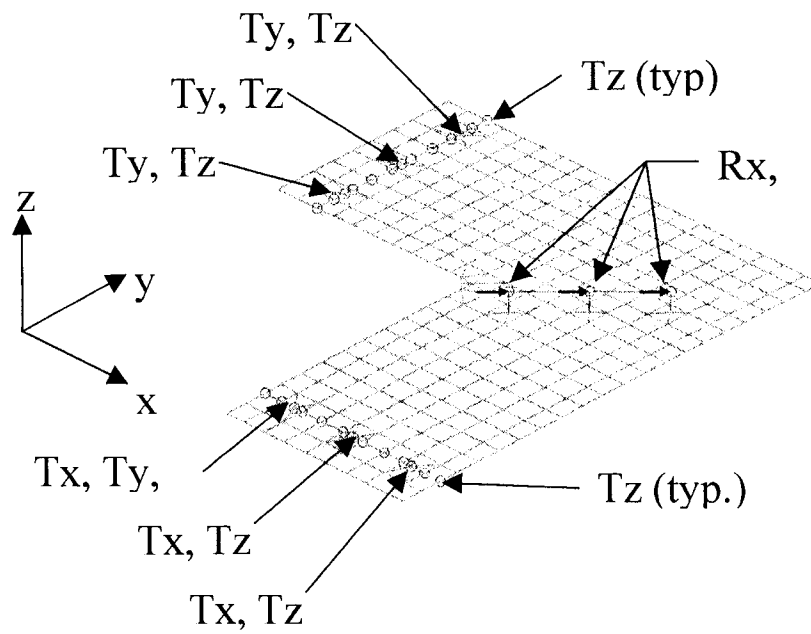


Fig. 4. Boundary conditions.

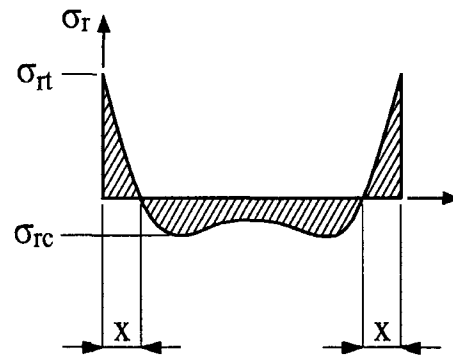


Fig. 5. Residual stress pattern in a flame-cut plate.

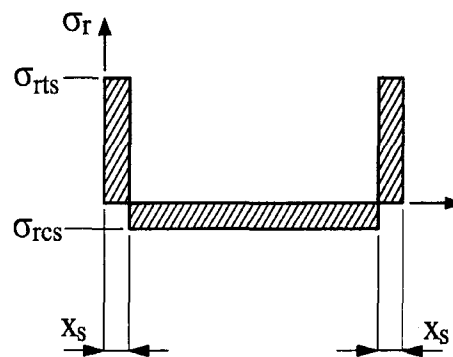
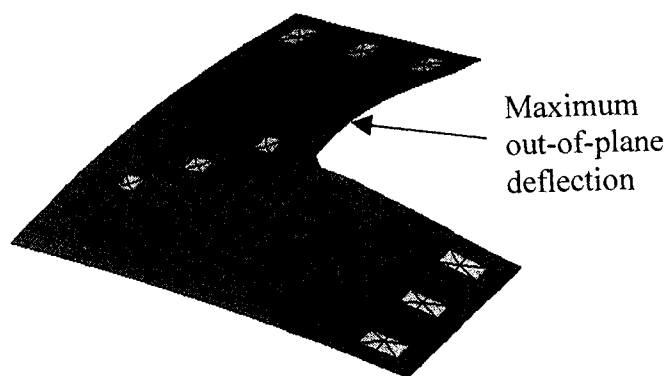
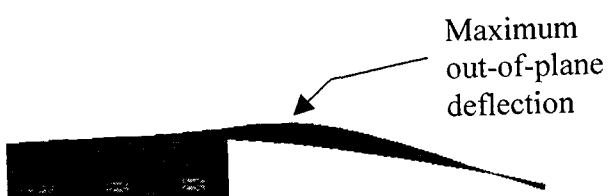


Fig. 6. Simplified residual stress pattern.



a. Top view.



b. Side View.

Fig. 7. Buckled shape for Model 2T.

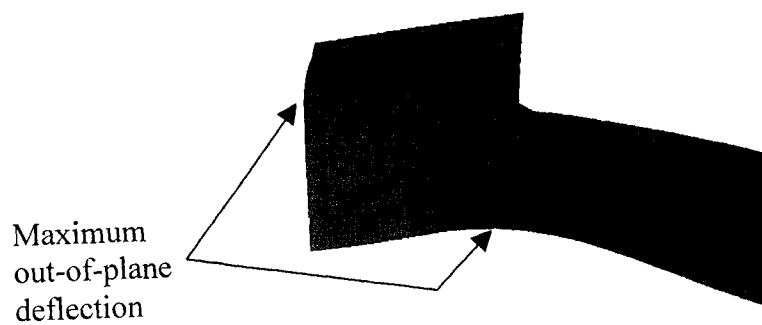
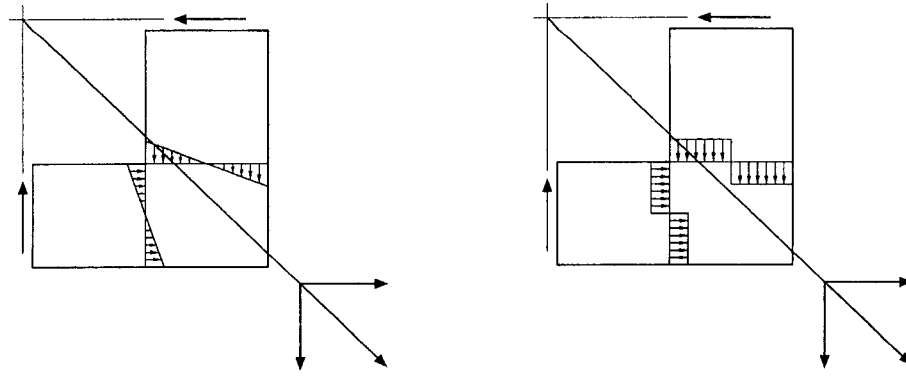


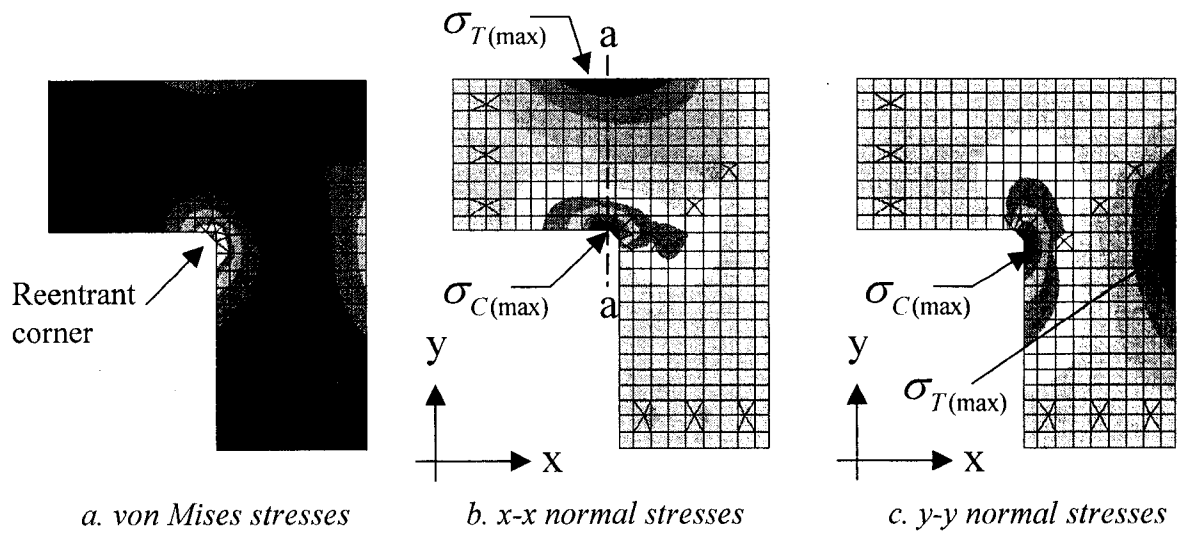
Fig. 8. Buckled shape for Model 6C.



a. Elastic

b. Plastic

Fig. 9. Bending stresses in gusset plate legs.



a. von Mises stresses

b. x-x normal stresses

c. y-y normal stresses

Fig. 10. Elastic stress contours for Model 2T.

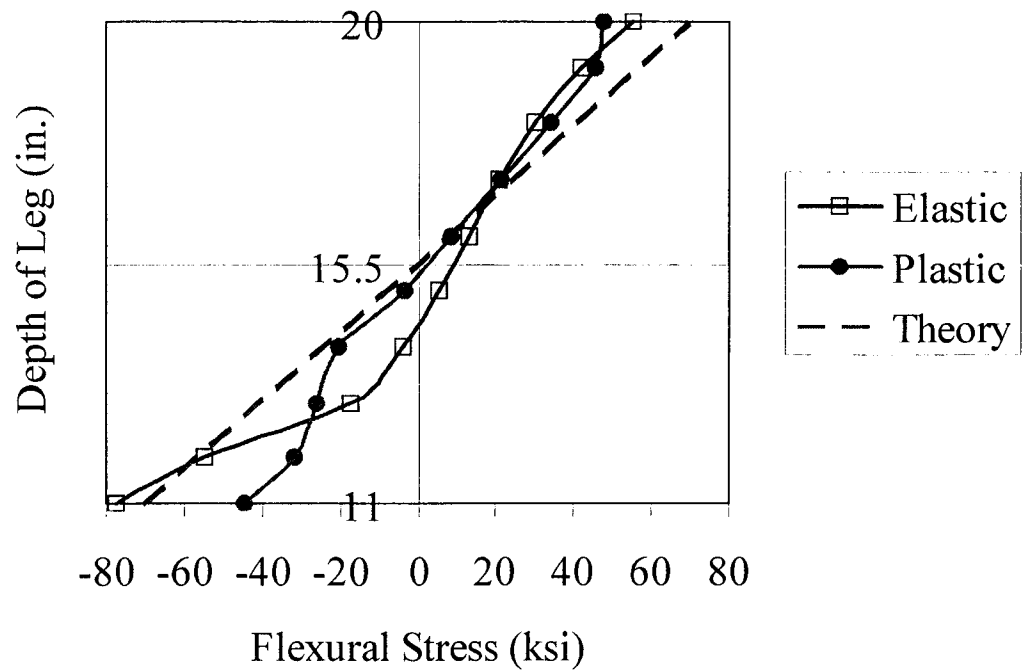
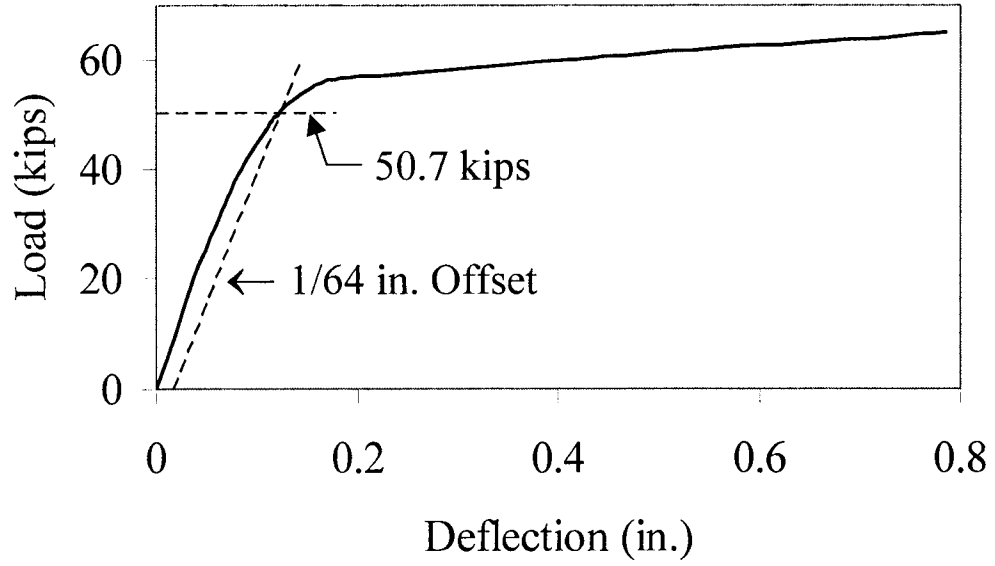
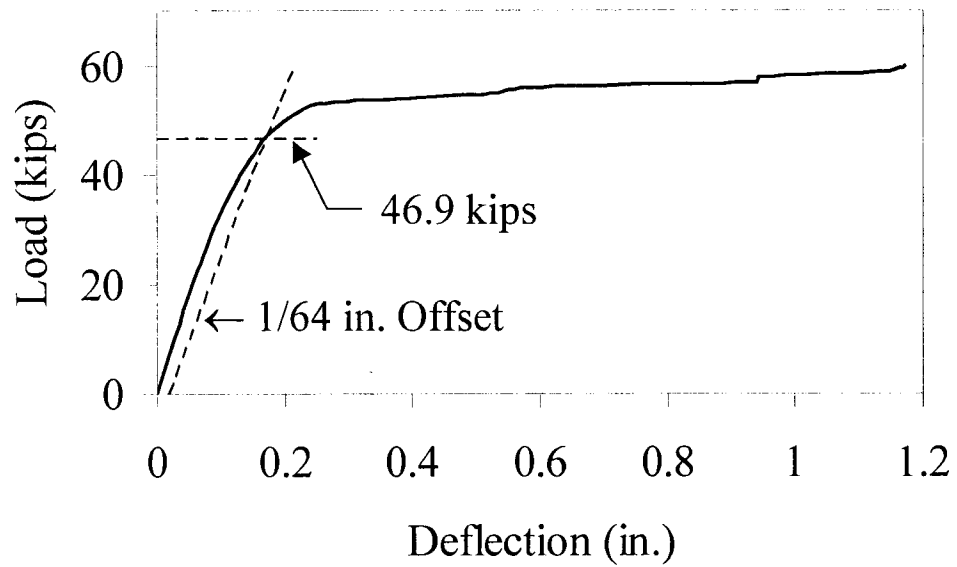


Fig. 11. Flexural stresses in 8-in. leg of plate 2T at a brace load of 65 k

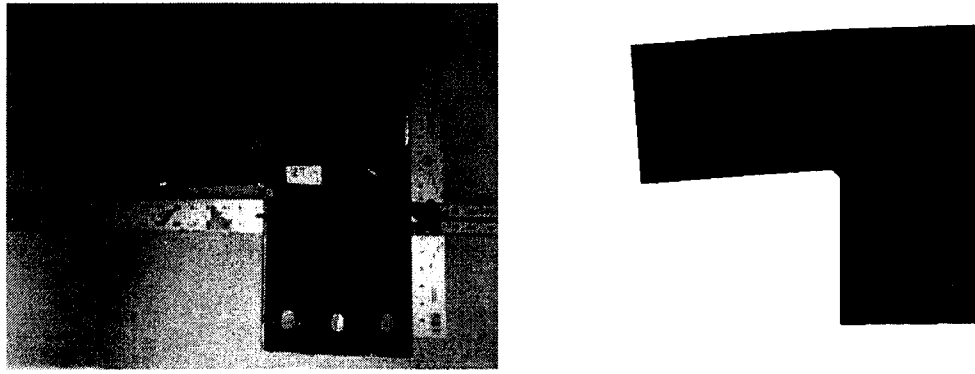


a. Model 2T



b. Model 9T

Fig. 12. Load versus deflection plots for finite element models.



a. Specimen 2T

b. Model 2T

Fig. 13. In-plane deformation of Model 2T.

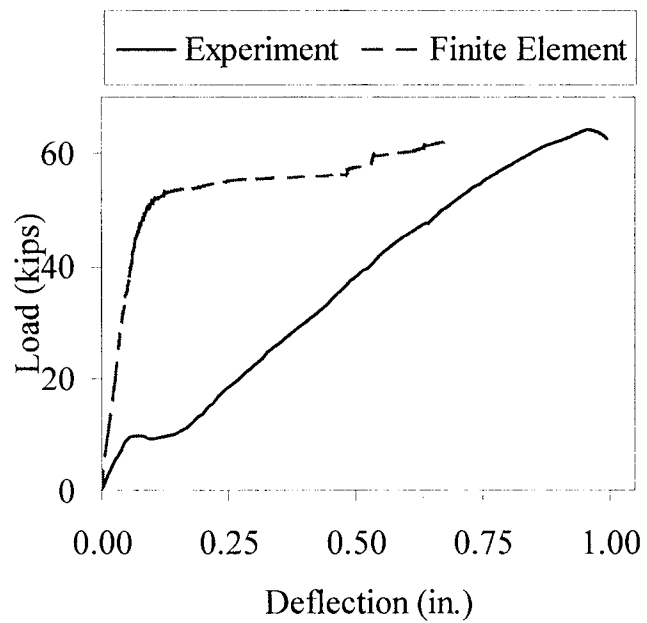


Fig. 14. Load versus deflection data for Model 2C and Specimen 2C.

A PROPOSED DESIGN METHOD FOR WRAP-AROUND GUSSET PLATES

by

BO DOWSWELL AND FOUAD FOUAD

In preparation for American Institute of Steel Construction Engineering Journal

Format adapted for dissertation

INTRODUCTION

Gusset plates are used in steel buildings to connect bracing members to other structural members in the lateral force resisting system. Horizontal bracing is commonly used to resist lateral loads in industrial structures and in commercial buildings where floor and roof diaphragms cannot carry the loads. Wrap-around gusset plates are L-shaped plates that are used where an opening is required at the corner of the plate. This typically occurs at horizontal bracing where the gusset plate is cut out around a column, as shown in Figure 1. Results from experiments and finite element models have been used to formulate a design method for wrap-around gusset plates subjected to tension or compression loads.

Problem Statement

Design procedures for standard gusset plates are well-documented in the literature; however, a design method for wrap-around gusset plates needs to be established.

Objectives

The purpose of this paper is to present a design method for wrap-around gusset plates. The accuracy of the proposed design method is verified by comparing the calculated capacities to experimental and finite element results.

BACKGROUND

The design procedure proposed in this paper is based on the research of Dowswell et al. (2005), Dowswell and Fouad (2005a), Dowswell and Fouad (2005b), and Dowswell and Fouad (2005c). The design procedure was developed for failure modes unique to wrap-around gusset plates. Some failure modes common to standard gusset plates are also potential failure modes for wrap-around gusset plates. Because these are adequately documented in the literature, they will not be reviewed here.

PROPOSED DESIGN METHOD

Force Distribution

Dowswell and Fouad (2005a) showed that the most practical force distribution in wrap-around gusset plates has each leg acting in shear, as shown in Figure 2. Using finite element models, Dowswell et al. (2005) showed that this force distribution is reasonable based on the flexural stresses in the legs. The research indicates that wrap-around gusset plates are subject to limit states common to flexural members; therefore, the proposed design method is based on a cantilever beam model at each leg.

Shear Stresses

The current design method for the limit state of shear at the gusset plate legs was summarized by Dowswell and Fouad (2005). All of the experimental specimens and finite element models failed by flexural yielding or buckling of the gusset plate legs; therefore, no information was gained relating to the shear behavior. The nominal shear capacity of each leg is:

$$V_{n1} = 0.6F_y d_1 t \quad (1a)$$

$$V_{n2} = 0.6F_y d_2 t \quad (1b)$$

where t is the gusset plate thickness, d_1 and d_2 are the depths of the gusset plate legs, and F_y is the yield strength. For the design to be adequate, the following must be satisfied:

$$\phi V_{n1} \geq P_1 \quad (2a)$$

$$\phi V_{n2} \geq P_2 \quad (2b)$$

where P_1 and P_2 are the factored components of P . For shear yielding, $\phi = 0.9$.

Flexural Stresses

Strain gages mounted on the specimens tested by Dowswell and Fouad (2005b) and Dowswell and Fouad (2005c) showed that the gusset legs were in almost pure flexure. Dowswell et al. (2005) confirmed this using finite element models. Each leg of the gusset plate must resist the flexural stresses generated by the force system in Figure 2. This force system results in maximum bending moments at the reentrant corner in each leg, as shown in Figure 3. Figure 4 shows the stress contour plots for a typical finite element model loaded in tension. In Figure 4a, it can be seen that the highest von Mises stresses are concentrated at the reentrant corner where the two legs meet. Figure 4b shows the normal stresses in the x-direction, and Figure 4c shows the normal stresses in the y-direction. The stresses are largest at the edges of the gusset plate legs. The stresses in the y-direction are higher than the stresses in the x-direction because of the larger

cutout dimension in the y-direction. These stress patterns verify the accuracy of the proposed design model in determining the location of the maximum flexural stresses.

From the strain gage data and finite element models, it was determined that the flexural stresses in the gusset plates exceeded the yield stress throughout much of the gusset plate. Although most of the plates had a substantial amount of the material above the proportional limit, none of the plates reached full plasticity before buckling. A typical plot of the elastic and inelastic stresses is shown in Figure 5 for a finite element model loaded to its failure load. The theoretical stresses, which were calculated using simple beam theory, are also shown in the figure. The proposed design method is based on an elastic bending stress distribution.

The bending moments at the critical sections of the plate are:

$$M_{u1} = P_1 e_2 \quad (3a)$$

$$M_{u2} = P_2 e_1 \quad (3b)$$

where P_1 and P_2 are the components of the factored brace load, P . e_1 and e_2 are the cutout dimensions at each leg, as shown in Figure 2. The nominal moment capacity of each leg is:

$$M_{n1} = F_y \frac{t d_1^2}{6} \quad (4a)$$

$$M_{n2} = F_y \frac{t d_2^2}{6} \quad (4b)$$

For the design to be adequate, the following must be satisfied:

$$\phi M_{n1} \geq M_{u1} \quad (5a)$$

$$\phi M_{n2} \geq M_{u2} \quad (5b)$$

where $\phi = 0.9$ for flexural yielding.

Sometimes wrap-around gusset plates have the interior corner cut on a diagonal, as shown in Figure 6b, in an effort to increase their capacity. The test Specimens 8 and 10, shown in Figure 6, were identical except for the diagonal cut on Specimen 10. The tests and finite element models showed that the average capacity for Specimen 10 was 22 percent higher than the average capacity for Specimen 8. Figure 7 shows the stress contour plots for Specimen 10. Figure 7a shows the normal stresses in the x-direction and Figure 7b shows the normal stresses in the y-direction. The moment capacity at cross sections *a-a* and *b-b* should be checked at each leg using Equations 3, 4, and 5. Calculations show that the flexural stresses in the x-direction at Section b-b are 2.40 times the stresses at Section a-a. The finite element stresses in Figure 7a confirm this. Similarly, Figure 7b confirms that Section a-a controls the design for the stresses in the y-direction. The calculated flexural stresses in the y-direction are 89 percent higher at Section a-a than they are at Section b-b.

Lateral-Torsional Buckling

Due to the flexural stresses in the gusset plate legs, they are subject to lateral-torsional buckling. Tests by Dowswell and Fouad (2005c) showed that the flexural stresses in the legs can cause lateral-torsional buckling, even if the brace is loaded in tension. All of the specimens had a permanent out-of-plane deformation at the plate edges with flexural compression stresses. The out-of-plane deformation was accompanied by twisting of the gusset plate legs, indicating a lateral-torsional buckling

failure. This failure mode is shown in Figures 8 and 9 for tension and compression loads, respectively.

Each leg of the gusset plate can be modeled as a cantilever beam to determine the buckling load. The buckled shape of the gusset legs was similar to the buckled shape of the wide flange cantilever beams with lateral bracing at the free end studied by Dowswell (2004). Although the equations presented by Dowswell (2004) are for wide flange cantilever beams, the equations can be used for rectangular beams. According to his research, the critical buckling moment of a cantilever beam is:

$$M_{cr} = C_L C_H C_B \frac{\sqrt{EI_y GJ}}{L} \quad (6)$$

where L is the beam length, C_L is a coefficient to account for the moment distribution along the length of the beam, C_H is a coefficient to account for the effect of load height, and C_B is a coefficient to account for the effect of bracing. The following values from Dowswell (2004) are substituted into the equation,

$C_L = 3.95$ for beams with no warping stiffness and a point load at the free end,

$C_H = 1.0$ for beams loaded at the shear center,

$C_B = 1.42$ for beams braced at the free end.

For a rectangular cross-section, the weak-axis moment of inertia, I_y is

$$I_y = \frac{t^3 d_i}{12} \quad (7)$$

and the torsion constant, J is

$$J = \frac{t^3 d_i}{3} \quad (8)$$

Substituting I_y , J , the modulus of elasticity, $E = 29,000 \text{ ksi}$, and the shear modulus, $G = 11,200 \text{ ksi}$, the resulting equation is:

$$M_{cr} = 16,848 \frac{d_i t^3}{L_i} \quad (9)$$

It is important to note that this equation is for elastic buckling and does not account for residual stresses. The problem is further complicated by stress concentrations at the reentrant corner and the unknown boundary conditions with respect to rotation at the root of the cantilever. The effect of non rigid torsional restraint at the support has been studied by Bose (1982), Bradford and Wee (1994), Bradford (1989), Bradford and Trahair (1983), and Hancock et al. (1980); however, it was determined that any further refinement of Equation 9 is not justified with the limited data available.

The design buckling capacity must be greater than the internal moment at each gusset plate leg.

$$\phi M_{cr1} \geq M_{u1} \quad (10a)$$

$$\phi M_{cr2} \geq M_{u2} \quad (10b)$$

where M_{u1} and M_{u2} are determined with Equations 3a and 3b, respectively, and $\phi = 0.9$ for lateral-torsional buckling.

To determine the buckling length, L_i , to be used in Equation 9, the buckled shape of the specimens and finite element models was observed. For the specimens loaded in tension, the inside edges buckled farther than the outside edges. This behavior was expected because the maximum compressive flexural stresses are on the inside edges, at the reentrant corner. The specimens loaded in compression buckled farther on the outside edges. Figure 10 shows how this behavior affects the buckling length of the legs. The

plate in Figure 10a was loaded in tension. The buckling of each leg is restrained at the reentrant corner, and the buckling length, L_i , is the length of the cutout. The following buckling lengths can be used when the plate is loaded in tension: $L_1 = e_2$ for Leg 1, and $L_2 = e_1$ for Leg 2. For plates loaded in compression, as shown in Figure 10b, the buckling length ends approximately at the center of the adjacent leg. For design purposes, the following buckling lengths can be used when the plate is loaded in compression: $L_1 = e_2 + d_2/2$ for Leg 1, and $L_2 = e_1 + d_1/2$ for Leg 2.

For plates with a diagonal cut, as shown in Figure 6b, which are loaded in tension, the buckling length can be taken as the portion of the leg with parallel edges, measured to the start of the diagonal cut. For plates with a diagonal cut loaded in compression, the buckling length is determined the same as for standard gusset plates.

VALIDATION OF PROPOSED DESIGN METHOD

The nominal capacity of the plate, P_{min} , is the minimum of the bending, shear, and buckling limit states. The capacities for each specimen tested by Dowswell and Fouad (2005b, 2005c) were calculated using the proposed design method and are summarized in Table 1. All of the loads are expressed as the maximum nominal load parallel to the brace based on the minimum capacity of the two legs. P_e is the bending capacity, P_v is the shear capacity, P_b is the lateral-torsional buckling capacity, and P_{min} is the minimum of P_e , P_v and P_b . The specimen numbers are suffixed with “T” if the plate was loaded in tension, and “C” if it was loaded in compression.

Table 1. Calculated Capacities

Spec. No.	P_e	P_v	P_b	P_{min}	Pred. Failure Mode
2T	33.12	145.7	105.94	33.12	Y
6T	31.79	101.7	43.48	31.79	Y
8T	46.00	155.8	141.92	46.00	Y
9T	35.77	115.6	84.90	35.77	Y
10T	68.00	204.0	145.27	68.00	Y
1C	39.52	115.9	56.80	39.52	Y
2C	32.87	144.6	73.46	32.87	Y
3C	36.14	115.6	96.08	36.14	Y
4C	23.12	101.7	16.32	16.32	B
5C	25.84	82.70	22.43	22.43	B
6C	31.79	101.7	27.83	27.83	B
7C	45.07	144.2	124.29	45.07	Y
8C	46.48	157.4	94.73	46.48	Y
9C	36.71	118.6	69.46	36.71	Y
10C	67.47	202.4	91.83	67.47	Y

P_e calculated elastic bending capacity

P_v calculated shear capacity

P_b calculated lateral-torsional buckling capacity

P_{min} minimum of P_e , P_v and P_b (proposed nominal capacity)

Y: yielding

B: buckling

The experimental results of Dowswell and Fouad (2005b, 2005c) and the finite element results of Dowswell et al. (2005) are summarized in Table 2. Because the load vs. deflection curves did not have a well-defined yield point, the experimental and finite element yield loads were determined using a 1/64-in. offset line, as shown in Figure 11. The yield load is where the load vs. deflection curve crossed the 1/64-in. offset line. P_{ey}

is the experimental yield load, P_{fy} is the yield load from the finite element models, and P_{avg} is the average of P_{ey} and P_{fy} .

Table 2. Experimental and Finite Element Loads

Spec. No.	P_{ey}	P_{fy}	P_{avg}	$\frac{P_{avg}}{P_{min}}$	Exp. Failure Mode
2T	69.0	50.7	59.85	1.81	Y/B
6T	42.3	39.9	41.10	1.29	Y/B
8T	85.3	73.8	79.55	1.73	Y/B
9T	51.5	46.9	49.20	1.38	Y/B
10T	96.2	84.8	90.50	1.33	Y/B
1C	33.3	51.6	42.45	1.07	Y/B
2C	47.3	44.7	46.00	1.40	Y
3C	46.6	45.0	45.80	1.27	Y/B
4C	32.0	30.2	31.10	1.91	B
5C	28.7	36.3	32.50	1.45	Y/B
6C	25.3	34.5	29.90	1.07	B
7C	46.4	51.3	48.85	1.08	Y/B
8C	38.4	67.6	53.00	1.14	Y
9C	44.4	38.7	41.55	1.13	Y/B
10C	57.0	76.6	66.80	0.99	Y/B

P_{ey} experimental yield load determined using a 1/64-in. offset

P_{fy} finite element yield load determined using a 1/64-in. offset

P_{avg} average of P_{ey} and P_{fy}

The P_{avg} to P_{min} ratios are in the fifth column of Table 2. P_{avg}/P_{min} varied from 0.99 to 1.91, with an average of 1.34 and a standard deviation of 0.28. Dowswell and Barber (2004) summarized the test results for compact corner gusset plates in compression and found the current design equations to be conservative by an average of 47 percent with a standard deviation of 0.23. Based on this data, the accuracy of the

proposed design procedure for wrap-around gusset plates is similar to the accuracy of the current design procedure for standard gusset plates.

The experimental failure modes are summarized in the sixth column of Table 2. All of the specimens failed by a combination of buckling and yielding; therefore it was difficult to determine whether the correct failure mode was predicted with the proposed design method. Two of the specimens, Specimens 2C and 8C, were almost fully yielded before buckling occurred due to a loss of stiffness. Both of these specimens also had a predicted failure mode of yielding as shown in Table 1. Specimens 4C and 6C buckled while most of the plate material was in the elastic range. The predicted failure mode for both of these plates was also buckling. For these four tests with definite failure modes, the design model predicted the correct failure mode.

CONCLUSIONS

Results from experiments and finite element models have been used to formulate a design method for wrap-around gusset plates subjected to tension or compression loads. The proposed design method is based on a cantilever beam model at each leg of the gusset plate and uses an elastic bending stress distribution. Due to the flexural stresses in the gusset plate legs, lateral-torsional buckling is a limit state that must be considered. The buckled shape of the gusset legs was similar to the buckled shape of the wide flange cantilever beams with lateral bracing at the free end. The cantilever beam model was used to determine the lateral-torsional buckling resistance of the gusset plate legs.

The accuracy of the proposed design method was verified by comparing the calculated capacities to experimental and finite element results. The mean calculated

capacities were 34 percent higher than the experimental and finite element capacities.

The accuracy of the proposed method is similar to that of the current design procedure for standard gusset plates without cutouts. The experimental specimens failed by a combination of buckling and yielding; therefore it was difficult to determine whether the correct failure mode was predicted with the proposed design method. For the four tests with definite failure modes, the design model predicted the correct failure mode.

In addition to the limit states presented in this paper, the designer should also investigate the limit states that would normally be checked for standard gusset plates, such as bolt strength, weld strength, shear fracture, and block shear.

EXAMPLES

Example 1

The capacity of the gusset plate in Figure 12 will be checked. Only the limit states presented in this paper will be checked. For a complete design, additional limit states common to standard gusset plates should be checked.

Axial force in brace: 35 kips tension/35 kips compression

Plate thickness: 3/8 in.

Plate material: A572 Grade 50, $F_y = 50 \text{ ksi}$

Shear in Leg 1

$$\phi V_n = (0.9)(0.6)F_y d_1 t = (0.9)(0.6)(50 \text{ ksi})(10 \text{ in.})(0.375 \text{ in.}) = 101.2 \text{ k}$$

$$101.2 \text{ k} > 22.5 \text{ k} \rightarrow \text{OK}$$

Shear in Leg 2

$$\phi V_{n2} = (0.9)(0.6)F_y d_2 t = (0.9)(0.6)(50 \text{ ksi})(10 \text{ in.})(0.375 \text{ in.}) = 101.2 \text{ k}$$

$$101.2 \text{ k} > 26.8 \text{ k} \rightarrow OK$$

Bending in Leg 1

$$\phi M_{n1} = (0.9)F_y \frac{t d_1^2}{6} = (0.9)(50 \text{ ksi}) \frac{(0.375 \text{ in.})(10 \text{ in.})^2}{6} = 281.2 \text{ in} \cdot \text{k}$$

$$M_{u1} = P_1 e_2 = (22.5 \text{ k})(12 \text{ in.}) = 270.0 \text{ in} \cdot \text{k}$$

$$281.2 \text{ in} \cdot \text{k} > 270.0 \text{ in} \cdot \text{k} \rightarrow OK$$

Bending in Leg 2

$$\phi M_{n2} = (0.9)F_y \frac{t d_2^2}{6} = (0.9)(50 \text{ ksi}) \frac{(0.375 \text{ in.})(10 \text{ in.})^2}{6} = 281.2 \text{ in} \cdot \text{k}$$

$$M_{u2} = P_2 e_1 = (26.8 \text{ k})(8.25 \text{ in.}) = 221.1 \text{ in} \cdot \text{k}$$

$$281.2 \text{ in} \cdot \text{k} > 221.1 \text{ in} \cdot \text{k} \rightarrow OK$$

Buckling at Leg 1

$L=17 \text{ in.}$ for compression loads and 12 in. for tension loads. Use $L=17 \text{ in.}$

$$\phi M_{cr1} = (0.9)(16,848) \frac{d_1 t^3}{L_1} = (0.9)(16,848) \frac{(10 \text{ in.})(0.375 \text{ in.})^3}{17 \text{ in.}} = 470.4 \text{ in} \cdot \text{k}$$

$$470.4 \text{ in} \cdot \text{k} > 270.0 \text{ in} \cdot \text{k} \rightarrow OK$$

Buckling at Leg 2

$L=13.25 \text{ in.}$ for compression loads and 8.25 in. for tension loads. Use $L=13.25 \text{ in.}$

$$\phi M_{cr2} = (0.9)(16,848) \frac{d_2 t^3}{L_2} = (0.9)(16,848) \frac{(10 \text{ in.})(0.375 \text{ in.})^3}{13.25 \text{ in.}} = 603.5 \text{ in} \cdot \text{k}$$

$$603.5 \text{ in}\cdot k > 221.1 \text{ in}\cdot k \rightarrow OK$$

Example 2

The capacity of the gusset plate in Figure 13 will be checked. The connection is identical to the one in Example 2, except that the cutout has a diagonal cut, and the load has been increased to 50 kips. Only the limit states presented in this paper will be checked. For a complete design, additional limit states common to standard gusset plates should be checked.

Axial force in brace: 50 kips tension/50 kips compression

Plate thickness: 3/8 in.

Plate material: A572 Grade 50, $F_y = 50 \text{ ksi}$

Shear in Leg 1

$$\phi V_{n1} = (0.9)(0.6)F_y d_1 t = (0.9)(0.6)(50 \text{ ksi})(10 \text{ in.})(0.375 \text{ in.}) = 101.2 \text{ k}$$

$$101.2 \text{ k} > 32.1 \text{ k} \rightarrow OK$$

Shear in Leg 2

Shear capacity will be analyzed at a plane immediately beyond the clip angle leg. The leg width at this location is,

$$d_2 = 10 \text{ in.} + (4 \text{ in.})(3.5 \text{ in.}/8.25 \text{ in.}) = 11.70 \text{ in.}$$

$$\phi V_{n2} = (0.9)(0.6)F_y d_2 t = (0.9)(0.6)(50 \text{ ksi})(11.70 \text{ in.})(0.375 \text{ in.}) = 118.4 \text{ k}$$

$$118.4 \text{ k} > 38.3 \text{ k} \rightarrow OK$$

Bending in Leg 1

$$\phi M_{n1} = (0.9) F_y \frac{td_1^2}{6} = (0.9)(50 \text{ ksi}) \frac{(0.375 \text{ in.})(10 \text{ in.})^2}{6} = 281.2 \text{ in} \cdot \text{k}$$

$$M_{u1} = P_1 e_2 = (32.1 \text{ k})(8 \text{ in.}) = 256.8 \text{ in} \cdot \text{k}$$

$$281.2 \text{ in} \cdot \text{k} > 256.8 \text{ in} \cdot \text{k} \rightarrow OK$$

Bending in Leg 2 (Case 1: Immediately beyond the clip angle leg)

$$d_2 = 10 \text{ in.} + (4 \text{ in.})(3.5 \text{ in.}/8.25 \text{ in.}) = 11.70 \text{ in.}$$

$$\phi M_{n2} = (0.9) F_y \frac{td_2^2}{6} = (0.9)(50 \text{ ksi}) \frac{(0.375 \text{ in.})(11.70 \text{ in.})^2}{6} = 385.0 \text{ in} \cdot \text{k}$$

$$M_{u2} = P_2 e_1 = (38.3 \text{ k})(3.5 \text{ in.}) = 134.0 \text{ in} \cdot \text{k}$$

$$385.0 \text{ in} \cdot \text{k} > 134.0 \text{ in} \cdot \text{k} \rightarrow OK$$

Bending in Leg 2 (Case 2: End of diagonal cut)

$$\phi M_{n2} = (0.9) F_y \frac{td_2^2}{6} = (0.9)(50 \text{ ksi}) \frac{(0.375 \text{ in.})(14 \text{ in.})^2}{6} = 551.2 \text{ in} \cdot \text{k}$$

$$M_{u2} = P_2 e_1 = (38.3 \text{ k})(8.25 \text{ in.}) = 316.0 \text{ in} \cdot \text{k}$$

$$551.2 \text{ in} \cdot \text{k} > 316.0 \text{ in} \cdot \text{k} \rightarrow OK$$

Buckling at Leg 1

$L = 17 \text{ in.}$ for compression loads and 8 in. for tension loads. Use $L = 17 \text{ in.}$

$$\phi M_{cr1} = (0.9)(16,848) \frac{d_1 t^3}{L_1} = (0.9)(16,848) \frac{(10 \text{ in.})(0.375 \text{ in.})^3}{17 \text{ in.}} = 470.4 \text{ in} \cdot \text{k}$$

$$470.4 \text{ in}\cdot k > 256.8 \text{ in}\cdot k \rightarrow OK$$

Buckling at Leg 2

$L=13.25 \text{ in.}$ for compression loads and 0 in. for tension loads. Use $L=13.25 \text{ in.}$

$$\phi M_{cr2} = (0.9)(16,848) \frac{d_2 t^3}{L_2} = (0.9)(16,848) \frac{(10 \text{ in.})(0.375 \text{ in.})^3}{13.25 \text{ in.}} = 603.5 \text{ in}\cdot k$$

$$603.5 \text{ in}\cdot k > 134.0 \text{ in}\cdot k \rightarrow OK$$

REFERENCES

AISC (2001), "Manual of Steel Construction, Load and Resistance Factor Design," 3rd ed., American Institute of Steel Construction, Inc., Chicago, Illinois.

AISC (1999), Load and Resistance Factor Design Specification for Structural Steel Buildings, American Institute of Steel Construction, Inc., Chicago, Illinois.

Bose, B. (1982), "The Influence of Torsional Restraint Stiffness at Supports on the Buckling Strength of Beams," *The Structural Engineer*, Vol. 60b, No. 4, December.

Bradford, M. A. and Wee, A. (1994), "Analysis of Buckling Tests on Beams on Seat Supports," *Journal of Constructional Steel Research*, Vol. 28, pp. 227-242.

Bradford, M. A. (1989), "Buckling of Beams Supported on Seats," *The Structural Engineer*, Vol. 67, No. 23, December.

Bradford, M. A. and Trahair, N. S. (1983), "Lateral Stability of Beams on Seats," *Journal of Structural Engineering*, ASCE, Vol. 109, No. 9, September.

Dowswell, B., Whyte, R., Davidson, J., and Fouad, F. (2005), "Finite Element Analysis of Wrap-Around Gusset Plates," Page 102 of this document.

Dowswell, B. and Fouad, F. H. (2005a), "Design Considerations for Wrap-Around Gusset Plates," Page 3 of this document.

Dowswell, B. and Fouad, F. H. (2005b), "Wrap-Around Gusset Plates in Compression," Page 50 of this document.

Dowswell, B. and Fouad, F. H. (2005c), "Wrap-Around Gusset Plates in Tension," Page 33 of this document.

Dowswell, B. and Barber, S. (2004), "Buckling of Gusset Plates: A Comparison of Design Equations to Test Data," *Proceedings, 2004 Annual Stability Conference*, Structural Stability Research Council, pp. 199-221.

Dowswell, B. (2004), "Lateral-Torsional Buckling of Wide Flange Cantilever Beams," *AISC Engineering Journal*, Third Quarter, pp. 135-147.

Hancock, G. H., Bradford, M. A., and Trahair, N. S. (1980), "Web Distortion and Flexural-Torsional Buckling," *Journal of the Structural Division*, ASCE, Vol. 106, No. ST7, July.

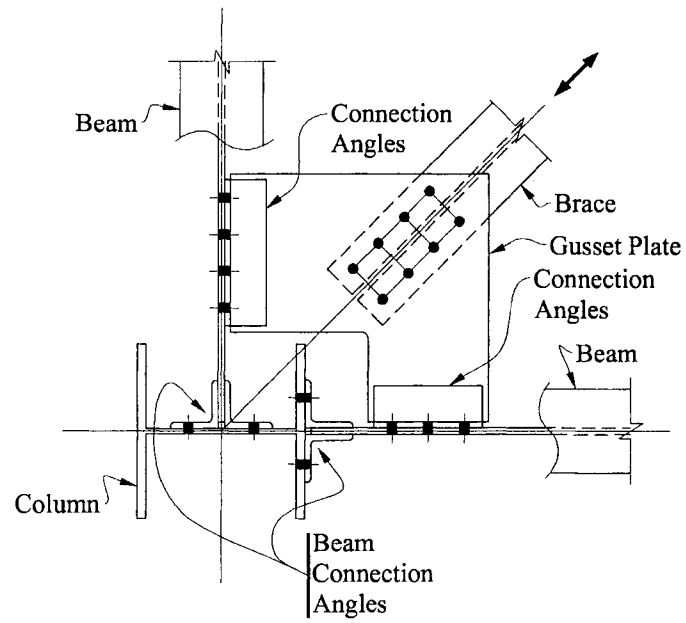


Fig. 1. Horizontal brace connection at beam-to-column intersection.

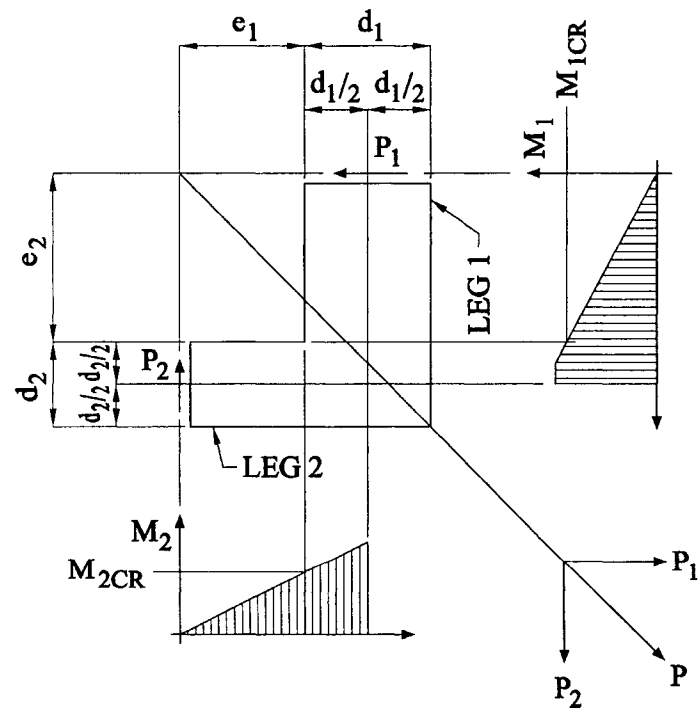


Fig. 2. Force system for wrap-around gusset plates.

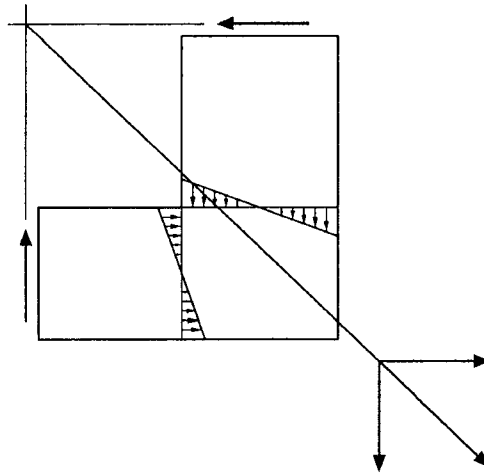


Fig. 3. Bending stresses in each leg.

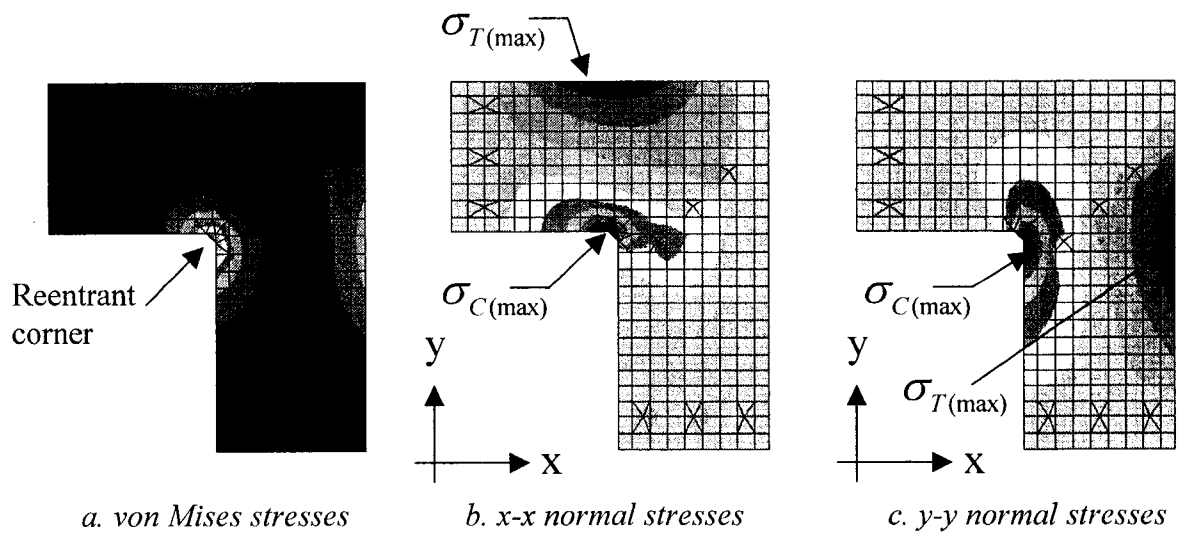


Fig. 4. Elastic stress contours for a typical model loaded in tension.

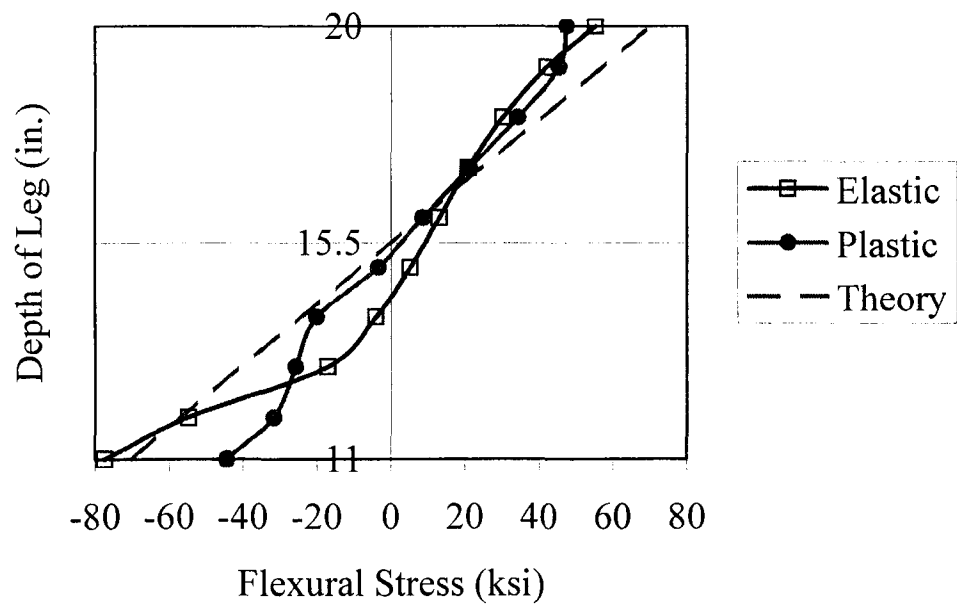
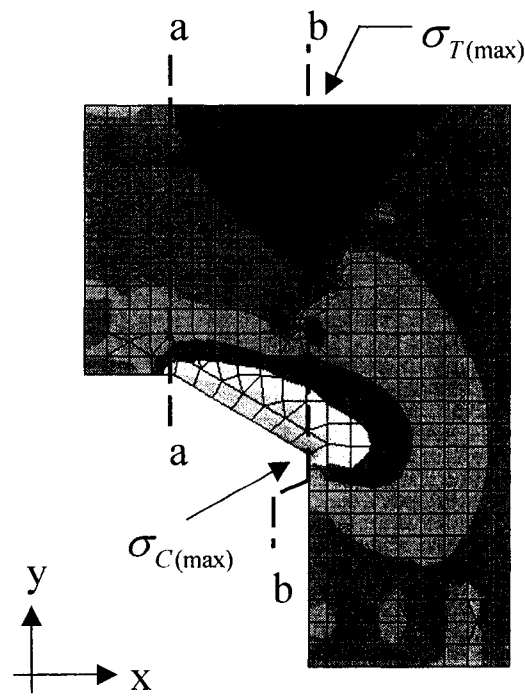
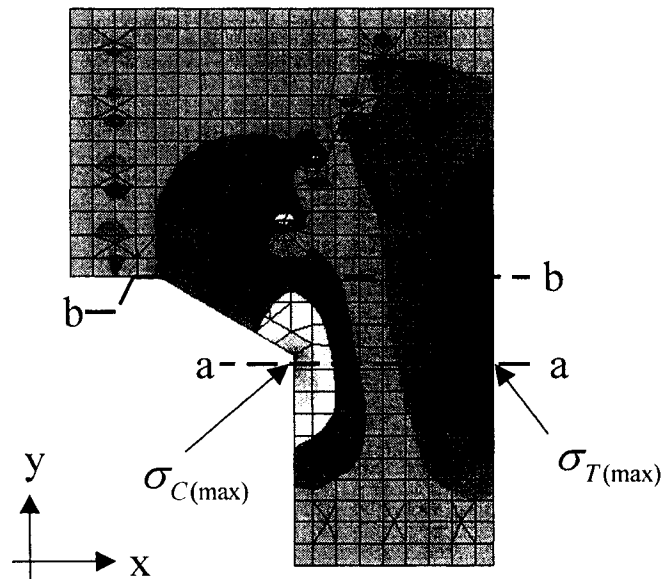


Fig. 5. Typical flexural stresses in gusset plate legs.

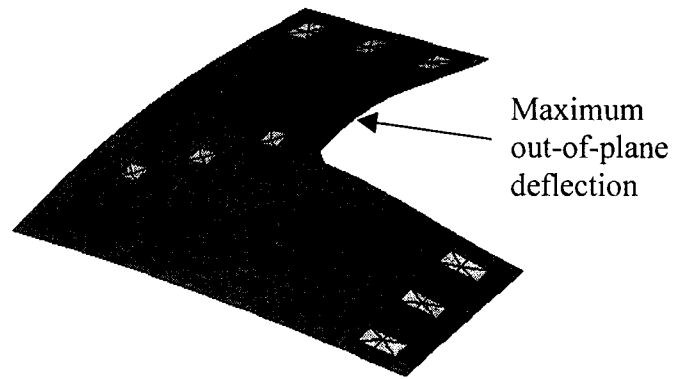


a. x-direction normal stresses

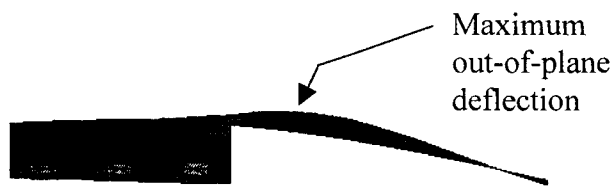


b. y-direction normal stresses

Fig. 7. Elastic stress contours for a typical model loaded in tension.



a. Top view.



b. Side View.

Fig. 8. Typical buckled shape for the models loaded in tension.

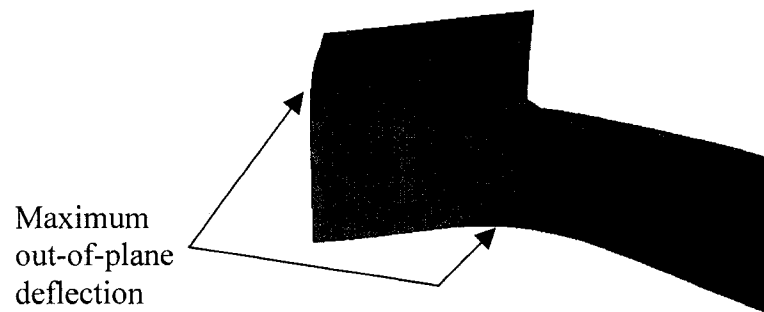
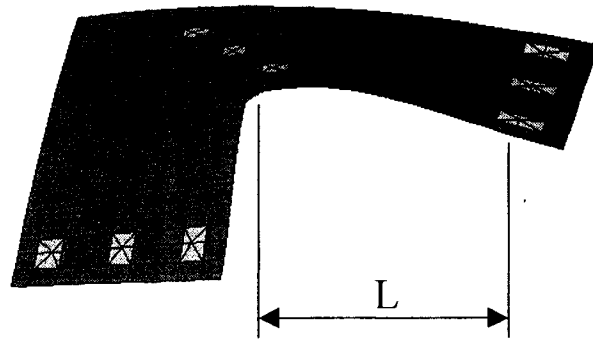
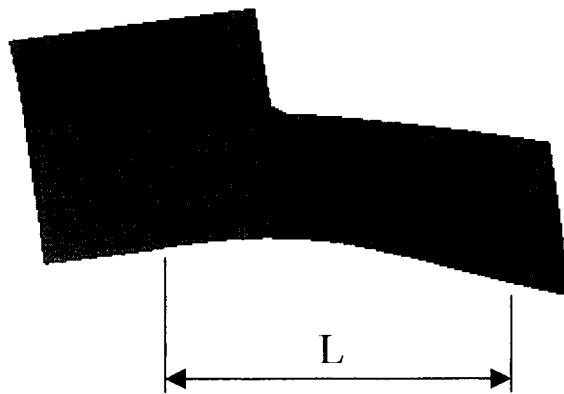


Fig. 9. Typical buckled shape for the models loaded in compression.



a. Plates loaded in tension.



b. Plates loaded in compression.

Fig. 10. Effective length of gusset legs.

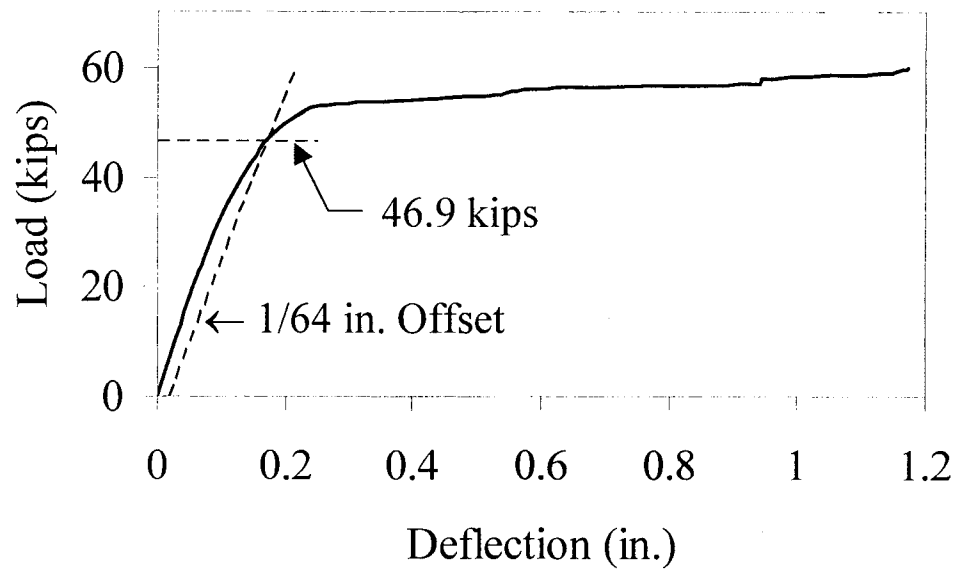


Fig. 11. Load versus deflection plot for finite element model 9T.

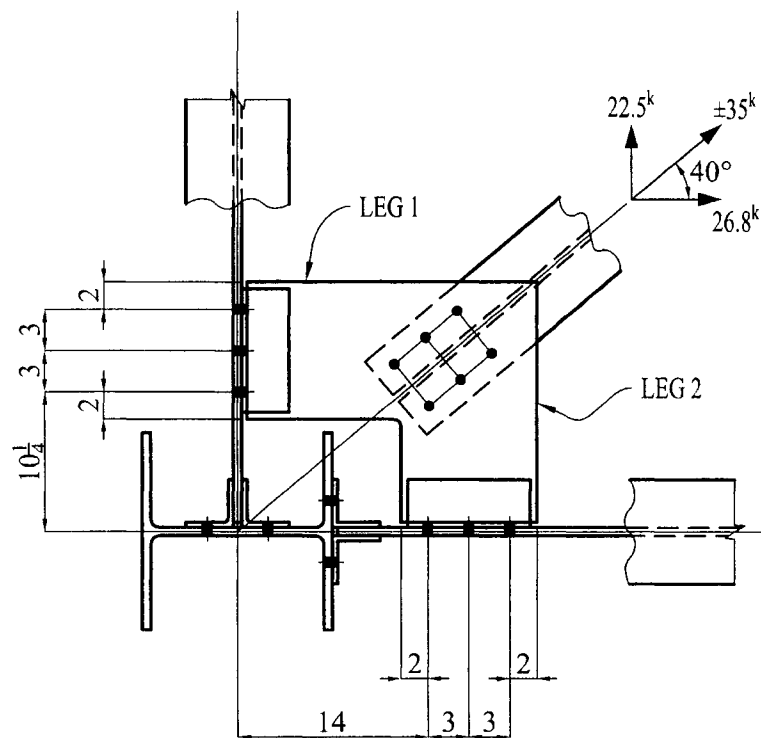


Fig. 12. Connection for Example 1.

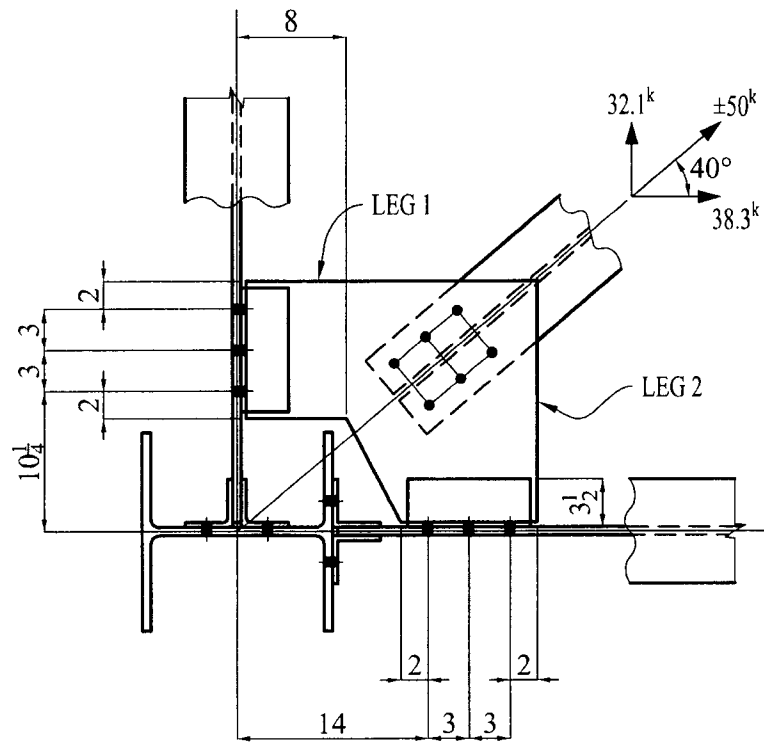


Fig. 13. Connection for Example 2.

CONCLUSION

The purposes of this research were to gain a better understanding of the behavior of wrap-around gusset plates, identify potential failure modes, and formulate a design method for these connections. Ten experimental specimens were tested in compression and five were tested in tension. All of the specimens were modeled using the finite element method with material and geometric nonlinearities.

The experiments and finite element models indicated that wrap-around gusset plates are subject to limit states common to flexural members. The results were used to formulate a design method for wrap-around gusset plates based on a cantilever beam model. The accuracy of the proposed design method was verified by comparing the calculated capacities to experimental and finite element results. The accuracy of the proposed method is similar to that of the current design procedure for standard gusset plates without cutouts.

The findings of this research project will provide information on the design and behavior of wrap-around gusset plates. The results of this project are presented in a way that can be easily used by design engineers. It is expected that the findings will impact national specifications and will be used in design guides on steel connection design.

Future research on wrap-around gusset plates could include experimental and finite element studies with the geometric parameters varied from the specimens detailed in this project. Cyclic testing would be beneficial to determine their behavior in seismic events. Because wrap-around gusset plates are common in industrial structures, research

on the fatigue capacity would help to provide safer support structures for cranes and vibrating machinery.

APPENDIX

NOTATION

A	cross sectional area
c	distance to extreme fiber
C_B	coefficient to account for the effect of bracing
C_H	coefficient to account for the effect of load height
C_L	coefficient to account for the moment distribution along the length of the beam
d_1	width of leg 1
d_2	width of leg 2
e_1	cutout dimension at leg 1
e_2	cutout dimension at leg 2
E	modulus of elasticity
F	axial load in brace
F_E	component of force F
F_N	component of force F
F_{rt}	tensile force generated by the actual residual stress pattern
F_{rts}	tensile force generated by the simplified residual stress pattern
F_y	yield strength
G	shear modulus
I	moment of inertia
I_y	weak-axis moment of inertia
J	torsion constant
l_1	buckling length at the work line

l_2	buckling length at the edge of the effective width
l_3	buckling length at the edge of the effective width
l_{avg}	average buckling length
L	beam length
L_1	buckling length for leg 1
L_2	buckling length for leg 2
L_w	effective width
M	moment
M_{1cr}	critical bending moment in leg 1
M_{2cr}	critical bending moment in leg 2
M_{cr}	critical buckling moment of a cantilever beam
M_{n1}	nominal bending capacity of leg 1
M_{n2}	nominal bending capacity of leg 2
ϕM_{n1}	design bending capacity of leg 1
ϕM_{n2}	design bending capacity of leg 2
M_u	applied moment
M_{u1}	bending moment at the critical section of leg 1
M_{u2}	bending moment at the critical section of leg 2
M_p	plastic moment capacity
ϕM_{cr1}	design buckling capacity of leg 1
ϕM_{cr2}	design buckling capacity of leg 2

P	factored axial load in brace
P_1	component of the factored brace load, P
P_2	component of the factored brace load, P
P_{avg}	average of P_{ey} and P_{fy}
P_b	calculated lateral-torsional buckling capacity
P_e	calculated elastic bending capacity
P_{eu}	maximum experimental load
P_{ey}	experimental yield load determined using a 1/64 in. offset
P_{fu}	maximum load from finite element model
P_{fy}	finite element yield load determined using a 1/64 in. offset
P_{min}	minimum of P_e , P_v and P_b (proposed nominal capacity)
P_v	calculated shear capacity
t	gusset plate thickness
V	shear force
V_{n1}	nominal shear capacity of leg 1
V_{n2}	nominal shear capacity of leg 2
ϕV_{n1}	design shear capacity of leg 1
ϕV_{n2}	design shear capacity of leg 2
V_u	applied shear
V_p	plastic shear capacity
x	width of tension portion of actual residual stress pattern

x_s	width of tension portion of simplified residual stress pattern
σ_e	effective stress
σ_{rt}	tension residual stress at the plate edge
σ_x	applied normal stress in the x-direction
σ_y	applied normal stress in the y-direction
τ	applied shear stress
ϕ	resistance factor

**GRADUATE SCHOOL
UNIVERSITY OF ALABAMA AT BIRMINGHAM
DISSERTATION APPROVAL FORM
DOCTOR OF PHILOSOPHY**

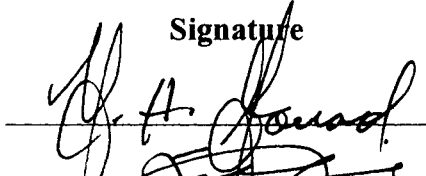

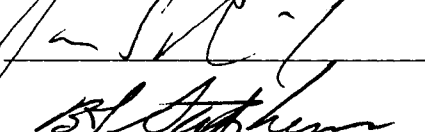

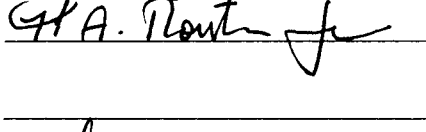
Name of Candidate Ronald Scott Dowswell

Graduate Program Civil Engineering

Title of Dissertation Design of Wrap Around Steel Gusset Plates

I certify that I have read this document and examined the student regarding its content. In my opinion, this dissertation conforms to acceptable standards of scholarly presentation and is adequate in scope and quality, and the attainments of this student are such that he may be recommended for the degree of Doctor of Philosophy.

Dissertation Committee:

Name	Signature
<u>Fouad H. Fouad</u> , Chair	
<u>Talat Abu-Amra</u>	
<u>James Davidson</u>	
<u>Bobby J. Stephens</u>	
<u>Houssam Toutanji</u>	

Director of Graduate Program

Dean, UAB Graduate School

Date JAN 03 2006

